IN THE UNITED STATES PATENT AND TRADEMARK OFFICE

Attorney Docket No. 028622-0102

In re patent application of
Dorken, *et al.*

Group Art Unit: 1643

Serial No. 09/673,735

Examiner: P Tungaturthi

Filed: 12/27/2000

For: Novel CD19 x CD3 Specific Polypeptides and Uses Thereof

DECLARATION UNDER 37 CFR § 1.132

Commissioner for Patents
PO Box 1450
Alexandria, Virginia 22313-1450

We, Patrick A. Baeuerle and Peter Kufer, hereby declare:

1. I, Patrick A. Baeuerle, have worked in the field of immunology for almost twenty years. I have over 200 publications with most of the papers published in the field of immunology. I received a Ph.D. in 1987 from the University of Munich and I am presently a Professor of Immunology at the Ludwig-Maximilians University in Munich. I also serve as Chief Scientific Officer at Micromet. My curriculum vitae and a list of publications to further explain my experience and background is attached as **APPENDIX A**.

I, Peter Kufer, am an inventor on the present application. I have worked in the field of immunology for almost twenty years and have numerous publications in the field of immunology. I received a M.D. in 1991 and a Ph.D. in 1994 from the University of Munich. I am an affiliated lecturer with Ludwig-Maximilians University in Munich. I also serve as Vice President, Immunotherapy at Micromet. My curriculum vitae is attached as **APPENDIX B**.

2. We have read and understood the Office Action dated August 3, 2005, and particularly the Examiner's comments regarding Bohlen *et al.* (1993), Blattler *et al.* (1993), Mack *et al.* (1995), and the orientation of the claimed bispecific single chain (bsc) antibody (Ab) invention, namely V_LCD19-V_HCD19-V_HCD3-V_LCD3. We will first provide our understanding of the cited publications and later discuss the orientation and activity of the claimed invention.

Bohlen (1993) does not study the single chain bispecific CD19 x CD3 antibody. In addition, the article does not describe methods for the treatment of non-Hodgkin's lymphoma with an antibody.

Blattler (1993) describes the targeting of cells with toxic molecules, such as ricin. Toxic molecules are delivered to the cells by, for example, the use of antibodies that bind CD19. The invention requires the transport of the toxic molecule into the target cells. During this process the antibody used to target the cells is internalized together with the toxic molecule, thereby killing the cell. For example, in column 19, lines 20-51, Blattler discusses embodiments of his invention that include antibodies to the CD19 antigen covalently linked to a toxic molecule capable of binding and being transported into the target cell. Column 5, lines 23-52, further describes the previously unknown ability to separate the binding and translocation function of the two chains in the ricin molecule. Blattler shows how an antibody such as anti-CD19 can be used in conjunction with a portion of the ricin molecule to target and translocate into a target cell of interest. In stark contrast, the single-chain bispecific antibodies to be effective cancer treatments must not be internalized in order to effectively function as an anti-cancer agent recruiting tumor cells. See below, discussion of Mack.

Mack (1995) describes the use of a 17-1A x CD3 bispecific antibody construct (17-1A x CD3 bsc Ab). The potency of the 17-1A x CD3 bsc-Ab construct in redirected lysis of various tumor cells is not different from the potency of monoclonal antibodies described in the literature. (See Figures 5 and 6, page 7024). Half maximal target cell lysis is observed at concentrations of 17-1A x CD3 bsc-Ab between 1.6 (Kato cells) and 40 ng/ml (HT-29 cells). This low level of activity is achieved by whole antibodies as well, and is not attractive given the low productivity of 17-1A x CD3 bsc-Ab of only 12-15 mg/L in CHO cells (see page 7023). This particular bispecific antibody is not suited for clinical use because of the excessive costs associated with production and treatment. Either productivity of 17-1A x CD3 bsc-Ab requires dramatic improvement, or 17-1A x CD3 bsc-Ab needs to be more efficacious by at least 100 fold. Neither of these shortcomings is solved by Mack.

Mack proposes the use of 17-1A x CD3 bsc-Ab for the treatment of minimal residual disease as is characterized by a low burden of tumor cells and the presence of very small tumors. See p. 7025 and the discussion of 17-1A x CD3 bsc-Ab in the treatment of disseminated residual tumor cells after resection of the primary tumor. By contrast, the present

invention may be used in late-stage lymphoma, such as non-Hodgkin lymphoma (NHL). In NHL, massive amounts of tumor cells, sometimes in the kg-range, must be eliminated by a bispecific antibody. These tumor cells can float freely in peripheral blood or lymph nodes, but can also manifest as very large tumors. A bispecific antibody that can remove large tumor masses as found with certain blood-borne cancers is not described by Mack.

An antibody for the treatment of NHL must have a different specificity than the 17-1A x CD3 bsc-Ab because lymphoma cells are devoid of 17-1A antigen. The selection of an appropriate target antigen to address lymphoma is a challenging task. Although CD19 is very frequently expressed on human B cell malignancies and has previously been employed for immunotherapeutic approaches, CD19 is also known to rapidly internalize upon binding by monoclonal antibodies. See discussion above. While certain therapies, such as an antibody with a toxic molecule, seek to exploit internalization of CD19, internalization of CD19 in the case of bispecific antibodies would prevent recruitment of T cells and redirected lysis of tumor cells. As discussed below, the efficacy of the present invention relative to 17-1A x CD3 bsc-Ab on 17-IA expressing tumor cells and to other CD19/CD3 bispecific antibodies such as diabody, tandem diabody or quadroma is higher by 2-4 orders of magnitude.

3. In response to the Examiner's comments on pages 3-4 of the Office Action that the orientation of the claimed invention would be obvious over the cited scientific articles, we provide the following information which demonstrates that the claimed single-chain CD19 x CD3 antibodies have activity that could not have been predicted from the prior art. In fact, the prior art taught that bispecific single-chain CD3-C19 antibody "failed to recognize human CD3" (Kipriyanov *et al.*, The Fourteenth International Conference Adv. in the Applications of Monoclonal Antibodies in Clinical Oncology, p. 29 Thira Santorini, Greece (May 5-7, 1997) **APPENDIX C**). In the same report, Kipriyanov teaches making a non-covalent heterodimer diabody and reports this diabody "is potent in retargeting peripheral blood lymphocytes to lyse tumour cells expressing CD19 antigen." Our research group has conducted direct comparisons of the claimed bispecific single-chain CD19-CD3 antibody with a covalent heterodimer diabody and found that the claimed antibody has a vastly superior activity. A covalent heterodimer diabody was selected for comparative purposes because it has been shown to be more active than non-covalent heterodimer diabodies (see below). Our research group compared side-by-side the

claimed bispecific single-chain antibody with a diabody (Tandab), a well-characterized, covalent heterodimer diabody having specificity for the B cell antigen CD19. The claimed bispecific single-chain antibody has significantly superior activity. In addition, we have prepared and tested multiple sequences with the structure of the claimed bispecific single-chain antibody and found them to have similar activity. These data verify the extraordinary efficacy of the claimed invention over the claimed scope of single-chain bispecific antibodies having the structure V_LCD19-V_HCD19-V_HCD3-V_LCD3.

4. The bsc CD19xCD3 Ab in the claimed orientation was produced by CHO cells and purified from cell culture supernatant. Multiple variants of bsc CD19xCD3, called MT103, MB2.1, MB4 and VH19 were used in the following experiments. See the attached sequences. These variants were produced using techniques described in the specification on pages 6-8 and throughout the Examples.

MT103: The bsc CD19xCD3 amino acid sequence is provided in Figure 8 of the application. MT103 includes the C-terminal His tag to assist in purification, but not the Flag-Tag provided in Figure 8.

MB2.1: V_HCD3 portion of MB2.1 has 4 amino acid substitutions in positions 1 (D->H), 2(I->V), 3 (K->Q), 24 (T->A) compared to MT103. The V_LCD3, V_HCD19, and V_LCD19 are identical to MT103.

MB4: V_HCD3 portion of MB4 has several amino acid substitutions (more than 30) compared to MT103. The V_LCD3, V_HCD19, and V_LCD19 are identical to MT103.

VH19: V_HCD19 portion of VH19 has one amino acid substitution in position 89 (E->N) compared to MT103 introducing a potential glycosylation site. V_LCD19, V_HCD3, and V_LCD3 are identical to MT103.

We compared the claimed construct to a well characterized covalent heterodimer diabody called Tandab. For a comparison of the domain structures in the disclosed antibodies, please see the attached Summary of Constructs. The amino acid sequence of Tandab is shown in Figure 1. Previous studies showed by direct side-by-side comparison that Tandab (called LL-Tandab in the citation below) was more active than non-covalent heterodimer diabodies. (Kipriyanov et al, (1999), *J Mol Biol* **293**, 41-56 **APPENDIX D**). For example, Kipriyanov states on page 51 that "[t]he Tandabs were consistently more effective than the diabody for inducing T cell

proliferation in the presence of tumor cells and in effector cell retargeting." Tandab is one of the best documented and studied heterodimer diabodies in this area of study. Tandab is therefore a well documented benchmark by which to compare the claimed invention with other similar constructs.

Tandab was produced in *E. coli* using the pBAD expression system (Invitrogen, Carlsbad, CA). A coding region was synthesized and sequenced (DNA 2.0 Inc., Menlo Park, CA) with a protein sequence as deduced from descriptions of the LL-Tandab protein by Kipriyanov et al, (1999) *J Mol Biol* **293**, 41-56 and Kipriyanov et al, (1998). *Int J Cancer* **77**, 763-72 (**APPENDIX E**), including PelB signal peptide, c-myc epitope and 6×histidine tag coding regions. The synthesized cDNA was cloned into a modified pBAD/*Myc*-His vector with the ampicillin cassette substituted with a kanamycin cassette giving the construct pBAD-Tandab KAN. The construct was transformed into *E. coli* strain BL21-AI (Invitrogen) and a 50 mL culture (LB medium, 50 µg/mL kanamycin, 37°C, 260 rpm) of a single transformant grown overnight was used to inoculate 12×1 L shake flask cultures (LB medium, 50 µg/mL kanamycin). The cultures were incubated at 25°C and 220 rpm until an $OD_{600\ of}$~0.5 was attained. Gene expression was induced by addition of 0.08% (w/v) L-arabinose (Sigma, Taufkirchen, Germany) and further incubation for approximately 15 hours. The cells were harvested by centrifugation at 5,000× g for 12 min and resuspended in 900 mL 1×D-PBS (Invitrogen).

Periplasmic proteins were extracted by sequential freezing in ethanol/dry ice and thawing in a 37°C warm water bath for a total of six cycles. The crude extract was centrifuged at 9.000×g for 20 min and Complete EDTA-free protease inhibitor cocktail (Roche, Mannheim, Germany) added according to the manufacturers protocol, filtered (0.2 µm) and chromatographed on a 11 mL ProSep Chelating I (Millipore, Schwalbach, Germany) metal affinity chromatography column, equilibrated with 20 mM sodium phosphate, 400 mM NaCl, pH 7.0. Using a flow rate of 3 mL/min, the column was washed with 7 volumes of 20 mM sodium phosphate, 400 mM NaCl, 50 mM imidazole, pH 7.0, and bound protein was eluted with the same buffer added imidazole to 500 mM. Eluted fractions containing Tandab were added EDTA to 10 mM, concentrated four-fold and subjected to gel filtration on a HiLoad 16/60 Superdex 200 column (Amersham Biosciences, Freiburg, Germany) equilibrated with 1x D-PBS and running at a flow rate of 1 mL/min. Absorbance at 280 and 254 nm and conductivity were used to monitor

the purification. All purification procedures were performed at 4°C. The purity of Tandab was assessed by non-reducing SDS-PAGE. The corrected extinction coefficient ($Absorbance_{280} = 1$) used was 0.49 mg/mL.

Non-reducing and reducing SDS-PAGE were performed in NuPage 4-12% Bis-Tris gels (Invitrogen), and proteins were stained with SimplyBlue SafeStain (Invitrogen, Carlsbad, California, USA) and destained in ultra pure water. For Western analysis, proteins were transferred onto a nitrocellulose transfer membrane by electroblotting. For immunological detection, the membranes were incubated overnight at 4°C with a 1:3000 dilution of a mouse anti-myc primary antibody (Invitrogen) followed by incubation with a 1:3000 dilution of an alkaline phosphatase-conjugated goat anti-mouse IgG Fc secondary antibody (Sigma) for 3 hours at room temperature. Both incubations were carried out in 1×D-PBS, 0,01% (v/v) Tween20, 3% (w/v) BSA. Alkaline phosphatases were detected colorimetrically using BCIP/NBT liquid substrate (Sigma, Taufkirchen, Germany).

Bispecific functionality of the Tandab was analyzed via FACS using human B-leukemic cell line Nalm-6 or T-leukemic cell line HP-Ball for CD19 or CD3 specificity, respectively. In brief, approximately 10^5 cells were incubated with 50 µL of the Tandab preparation (1 and 10 µg/ml) for 50 min. on ice. After washing with PBS/10%FCS/0.05% sodium azide, the cells were incubated with 30 µL of 2 µg/mL Penta-His IgG (Qiagen, Hilden, Germany) in PBS/10%FCS/0.05% sodium azide for 40 min on ice. After a second wash, the cells were incubated with 30 µL of a R-phycoerythrin (PE)-labeled goat anti-mouse IgG (Jackson ImmunoResearch, Cambridgeshire, UK; 1:100 in PBS/10%FCS/0.05% sodium azide) for 40 min. on ice. The cells were then washed again and resuspended in 200 µL PBS/10%FCS/0.05% sodium azide. The relative fluorescence of stained cells was measured using a FACSCalibur™ flow cytometer (BD Biosciences, San Jose, CA).

All cell lines were purchased from the 'Deutsche Sammlung von Mikroorganismen und Zelllinien' (DSMZ, Braunschweig, Germany). MEC-1 cells were cultured in Basal Iscove's Medium, (Biochrom, Berlin, Germany), supplemented with 10% heat-inactivated fetal calf serum (FCS) from Invitrogen, Heidelberg, Germany. Nalm-6 and Raji cells were cultured in RPMI 1640 phenol red free medium (Invitrogen), supplemented with 10% FCS. For the cytotoxicity assays, all target cells were co-cultured with effector cells in RPMI 1640 phenol red-free medium supplemented with 10% FCS.

Peripheral blood mononuclear cells (PBMCs) were prepared by Ficoll density gradient centrifugation from leukocytes reduction filters as provided by local blood donor centers (Munich, Germany). Erythrocytes were removed by incubation in erythrocyte lysis buffer (155 mM NH_4Cl, 10 mM $KHCO_3$, 100 µM EDTA) for 15 minutes at room temperature. Cells were centrifuged for 5 minutes at 600x g. The supernatant containing the lysed erythrocytes was discarded and the pellet washed with PBS. Thrombocytes were removed in an additional centrifugation step for 15 minutes at 100x g. PBMCs were finally resuspended and cultured in RPMI 1640 medium supplemented with 10% heat-inactivated FCS until use.

CD3 positive T cells were isolated from PBMCs using the Human T Cell Enrichment Column Kit (R&D Systems) according to the manufacturer's instructions. T cells used without pre-stimulation were isolated shortly before setting up the cytotoxicity assay.

A 75 cm^2 culture flask was coated for 90 min at 37°C with 10 µg/mL of OKT3, purified from hybridoma supernatant, and 2 µg/mL of anti-CD28 (15E8, Chemicon, Hampshire, UK) antibodies diluted in PBS. Approximately 1.7x 10^7 isolated T cells were resuspended in 10 mL of cell culture medium and activated for 4 days in the coated culture flask in presence of 30 U/mL of IL-2. After 4 days of incubation, T cells were pelleted and resuspended in 25 mL of fresh cell culture medium containing 30 U/mL of IL-2. T cell suspension was transferred in a new 75 cm^2 culture flask and further incubated for one another day.

Target cells (MEC-1, Nalm-6 and Raji cells) were labeled using the PKH-26 Red Fluorescent Cell Linker Kit (Sigma, Taufkirchen, Germany) according to the manufacturer's instructions. In brief, 5x 10^6 target cells were washed with PBS and resuspended in 250 µL of Diluent C. Cells were then mixed with 2.5 µL of PKH26 dye diluted in 250 µL of Diluent C and incubated at room temperature for 3 minutes with gentle agitation. After incubation, the staining reaction was quenched by addition of 1 mL FCS. Labeled target cells were then washed twice with cell culture medium.

All cytotoxicity assays were performed with isolated T cells as effector cells (pre-stimulated or not) and target cells pre-labeled with the membrane dye PKH-26. Effector and target cells were co-incubated in 96-well round-bottom plates at an E:T ratio of 5:1 for MEC-1 and Nalm-6 cells and at an E:T ratio of 10:1 for Raji cells. Per well, a defined number of 1.5x 10^5 T cells was used. For measurement of the concentration-dependent cell lysis, 10-fold serial

dilutions of MT103 or Tandab were added to the samples. Cells were incubated in a total volume of 200 µL for 18 hours in a 5% atmosphere at 37°C.

After incubation, cells were pelleted by centrifugation and washed with FACS buffer (PBS, 1% FCS, 0.05 Na_3N). Subsequently, cells were resuspended in 200 µL of FACS buffer containing 1 µg/mL of propidium iodide to distinguish live from dead cells. Cells were analyzed using a FACS Calibur flow cytometer (Becton Dickinson, Heidelberg, Germany). Per sample, a total of 30,000 target cells were acquired. Data were evaluated using the Cell Quest™ software (Becton Dickinson).

5. Hexahistidine-containing proteins were purified by metal affinity chromatography from periplasmic extracts of transformed *E. coli* cells. Tandab was separated from other species in the imidazole eluate by gel filtration (Fig. 2A). A dominant protein peak of approximately 120 kDa molecular size was collected by size exclusion as fraction I. Fraction I showed upon non-reducing SDS-PAGE a single polypeptide band of 114 kDa (Fig. 2B). This protein was fully converted to a 56-kDa band upon reducing SDS-PAGE (data not shown). The 114-kDa protein reacted in Western blot with an anti-myc antibody (Fig. 3B), indicating that it contained the C-terminal c-myc tag built into the Tandab protein (see Fig. 1). The protein was (i) absent from *E. coli* cells not transformed with Tandab cDNA (data not shown), (ii) was purified by metal chelate affinity chromatography, (iii) immunoreacted with anti-myc antibody and (iv) had the reported molecular size and dimeric structure. It therefore showed all features expected for a soluble Tandab protein expressed in *E. coli* periplasm (Kipriyanov et al., 1999; Reusch et al., 2004 **APPENDIX F**).

The identity of the 114-kDa protein in fraction I with Tandab was further supported by binding studies using fluorescence-activated cell sorting (FACS). Purified Tandab showed bispecific binding to CD3 on human T leukemia cell line HP-Ball (Figs. 3A and 3B) and to CD19 as expressed on human pre-B lymphoma line Nalm-6 (Figs. 3C and 3D). Binding was dose-dependent and showed robust shifts in mean fluorescence intensity of reporter cells at a concentration of 10 µg/ml Tandab.

In order to confirm that our Tandab protein was of equivalent biological activity as the published Tandab we analyzed the efficacy of Tandab for redirected target cell lysis. We first tested in a FACS-based cytotoxicity assay its efficacy with freshly isolated, unstimulated human

T lymphocytes as effector cells. The FACS-based assay determined the ratio between propidium iodide positive and negative target cells, and produced cytotoxicity data with ED_{50} values comparable to those derived from ^{51}Cr release, caspase 3,7 activation or adenylate kinase release assays (data not shown). A recent study with Tandab investigating redirected lysis of malignant B cells from chronic lymphocytic leukemia patients (Reusch et al., 2004) suggested that Tandab is also active with unstimulated T cells as are present in PBMC cultures, while previous studies with Tandab and diabodies used T lymphocytes pre-stimulated in cell culture with recombinant IL-2 and anti-CD3 monoclonal antibody OKT-3 (Kipriyanov et al., 1999). We confirmed here that Tandab could redirect unstimulated peripheral T cells for lysis of three human B lymphoma/leukemia cell lines. Raji, MEC-1 and Nalm-6 were all lysed in a Tandab concentration-dependent fashion at half maximal concentrations of 1.07, 1.27 and 0.24 nM, respectively (Figs. 4A, 4B and 4C; Tab. 1). We used E:T ratios of 10:1 for Raji and of 5:1 for MEC-1 and Nalm-6 cells. During the 18-hour assay period, between 40 and 80% of target cells were lysed. Nalm-6 cells were most sensitive to lysis, while Raji cells were most resistant.

Under identical assay conditions, MT103 also caused redirected lysis of all three cell lines with unstimulated peripheral T cells. Efficacy of cell lysis was, however, much higher than for the Tandab molecule. Values for half-maximal target cell lysis by MT103 were 0.4, 1.7 and 0.2 pM for Raji, MEC-1 and Nalm-6 target cell lines, respectively (Fig. 4A to C). This corresponds to a 736-2,605 fold higher cytotoxic activity of MT103 (Tab. 1). A larger proportion of MEC-1 cells were lysed by MT103-redirected T cells than by Tandab-redirected T cells, while Raji and Nalm-6 cells were lysed to a similar extent by the two kinds of bispecific antibodies during the 18-h assay period. Three sequence variants of bsc CD19xCD3 showed similar ED_{50} values as MT103 for redirected lysis of Nalm-6 cells with unstimulated T cells (see below).

In the next experiment, cultured T lymphocytes were used as effector cells, which had been stimulated for 4 days with immobilized recombinant OKT-3 and a T cell co-stimulatory agonistic anti-CD28 antibody, and for one day with human IL-2 prior to the cytotoxicity assay. Under these conditions of optimal pre- and co-stimulation of T cells, Tandab now reached close to 100% lysis of Nalm-6 cells, more than 80% of MEC-1 cells and 60% of Raji cells (Figs. 5A to C). Despite an enhanced overall cell lysis, no improvement of ED_{50} values was observed. ED_{50} values were 10.2, 6.0 and 0.24 nM for Raji, MEC-1 and Nalm-6 target cells, respectively (Tab.

1). Rather, there was a clear reduction by 10 and 6 fold in Tandab efficacy with Raji and MEC-1 cells, respectively, while it was unchanged for Nalm-6 cells.

Under identical assay conditions, MT103 reached close to complete lysis by redirecting pre-stimulated peripheral T cells of both MEC-1 and Nalm-6 target cells, and 80% lysis of Raji cells (Figs. 5A to C). Efficacy (ED_{50} values) for redirected target cell lysis with pre-stimulated T cells was improved for MEC-1 and Nalm-6 cells, and somewhat reduced for Raji cells compared to values obtained with unstimulated T cells (Tab. 1). All ED_{50} values of MT103 were at a low pM to fM level. With pre-stimulated T cells, the superiority of MT103 over Tandab was even more pronounced. MT103 was more potent in redirected lysis than Tandab by a factor between 2,218- and 8,062-fold (Tab. 1).

6. The bioactivities of the bsc CD19xCD3 Ab variants were analyzed in a cytotoxicity assay based on calcein release. Cytotoxicity assays were performed with target cells (Nalm-6, human B lymphoid cell line) loaded with Calcein AM (Molecular Probes) using human peripheral blood mononuclear cells (PBMCs) as effector cells. For the labeling of target cells calcein was added in a final concentration of 10 μM to a suspension of $1.5x10^7$ Nalm-6 cells in 5ml medium (RPMI medium with 10% heat-inactivated FCS and 25 mM Hepes) and incubated for 30 min. at 37°C at 5% CO_2. Calcein-loaded Nalm-6 cells ($0.5x10^5$) and human PBMC ($5x10^5$) were incubated with different concentrations of anti-CD19 x anti-CD3 for 4 hrs at 37°C at 5% CO_2 in triplicates. Mixed target and effector cells without addition of bispecific single-chain antibodies were used as controls. Cells were incubated with Saponin (0.1% final concentration) for 15 min in dark at room temperature and Calcein release was measured using a Spectrofluorometer at 535 nM emission. Percentage specific cytotoxicity was calculated according to the following formula: [(Sample value - control) : (maximum lysis – control)] x 100.

Cytotoxic activities of all variants with amino acid substitutions in the anti CD3 (Figure 6) and anti CD19 portion (Figure 7) were comparable to MT103. Both assays were performed with unstimulated human PBMCs as effector cells and Nalm-6 cells as target cells. In Figure 6, bispecific scFv anti EpCAM x anti CD3 was used as negative control. MT103 was used as positive control in comparing the bsc CD19xCD3 Ab variants MB2.1 and MB 4, both containing amino acid substitutions in the V_HCD3. The ED_{50} value of MT103 was 0.065 ng/ml. The ED_{50} values for MB2.1 and MB4 were comparable in magnitude.

In Figure 7, MT103 was also used as a reference molecule in comparison with the bsc CD19xCD3 Ab variant VH19 containing one amino acid substitution in the V_HCD19. The ED_{50} value of MT103 was 0.024 ng/ml. A comparable, even slightly smaller ED_{50} value was obtained for VH19.

Comparable conditions were used in Fig. 4C showing cytotoxic activities of MT103 and Tandab in direct comparison. In Fig. 4C the assay was also performed with Nalm 6 as target cells and with unstimulated human effector cells. The ED_{50} value of MT103 was 0.0156 ng/ml or 0.3 pM. The bioactivities of MT103 obtained in the different experiments were comparable and in the same range of magnitude. In contrast, the ED_{50} value of the Tandab was 28.5 ng/ml or 231 pM.

7. These experiments directly compare bispecific single-chain antibodies with domain arrangement V_LCD19-V_HCD19-V_HCD3-V_LCD3 with other constructs for potency of redirected target cell lysis. V_LCD19-V_HCD19-V_HCD3-V_LCD3 was consistently more active than Tandab and, depending on target cell line and pre-treatment of T cells had ED_{50} values between three and four orders of magnitude improved over Tandab. Tandab was selected since previous studies showed by direct side-by-side comparison that Tandab was more active than CD19/CD3-bispecific diabodies. Accordingly, V_LCD19-V_HCD19-V_HCD3-V_LCD3 is also much more active than these two other well-characterized bispecific antibody formats. In addition, we have characterized multiple V_LCD19-V_HCD19-V_HCD3-V_LCD3 constructs and verified that they all have similar assay activity. These findings underscore the remarkable and unexpected efficacy of the claimed invention in comparison to other modes of antibody treatment.

8. We hereby declare further that all statements made herein of our own knowledge are true and that all statements made on information and belief are believed to be true and further that these statements were made with the knowledge that willful false statements and the like so made are punishable by fine or imprisonment, or both, under Section 1001 of Title 18 of the United States Code and that such willful false statements may jeopardize the validity of the application or any patent issuing thereon.

By: _____ Date: _____
Dr. Patrick A. Baeuerle

By: _____ Date: _____
Dr. Peter Kufer

Sequences for V_LCD19-V_HCD19-V_HCD3-V_LCD3 constructs

MT103 (Also provided in Figure 8 of application)

V_HCD3
DIKLQQSGAELARPGASVKMSCKTSGYTFTRYTMHWVKQRPGQGLEWIGYINPSRGYTNYNQKF
KDKATLTTDKSSSTAYMQLSSLTSEDSAVYYCARYYDDHYCLD YWGQGTTLTVSS
V_LCD3
DIQLTQSPAIMSASPGEKVTMTCRASSSVSYMNWYQQKSGTSPKRWIYDTSKVASGVPYRFSGS
GSGTSYSLTISSMEAEDAATYYCQQWSSNPLTFGAGTKLELK
V_HCD19
QVQLQQSGAELVRPGSSVKISCKASGYAFSSYWMNWVKQRPGQGLEWIGQIWPGDGDTNYNGKF
KGKATLTADESSSTAYMQLSSLASEDSAVYFCARRETTTVGRYYYAMDYWGQGTTVTVSS
V_LCD19
DIQLTQSPASLAVSLGQRATISCKASQSVDYDGDSYLNWYQQIPGQPPKLLIYDASNLVSGIPP
RFSGSGSGTDFTLNIHPVEKVDAATYHCQQSTEDPWTFGGGTKLEIK

MB2.1 (Variations from MT103 are highlighted)

V_HCD3
HVQLQQSGAELARPGASVKMSCKASGYTFTRYTMHWVKQRPGQGLEWIGYINPSRGYNYNQKFK
DKATLTTDKSSSTAYMQLSSLTSEDSAVYYCARYYDDHYCLD YWGQGTTLTVSS

V_LCD3, V_HCD19, and V_LCD19 - Identical to MT103.

MB4 (Variations from MT103 are highlighted)

V_HCD3
VQLQQSGPELVKPGASVKMSCKASGYKFSSSVMHWVKQKPGQGLEWIGYINPYNDVTKTEKFK
GKATLTSDKSSSTAYMEISSLTSEDSAVYFCARSPYYDYDGFAYWGQGTLVTVS

V_LCD3, V_HCD19, and V_LCD19 - Identical to MT103.

VH19 (Variation from MT103 is highlighted)

V_HCD19
QVQLQQSGAELVRPGSSVKISCKASGYAFSSYWMNWVKQRPGQGLEWIGQIWPGDGDTNYNGKF
KGKATLTADESSSTAYMQLSSLASNDSAVYFCARRETTTVGRYYYAMDYWGQGTTVTVSS

V_LCD19, V_HCD3, and V_LCD3 - Identical to MT103.

Summary of Constructs

I. Dörken, *et al.* Originally filed 1998 Bispecific single chain antibody	V_{LCD19} - V_{HCD19} - V_{HCD3} - V_{LCD3}
II. Kipriyanov, *et al.* Publications from 1997/1998 A. Bispecific single chain antibody	V_{LCD3} - V_{HCD3} - V_{LCD19} - V_{HCD19}
B. Non-covalent heterodimer diabody	V_{HCD3} - V_{LCD19} V_{LCD3} - V_{HCD19}
III. Kipriyanov, *et al.* Publication from 1999 Covalent heterodimer diabody (Tandab or tandem diabodies)	V_{HCD3} - V_{LC19} - V_{HCD19} - V_{LCD3} V_{LCD3} - V_{HCD19} - V_{LCD19} - V_{HCD3}

Figure and Table Legends

Figure 1. Primary structure of Tandab. The amino acid one letter code is used. Key structural features such as complementarity determining regions (CDRs) from heavy (H) and light chains (L), the c-myc epitope tag, hexahistidine sequence (6His) and PelB signal peptide for periplasmic expression in *E. coli* are shown underlined. The LL linker sequence is shown in bold.

Figure 2. Biochemical characterization of Tandab. (A) Gel filtration elution profile of imidazole affinity eluate containing Tandab. Absorbance at 280 nM (mAU; solid line), absorbance at 254 nm (gray line) and conductivity (dashed line) of the elution profile from a HiLoad 16/60 Superdex 200 column are shown. The position of the 114-kDa Tandab is marked as fraction I. The elution position of the 57-kDa diabody is marked as fractions II and III. (B) Non-reducing SDS-PAGE of fraction I. Protein was separated on a 4-12% Tris/Bis buffered poly-acrylamide gel, and stained by Coomassie blue. (C) Western blot analysis of fraction I. For immunological detection of Tandab, membranes were incubated with a mouse anti-myc primary antibody and an alkaline phosphatase-conjugated goat anti-mouse IgG Fc-specific secondary antibody. The position of five molecular mass markers is indicated.

Figure 3. Bispecific binding activity of Tandab. Binding of Tandab to human T-leukemic cell-line HP-Ball (A and B) and human B-leukemic cell line Nalm-6 (C and D) was analyzed by flow cytometry at 1 (A and C), 10 μg/mL Tandab (B and D) and a vehicle control (PBS). Cell-bound protein was detected via the His-tag using a mouse Penta-His IgG and a goat anti-mouse IgG-PE. The results are depicted as histograms plotting fluorescence intensity (log) versus relative cell number.

Figure 4. Redirected lysis of three human B lymphoma cell lines by unstimulated human peripheral T cells in the presence of Tandab or MT103. Raji (A), MEC- 1(B) and Nalm-6 (C) lines cells were cocultured with freshly isolated, unstimulated human T cells at E:T ratios of 10:1 (Raji) or 5:1 (MEC-1 and Nalm-6) and incubated at the indicated concentrations of either Tandab (filled circles) or MT103 (filled triangles) for 18 hours. Redirected specific lysis was determined

as percentage of propidium-iodide positive target cells against a control by a flow cytometry-based assay using FKH26 pre-labeled target cells. Bars give standard deviations from triplicate determinations.

Figure 5. Redirected lysis of three human B lymphoma cell lines by pre-stimulated human peripheral T cells in the presence of Tandab or MT103. Raji (A), MEC- 1(B) and Nalm-6 (C) lines cells were co-cultured with pre-stimulated human T cells at E:T ratios of 10:1 (Raji) or 5:1 (MEC-1 and Nalm-6) and incubated at the indicated concentrations of either Tandab (filled circles) or MT103 (filled triangles) for 18 hours. Pre-stimulation of T cells was for 4 days with anti-CD3 and anti-CD28 antibodies and for one day with human IL-2. Redirected specific lysis was determined as percentage of propidium iodide-positive target cells against a control by a flow cytometry-based assay using FKH26 pre-labeled target cells. Bars give standard deviations from triplicate determinations.

Figure 6 Comparison of cytotoxic activities of MT103, MB2.1, MB4, and anti EpCAM x anti CD3 antibodies.

Figure 7 Comparison of Cytotoxic Activity of MT103 and VH19

Table 1. Half-maximal concentrations for redirected target cell lysis by Tandab- and MT103-activated human T cells. ED_{50} values from dose response curves as are shown in Figures 4 and 5 were calculated by a curve fitting software. E:T ratios for Raji cells was 10:1, and for MEC-1 and Nalm-6 cells it was 5:1.

Figure 1

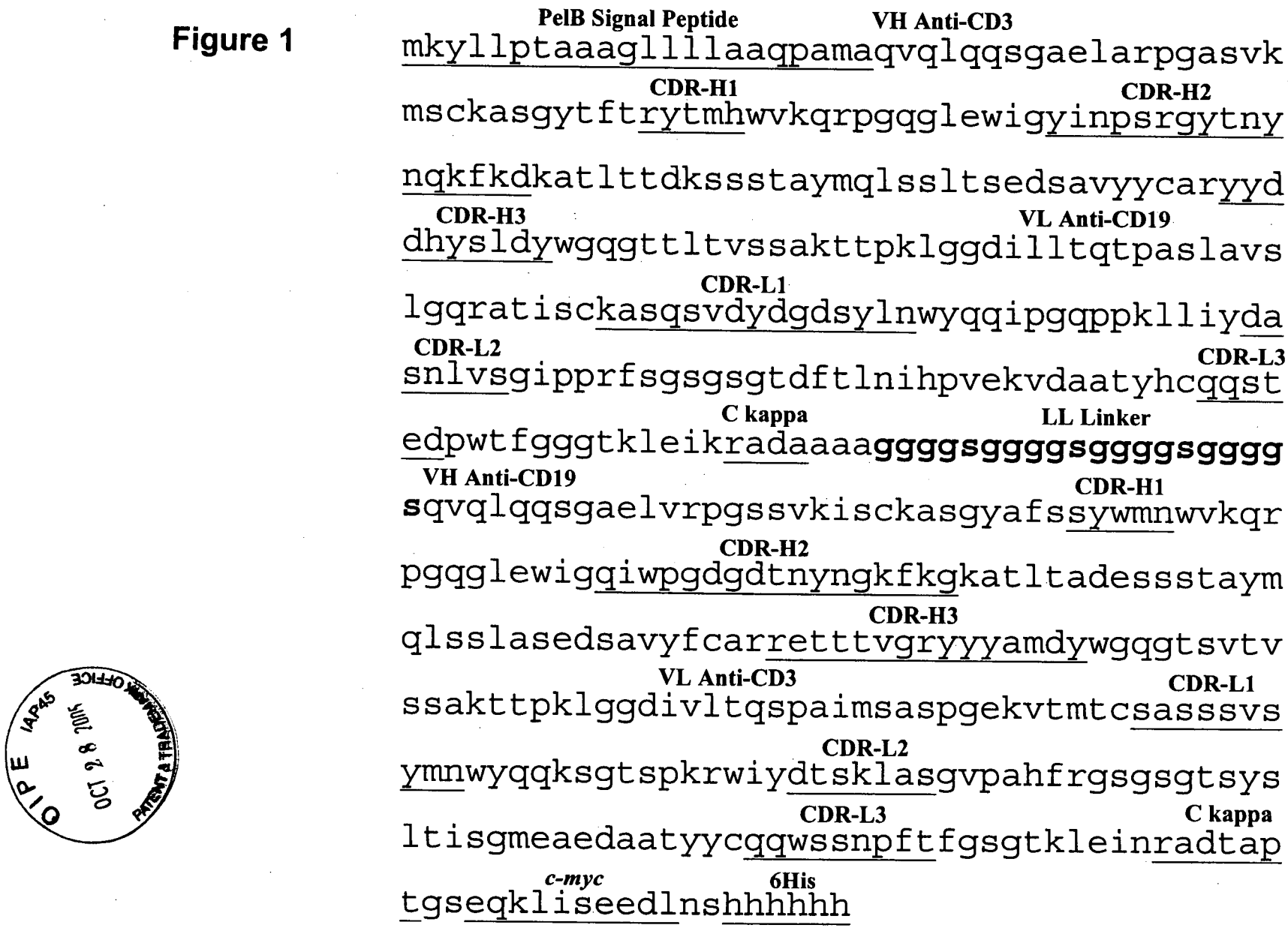

Figure 2

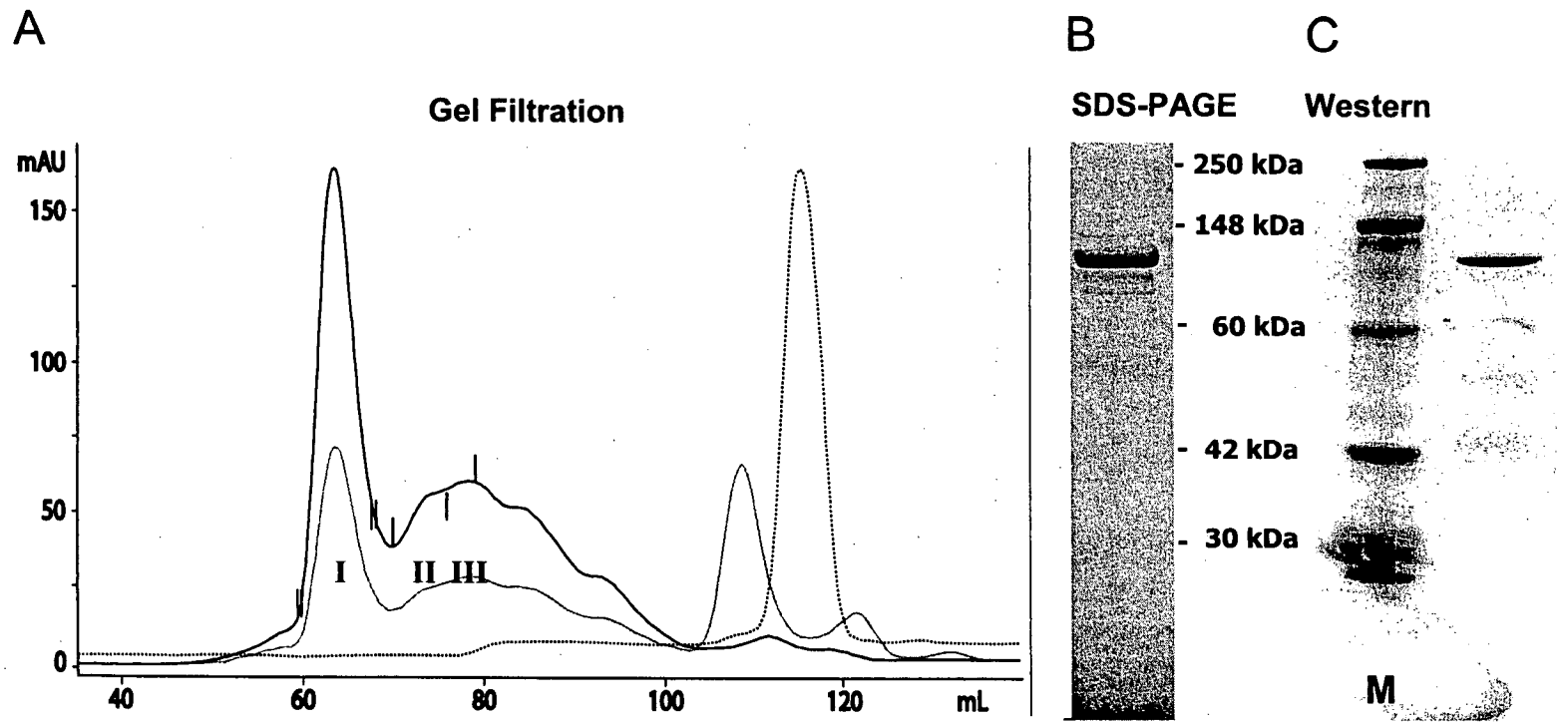

Figure 3

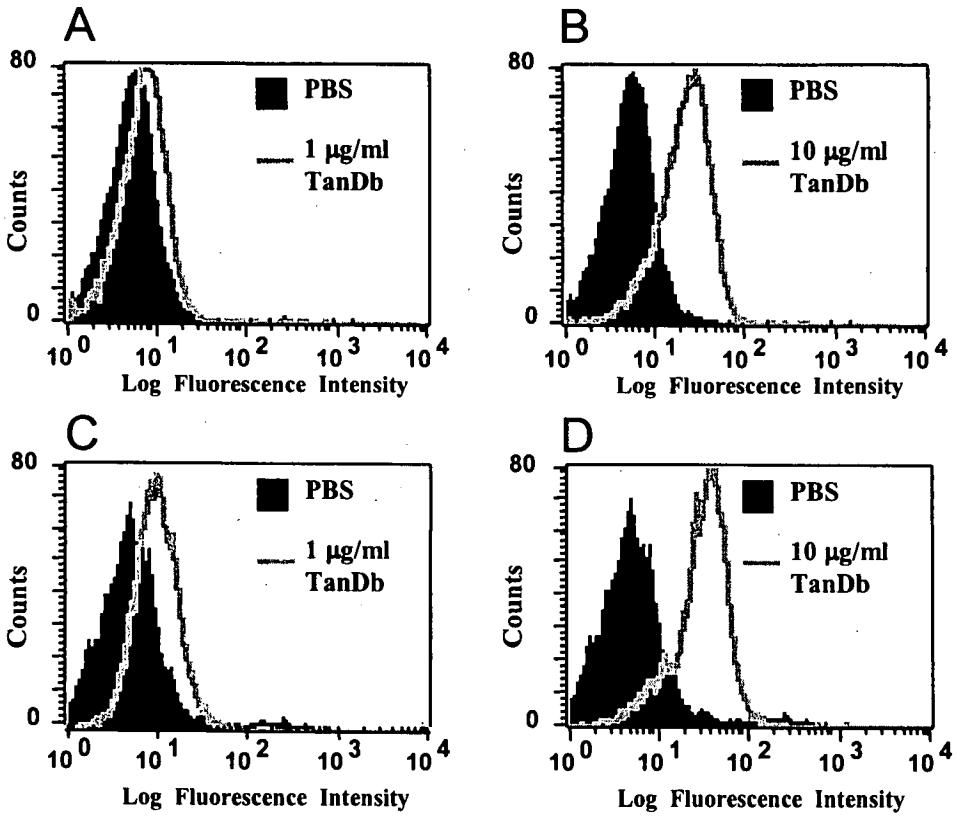

Figure 4

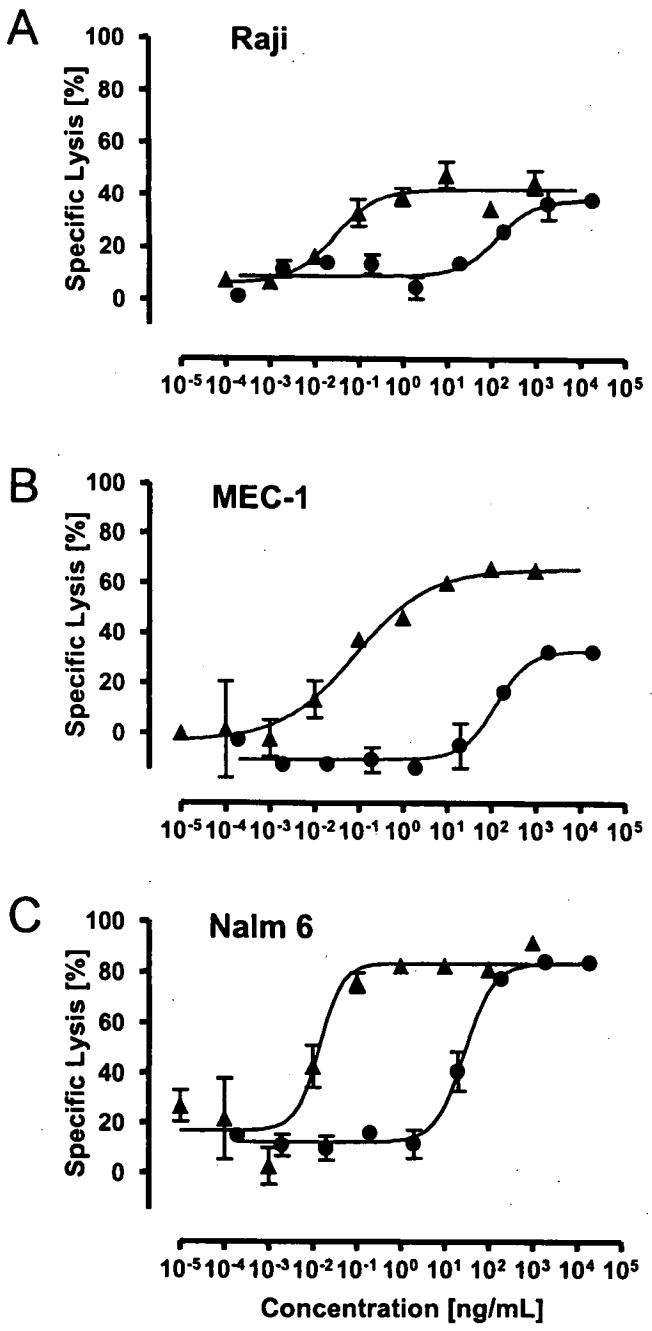

Figure 5

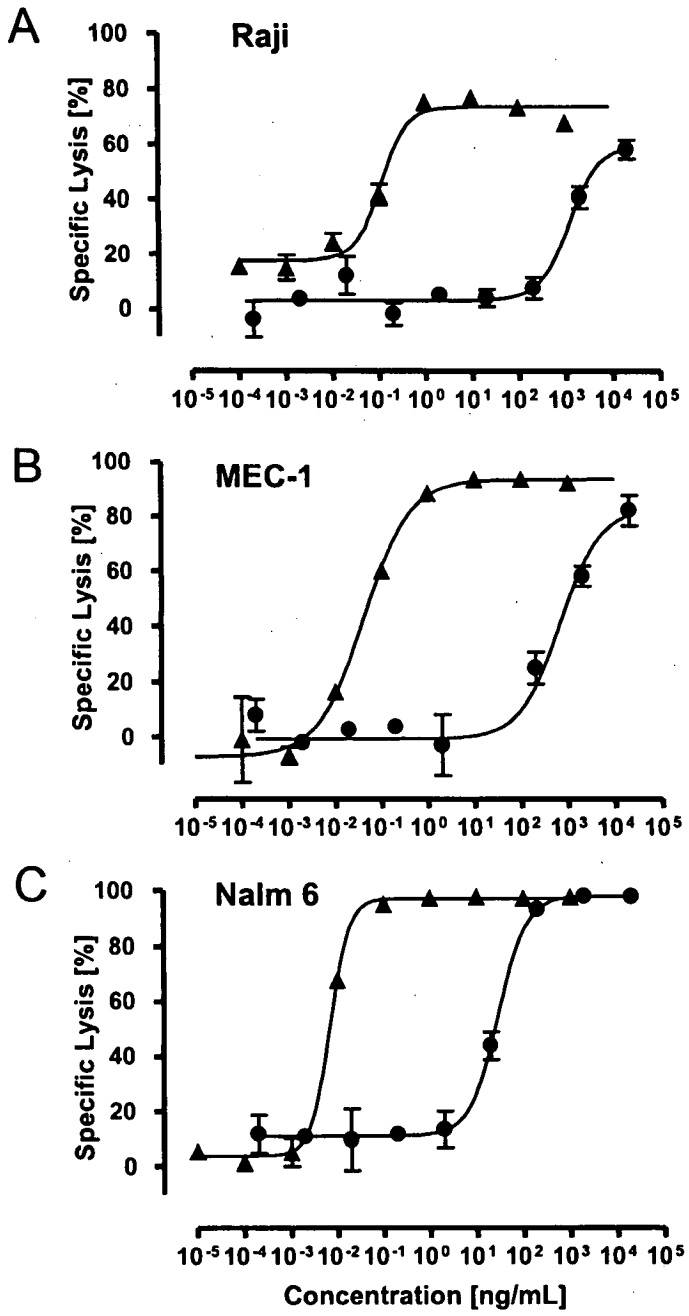

Figure 6

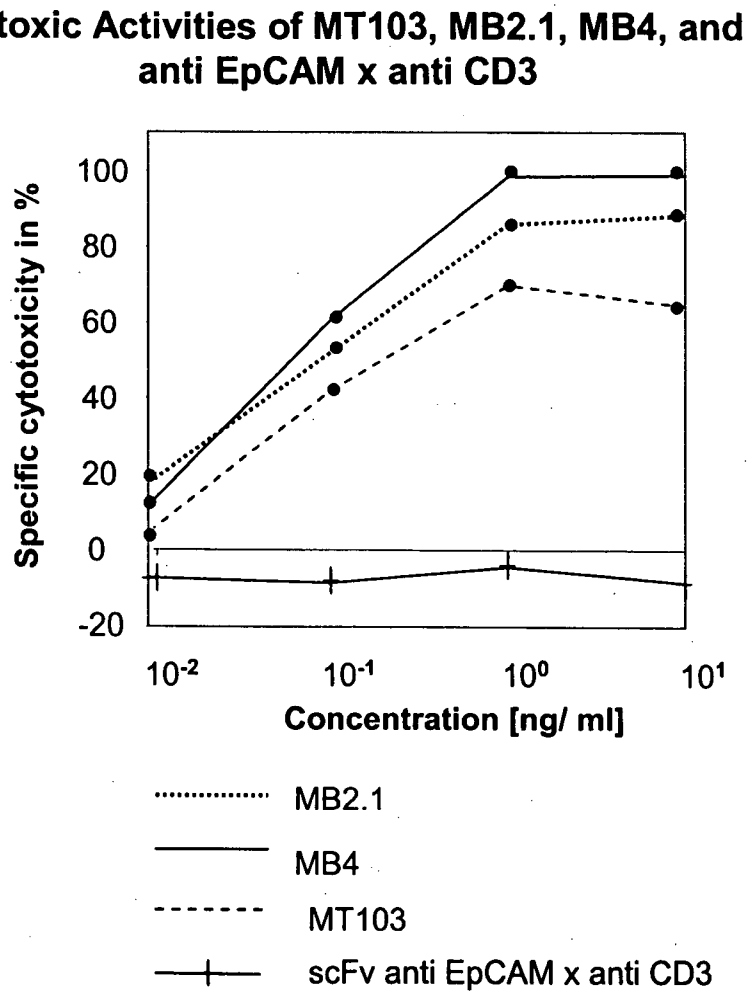

Figure 7

Cytotoxic Activity of MT103 and VH19

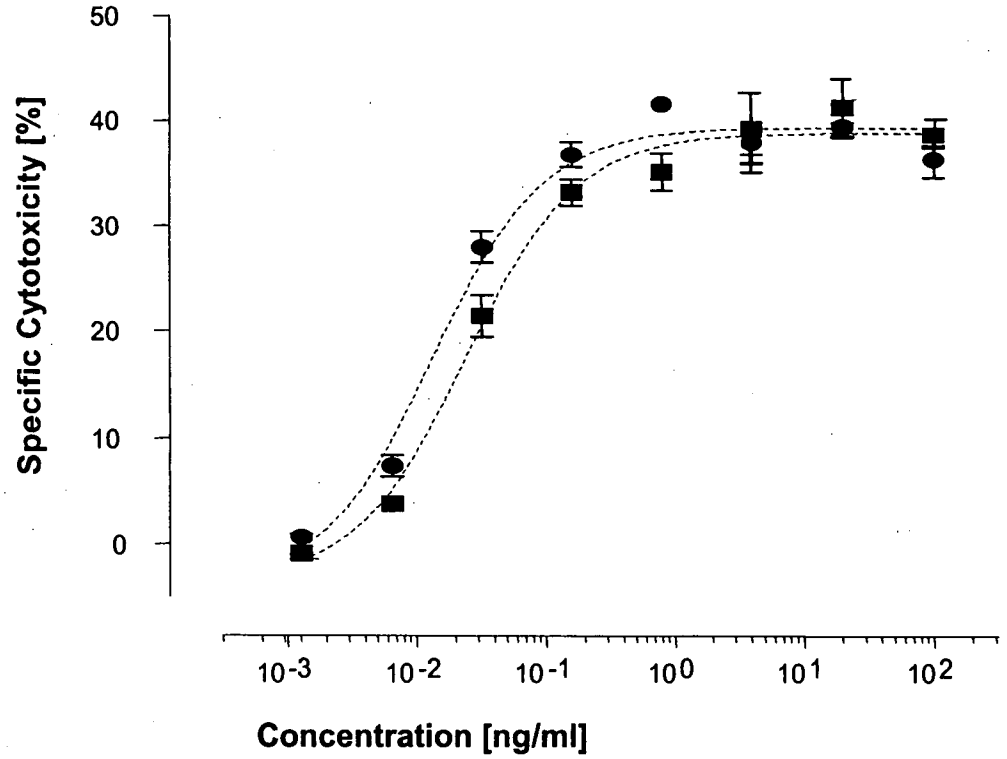

■ MT103 ● VH19

Table 1

Cell Type		E:T Ratio	ED50			
			MT103 [pM] (95% Confidence Interval)	Tandab [pM] (95% Confidence Interval)	Fold Difference	P Value for Difference of log ED50
Unstim. T Cells	Raji	10:1	**0.41** (0.13-1.26)	**1,068** (227-5,032)	**2,605**	**<0.005**
	MEC-1	5:1	**1.73** (0.38-7.90)	**1,273** (580-2,791)	**736**	**<0.0001**
	Nalm-6	5:1	**0.23** (0.12-0.43)	**237** (145-389)	**1,030**	**<0.0001**
Pre-stim. T Cells	Raji	10:1	**1.27** (0.55-2.96)	**10,239** (4,964-21,121)	**8,062**	**<0.0001**
	MEC-1	5:1	**0.88** (0.54-1.43)	**6,005** (1,995-18,079)	**6,824**	**<0.0001**
	Nalm-6	5:1	**0.11** (0.09-0.14)	**244** (146-404)	**2,218**	**<0.0001**

Curriculum vitae

Name	Patrick Alexander Baeuerle
Academic Titles	Honorary Professor of Immunology, Ph.D., M.Sc.
Nationality	German
Date of Birth	November 24, 1957
Place of Birth	Friedrichshafen, Germany
Marrital Status	Married; two children (13 and 17)

Academic Career

1978-1982	**Study of Biology** at University of Konstanz, Germany
1982-1983	**Diploma Work** at the Max-Planck-Institute for Psychiatry, Martinsried, Germany, in the laboratory of Prof. Dr. Wieland B. Huttner (now Director at Max-Planck-Institute for Cell Biology, Dresden).
April 5, 1983	Receival of Diploma (M.Sc.) in Biology from the University of Konstanz
1983-1986	**Study of Biochemistry** at Ludwig-Maximilians-University, Munich with **doctoral work** at the Max-Planck-Institute for Psychiatry, Martinsried, in the laboratory of Prof. Wieland Huttner
1986-1987	Continuation of Ph.D. work at the European Molecular Biology Laboratory (EMBL), Heidelberg, Germany, Cell Biology Program
Febr. 9, 1987	Receival of **Ph.D.** (*summa cum laude*) in Biochemistry from the Ludwig-Maximilians-University, Munich, Germany
1987-1989	**Postdoctorate** at the Whitehead Institute/Massachussetts Institute of Technology (MIT), Cambridge, USA, in the laboratory of Nobel laureate Dr. David Baltimore
1988	Calls as **independent research group leader** to the ZMBH in Heidelberg, the Spemann Laboratory of the Max-Planck-Institute for Immunobiology in Freiburg, and to the Gene Center of the Ludwig-Maximilians-University in Munich
1989-1993	Leader of an independent research group at the Gene Center, Martinsried, Germany
Nov. 28, 1991	**Habilitation** in Biochemistry at the Faculty for Chemistry and Pharmacy of the Ludwig-Maximilians-University, Munich
1992	Tertio loco for position of Professor and Chairman of Biochemistry at the University of Zurich; secundo loco for position of Chairman and Professor at the University of Freiburg
Nov. 23, 1992	**Professor and Chairman of Biochemistry** to the University of Freiburg, Medical School (follower of Prof. Dr. Karl Decker)
Jan. 14, 2000	Nomination as **Honorary Professor of Immunology**, Medical Faculty of the Ludwig-Maximilians-University, Munich

Positions Held

1999-2004	Scientific Advisory Board of the Istituto Scientifica San Raffaele (DIBIT), Milano, Italy (According to *Science* magazine, DIBIT is Italy's premier biomedical research institution)
1992, 1996, 2000	Faculty member of three Spetsai Summer Schools (NATO/FEBS), Island of Spetses, Greece
2002-	Member of the EMBL Alumni Association, Heidelberg, Germany
1998-	*Ad-hoc* consultant for several venture capital firms (e.g., Atlas, Schroeder Ventures, Abingworth, Wellington, Life Science Partners)
2005-	Scientific Advisory Board of the Institute for Multiple Sclerosis Research of the Hertie Foundation, Goettingen, Germany

Editorial Activities

1993-2001	Associate Editor of *Chemistry & Biology* (Cell Press)
1994-1997	Contributing Editor of *Journal of Inflammation*
1994-1998	Editorial Board of the *EMBO Journal*
1994-1998	Editorial Board of *Trends in Cell Biology*
1997-1999	Editorial Board of *Free Radical Biology & Medicine*
1998-2004	Section Editor of *Biochemica et Biophysica Acta*
1995	Editor of *Inducible Gene Expression* Volumes 1 and 2, Birkhäuser
1995-	Editorial Board of *European Cytokine Network*
1998	Editor of *Antioxidant and Redox Regulation of Genes*, Academic Press

Activities as Peer Reviewer

Frequent ad hoc reviewer for the following journals:

EMBO J., Nature, Cell, Immunity, Science, J. Biol. Chem., J. Immunol., J. Clin. Invest., Mol. Cell. Biol., Trends in Cell. Biol., Proc. Natl. Acad. Sci. USA, J. Neurosc., Intl. J. Cancer

and others

Reviewer for the following research funding organizations:

Deutsche Forschungsgemeinschaft, Swiss National Fonds, Leukemia Society, Medical Research Council, The Wellcome Trust, European Community, EMBO, Human Science Frontier Program

Meeting Organizations

10/1993	First Banbury Conference on "κB-binding Proteins", Cold Spring Harbor, USA
09/1994	First EMBL Conference on Transcription, Heidelberg, Germany
09/1994	First European Community Biotechnology Workshop on "Cytokine Gene Expression by NF-κB/Rel Factors", Freiburg, Germany
01/1998	Member of the International Scientific Committee organizing the 4th World Congress on "Inflammation" in Paris, France (June 1999)
02/1999	Workshop on "Minimal Residual Disease", Ringberg Castle, Tegernsee, Germany

List of Publications

Patrick A. Baeuerle

1. Tiggemann, R., H. Plattner, I. Rashed, P.A. Baeuerle and E. Wachter (1981). Quantitative data on peroxidatic markers for electron microscopy. *J. Histochem. Cytochem.* **29**: 1387-1396

2. Baeuerle, P.A. and W.B. Huttner (1984). Inhibition of N-glycosylation induces tyrosine sulfation of hybridoma immunoglobulin G. *EMBO J.* **3**: 2209-2215

3. Baeuerle, P.A. and W.B. Huttner (1985). Tyrosine sulfation of yolk proteins 1, 2 and 3 in *Drosophila melanogaster*. *J. Biol. Chem.* **260**: 6434-6439

4. Baeuerle, P.A. and W.B. Huttner (1986). Chlorate - a potent inhibitor of protein sulfation in intact cells. *Biochem. Biophys. Res. Commun.* **141**: 870-877

5. Benedum, U.M., P.A. Baeuerle, D.S. Konecki, R. Frank, J. Powell, J. Mallet and W.B. Huttner (1986). The primary structure of chromogranin A: a representative of a class of acidic secretory proteins common to a variety of peptidergic cells. *EMBO J.* **5**: 1495-1502

6. Huttner, W.B., P.A. Baeuerle, U.M. Benedum, E. Friederich, A. Hille, R.W.H. Lee, P. Rosa, U. Seydel and C. Suchanek (1986). Protein sulfation on tyrosine. In *Hormones and Cell Regulation* (J. Nunez, ed.), Colloque INSERM/John Libbey Eurotext Ltd. **139**: 199-217

7. Baeuerle, P.A. and W.B. Huttner (1987). Tyrosine sulfation is a trans Golgi-specific protein modification. *J. Cell. Biol.* **105**: 2655-2664

8. Benedum, U.M., A. Lamouroux, D.S. Konecki, P. Rosa, A. Hille, P.A. Baeuerle, R. Frank, F. Lottspeich, J. Mallet and W.B. Huttner (1987). The primary structure of human secretogranin I/chromogranin B: comparison with chromogranin A reveals homologous terminal domains and a large intervening variable region. *EMBO J.* **6**: 1203-1211

9. Huttner, W.B. and P.A. Baeuerle (1988). Sulfation of proteins on tyrosine. In *Modern Cell Biology* (B. Satir, ed.) **6**: 97-140

10. Baeuerle, P.A., F. Lottspeich and W.B. Huttner (1988). Purification of yolk protein 2 of *Drosophila melanogaster* and determination of its site of tyrosine sulfation. *J. Biol. Chem.* **263**: 14925-14929

11. Friederich, E., P.A. Baeuerle, H. Garoff, B. Hovemann and W. B. Huttner (1988). Expression, tyrosine sulfation and secretion of yolk protein 2 of *Drosophila melanogaster* in mouse fibroblasts. *J. Biol. Chem.* **263**: 14930-14938

12. Gerdes, H.-H., P. Rosa, E. Pillips, P.A. Baeuerle, R. Frank, P. Argos and W.B. Huttner (1989). The primary structure of human secretogranin II, a widespread tyrosine-sulfated secretory protein that exhibits low pH- and calcium-induced aggregation. *J. Biol. Chem.* **264**: 12009-12015

13. Baeuerle, P.A. and D. Baltimore (1988). Activation of DNA-binding in an apparently cytoplasmic precursor of the NF-κB transcription factor. *Cell* **53**: 211-217

14. Baeuerle, P.A. and D. Baltimore (1988). Activation of NF-κB - a transcription factor controlling expression of the κ light chain gene and HIV. In *The Control of Human Retrovirus Gene Expres-*

sion (B.R. Franza, B.R. Cullen and F. Wong-Staal, eds.) Cold Spring Harbor Laboratory, 217-226

15. Baeuerle, P.A., M. Lenardo, J.W. Pierce and D. Baltimore (1988). Phorbol ester-induced activation of the NF-κB transcription factor involves dissociation of an apparently cytoplasmic NF-κB/inhibitor complex. *Cold Spring Harbor Symp. Quant. Biol.* **53**: 786-798

16. Baeuerle, P.A. and D. Baltimore (1988). IκB: a specific inhibitor of the NF-κB transcription factor. *Science* **242**: 540-546

17. Baeuerle, P.A. and D. Baltimore (1989). A 65-kD subunit of active NF-κB is required for inhibition of NF-κB by IκB. *Genes Dev.* **3**: 1689-1698

18. Schreck, R. and P.A. Baeuerle (1990). NF-κB as inducible transcriptional activator of the granulocyte/macrophage colony stimulating factor gene. *Mol. Cell. Biol.* **10**: 1281-1286

19. Collart, M.A., P.A. Baeuerle and P. Vassalli (1990). Regulation of tumor necrosis factor alpha transcription in macrophages: involvement of four κB-like motifs and of constitutive and inducible forms of NF-κB. *Mol. Cell. Biol.* **10**: 1498-1506

20. Zabel, U. and P.A. Baeuerle (1990). Purified human IκB can rapidly dissociate the complex of the NF-κB transcription factor with its cognate DNA. *Cell* **61**: 255-265

21. Kieran, M., V. Blank, F. Logeat, J. Vandekerckhove, F. Lottspeich, O. Le Bail, M.B. Urban, P. Kourilsky, P.A. Baeuerle and A. Israël (1990). The DNA binding subunit of NF-κB is identical to factor KBF1 and homologous to the *rel* oncogene product. *Cell* **62**: 1007-1018

22. Urban, M.B. and P.A. Baeuerle (1990). The 65-kD subunit of NF-κB is a receptor for IκB and modulator of DNA binding specificity. *Genes Dev.* **4**: 1975-1984

23. Schreck, R., H. Zorbas, E.-L. Winnacker and P.A. Baeuerle (1990). The NF-κB transcription factor induces DNA bending which is modulated by its 65 kD subunit. *Nucl. Acids Res.* **18**: 6497-6502

24. Messer, G., E. Weiss and P.A. Baeuerle (1990). TNF-β induces binding of the NF-κB transcription factor to a high affinity κB motif in the TNF-β promoter. *Cytokine* **2**: 1-9

25. Hohmann, H.-P., M. Brockhaus, P.A. Baeuerle, R. Remy, R. Kolbeck and A.P.G.M. van Loon (1990). Expression of the types A and B receptors is independently regulated and both receptors mediate activation of the transcription factor NF-κB. *J. Biol. Chem.* **265**: 22409-22417

26. Haas, J.G., P.A. Baeuerle, G. Riethmüller and H.W.L. Ziegler-Heitbrock (1990). Molecular mechanism in downregulation of TNF expression. *Proc. Natl. Acad. Sci. USA* **87**: 9563-9567

27. Zabel, U., R. Schreck and P.A. Baeuerle (1991). DNA binding of purified transcription factor NF-κB: affinity, specificity, Zn dependence and differential half site recognition. *J. Biol. Chem.* **266**: 252-260

28. Baeuerle, P.A. and D. Baltimore (1991). The physiology of the NF-κB transcription factor. In *Molecular Aspects of Cellular Regulation Vol. 6*, Hormonal Control Regulation of Gene Transcription (P. Cohen and J.G. Foulkes, eds.) Elsevier/North Holland Biomedical Press, pp. 409-432

29. Rattner, A., M. Korner, H. Rosen, P.A. Baeuerle and Y. Citri (1991). NF-κB activates proenkephalin transcription in T lymphocytes. *Mol. Cell. Biol.* **11**: 1017-1022

30. Ruben, S., P.J. Dillon, R. Schreck, T. Henkel, C.-H. Chen, M. Maher, P.A. Baeuerle and C. Rosen (1991). Isolation of a *rel*-related human cDNA that potentially encodes the 65-kD subunit of NF-κB. *Science* **251**: 1490-1493

31. Baeuerle, P.A. (1991). The inducible transcription activator NF-κB: regulation by distinct protein subunits. *Biochem. Biophys. Acta, Reviews on Cancer* **1072**: 63-80

32. Urban, M.B. and P.A. Baeuerle (1991). The role of the p50 and p65 subunit of NF-κB in the recognition of cognate sequences. *The New Biologist* **3**: 279-288

33. Urban, M.B., R. Schreck and P.A. Baeuerle (1991). NF-κB contacts DNA by a heterodimer of the p50 and p65 subunit. *EMBO J.* **10**: 1817-1825

34. Schreck, R., P. Rieber and P.A. Baeuerle (1991). Reactive oxygen intermediates as apparently widely used messengers in the activation of the NF-κB transcription factor and HIV-1. *EMBO J.* **10**: 2247-2258

35. Schwemmle, S., D. Bevec, G. Brem, M.B. Urban, P.A. Baeuerle and E.H. Weiss (1991). Developmental and tissue-specific expression of the Q5k gene. *Immunogenetics* **34**: 28-38

36. Nigg, E., P.A. Baeuerle and R. Lührmann (1991). Nuclear import-export: in search of signals and mechanisms. *Cell* **66**: 15-22

37. Schreck, R. and P.A. Baeuerle (1991). A role of oxygen radicals as second messengers. *Trends Cell Biol.* **1**: 39-42

38. Kerr, L.D., I.-J. Inoue, N. Davis, E. Link, P.A. Baeuerle, H.R. Bose Jr. and I.M. Verma (1991). The rel-associated pp40 protein prevents DNA binding of rel and NF-κB: relationship with IκB-β and regulation by phosphorylation. *Genes Dev.* **5**: 1464-1476

39. Schmitz, M.L., T. Henkel and P.A. Baeuerle (1991). Proteins controlling the nuclear uptake of NF-κB, Rel and Dorsal. *Trends Cell Biol.* **1**: 130-137

40. Schmitz, M.L. and P.A. Baeuerle (1991). The p65 subunit is responsible for the strong transactivating potential of NF-κB. *EMBO J.* **10**: 3805-3817

41. Hansen, S.K., C.V. Nerlov, U. Zabel, P. Verde, M. Johnsen, P.A. Baeuerle and F. Blasi (1992). A novel complex between the p65 subunit of NF-κB and c-Rel binds to a DNA element involved in the phorbol ester induction of the human urokinase gene. *EMBO J.* **11**: 205-213

42. Link, E., L.D. Kerr, R. Schreck, U. Zabel, I. Verma and P.A. Baeuerle (1992). Purified IκB-β is inactivated upon dephosphorylation. *J. Biol. Chem.* **267**: 239-246

43. Henkel, T., U. Zabel, K. van Zee, J. Müller, E. Fanning and P.A. Baeuerle (1992). Intramolecular masking of the nuclear location signal and dimerization motif in the precursor of the p50 NF-κB subunit. *Cell* **68**: 1121-1133

44. Brach, M.A., F. Herrmann, Y. Hamada, P.A. Baeuerle and D.W. Kufe (1992). Identification of NF-jun, a novel inducible transcription factor that regulates c-jun gene transcription. *EMBO J.* **11**: 1479-1486

45. Schreck, R., B. Meier, D. Männel, W. Dröge and P.A. Baeuerle (1992). Dithiocarbamates as potent inhibitors of NF-κB activation in intact cells. *J. Exp. Med.* **175**: 1181-1194

46. Meyer, M., W.H. Caselmann, V. Schlüter, R. Schreck, P.H. Hofschneider and P.A. Baeuerle (1992). Hepatitis B virus transactivator MHBst: activation of NF-κB, selective inhibition by antioxidants and integral membrane localization. *EMBO J.* **11**: 2992-3001

47. Schreck, R., R. Grassmann, B. Fleckenstein and P.A. Baeuerle (1992). Antioxidants selectively suppress activation of NF-κB by human T cell leukemia virus type I protein Tax. *J. Virol.* **66**: 6288-6293

48. Lattion, A.-L., P. Reichenbach, E. Espel, C. Fromenthal, A. Israël, P.A. Baeuerle and M. Nabholz (1992). Characterization of a new tissue-specific transcription factor binding to the SV40 enhancer TC-II (NF-κB) element. *Mol. Cell. Biol.* **12**: 5217-5222

49. Schreck, R., D. Bevec, P. Dukor, P.A. Baeuerle, L. Chedid and G.M. Bahr (1992). Selection of a muramyl peptide based on its lack of activation of nuclear factor-κB as a potential adjuvant for AIDS vaccines. *Clin. Exp. Immunol.* **90**, 188-193

50. Kerr, L.D., C.S. Duckett, P. Wamsley, Q. Zhang, P. Chiao, G. Nabel, T.W. McKeithan, P.A. Baeuerle and I.M. Verma (1992). The proto-oncogene Bcl-3 encodes an IκB protein. *Genes Dev.* **6**: 2352-2363

51. Schreck, R., K. Albermann and P.A. Baeuerle (1992). NF-κB: an oxidative stress-responsive transcription factor of eukaryotic cells (a review). *Free Rad. Res. Comms.* **17**: 221-237

52. Zabel, U., T. Henkel, M.A. dos Santos Silva and P.A. Baeuerle (1993). Nuclear uptake control of NF-κB by MAD-3, an IκB protein present in the nucleus. *EMBO J.* **12**: 201-211

53. Grimm, S. and P.A. Baeuerle (1993). The inducible transcription factor NF-κB: structure/ function relationship of its protein subunits. *Biochem. J.* **290**: 297-308

54. Müller, J.M., H.W.L. Ziegler-Heitbrock and P.A. Baeuerle (1993). Nuclear factor kappa B: a mediator of lipopolysaccharide effects. *Immunobiology* **187**: 233-256

55. Meyer, M., R. Schreck and P.A. Baeuerle (1993). H_2O_2 and antioxidants have opposite effects on activation of NF-κB and AP-1 in intact cells: AP-1 as secondary antioxidant-responsive factor. *EMBO J.* **12**: 2005-2015

56. Costello, R.T., C.B. Lipsey, M.V. Algarte, P.A. Baeuerle, D.M. Olive and J.C. Imbert (1993). Activation of primary human T lymphocytes through CD2+CD28 adhesion molecules induces long-term nuclear expression of NF-κB. *Cell Growth Diff.* **4**: 329-339

57. Henkel, T., M.L. Schmitz and P.A. Baeuerle (1993). Rapid characterization of λ cDNA clones after amplification and radioactive labeling with the PCR technique. *BioTechniques* **14**: 906-908

58. Plaksin, D., P.A. Baeuerle and L. Eisenbach (1993). KBF1 (p50 NF-κB homodimer) acts as repressor of H-2K^b gene expression in metastatic tumor cells (1993). *J. Exp. Med.* **177**: 1651-1662

59. Henkel, T., T. Machleidt, I. Alkalay, M. Krönke, Y. Ben-Neriah and P.A. Baeuerle (1993). Rapid proteolysis of IκB-α is necessary for activation of transcription factor NF-κB. *Nature* **365**: 182-185

60. Ziegler-Heitbrock, H.W.L., T. Sternsdorf, J. Liese, B. Belohradsky, C. Weber, A. Wedel, R. Schreck, P.A. Baeuerle and M. Ströbel (1993). Pyrrolidinedithiocarbamate inhibits NF-κB mobilization and TNF production in human monocytes. *J. Immunol.* **151**: 6986-6993

61. Kaltschmidt, C., B. Kaltschmidt and P.A. Baeuerle (1993). Brain synapses contain inducible forms of the transcription factor NF-κB. *Mech. Dev.* **43**: 135-147

62. Henkel, T. and P.A. Baeuerle (1993). Rapid functional analysis of mutated cDNA clones by direct use of PCR products in in vitro transcription/translation reactions. *Analytical Biochemistry* **214**: 351-352

63. Kaltschmidt, B., P.A. Baeuerle and C. Kaltschmidt (1993). Potential role of transcription factor NF-κB in neurological disorder. Interdisciplinary Review. *Journal Molecular Aspects of Medicine*, Pergamon Press **14**: 171-190

64. Costello, R., C. Cerdan, C. Lipcey, M. Algarté, Y. Martin, P.A. Baeuerle, D. Olive and J. Imbert (1993). The role of NF-κB p50/p105 gene expression in activation of human blood T lymphocytes via CD2 and CD28 adhesion molecules. *Cell Growth Diff.* **4**: 947-954

65. Schreck, R. and P.A. Baeuerle (1994). Methods of assessing oxygen radicals as mediators in the activation of inducible eukaryotic transcription factor NF-κB. *Methods Enzymol.* **234**: 151-163

66. Meyer, M., R. Schreck, J.M. Müller and P.A. Baeuerle (1994). Redox control of gene expression by eukaryotic transcription factors NF-κB, AP-1 and SRF. In: *Oxidative Stress on Cell Activation and Viral Infection* (C. Pasquier et al., ed.). Birkhäuser Verlag, Basel, pp. 217-235

67. Baeuerle, P.A. and T. Henkel (1994). Function and activation of NF-κB in the immune system. *Annu. Rev. Immunol.* **12**: 141-179

68. Hansen, S.K., P.A. Baeuerle and F. Blasi (1994). Purification, reconstitution and IκB association of the c-Rel-p65(RelA) complex, a strong activator of transcription. *Mol. Cell. Biol.* **14**: 2593-2603

69. Kaltschmidt, C., B. Kaltschmidt, H. Neumann, H. Wekerle and P.A. Baeuerle (1994). Constitutive NF-κB activity in neurons. *Mol. Cell. Biol.* **14**: 3981-3992

70. Machleidt, T., K. Wiegmann, T. Henkel, S. Schütze, P.A. Baeuerle and M. Krönke (1994). Sphingomyelinase activates proteolytic IκB-α degradation in a cell-free system. *J. Biol. Chem.* **269**: 13760-13765

71. Grimm, S. and P.A. Baeuerle (1994). Failure of splicing variant p65Δ of the p65 NF-κB subunit to transform fibroblasts. *Oncogene* **9**: 2391-2398

72. Ziegler-Heitbrock, H.W.L., A. Wedel, W. Schraut, M. Ströbel, P. Wendelgass, T. Sternsdorf, P.A. Baeuerle, J.G. Haas and G. Riethmüller (1994). Tolerance to lipopolysaccharide involves mobilization of nuclear factor κB with predominance of p50 homodimers. *J. Biol. Chem.* **269**: 17001-17004

73. Pahl, H.L. and P.A. Baeuerle (1994). Oxygen and the control of gene expression. *Bioessays* **16**: 497-502

74. Meyer, M., H.L. Pahl and P.A. Baeuerle (1994). Regulation of the transcription factors NF-κB and AP-1 by redox changes. *Chemico-Biological Interactions* **91**: 91-100

75. Schmitz, M.L. and P.A. Baeuerle (1994). A vector, pHisGal, allowing bacterial production of proteins fused to a hexahistidine-tagged Gal4 DNA-binding domain. *Biotechniques* **17**: 714-718

76. Kaltschmidt, C., B. Kaltschmidt, J. Lannes-Vieira, G. Kreuzberg, H. Wekerle, P.A. Baeuerle and J. Gehrmann (1994). Activation of transcription factor NF–κB in microglia during experimental autoimmune encephalomyelitis. *J. Neuroimmunol.* **55**: 99-106

77. Schmitz, M.L., M.A. dos Santos Silva, H. Altmann, M. Czisch, T.A. Holak and P.A. Baeuerle (1994). Structural and functional analysis of the NF–κB p65 C-terminus: an acidic and modular transactivation domain with the potential to adopt an α-helical conformation. *J. Biol. Chem.* **269**: 25613-25620

78. Frankenberger, M., A. Pforte, T. Sternsdorf, B. Passlick, P.A. Baeuerle and H.W.L. Ziegler-Heitbrock (1994). Constitutive nuclear NF–κB in cells of the monocyte lineage. *Biochem. J.* **304**: 87-94

79. Traenckner, E.B.-M., S. Wilk and P.A. Baeuerle (1994). A proteasome inhibitor prevents activation of NF–κB and stabilizes a newly phosphorylated form of IκB-α that is still bound to NF–κB. *EMBO J.* **13**: 5433-5441

80. Los, M., W. Dröge, K. Stricker, P.A. Baeuerle and K. Schulze-Osthoff (1995). Hydrogen peroxide as a potent activator of T lymphocyte functions. *Eur. J. Immunol.* **25**: 159-165

81. Kaltschmidt, C., B. Kaltschmidt, T. Henkel, H. Stockinger and P.A. Baeuerle (1995). Selective recognition of the activated form of transcription factor NF–κB by a monoclonal antibody. *Biol. Chem. Hoppe-Seyler* **376**: 9-16

82. Pahl, H. and P.A. Baeuerle (1995). Expression of influenza hemagglutinin activates transcription factor NF–κB. *J. Virol.* **69**: 1480-1484

83. Schmidt, K.N., P. Amstad, P. Cerutti and P.A. Baeuerle (1995). The roles of hydrogen peroxide and superoxide as messengers in the activation of transcription factor NF–κB. *Chem.& Biol.* **2**: 13-22

84. Baeuerle, P.A. (1995). Enter a polypeptide messenger (News and Views). *Nature* **373**: 661-662

85. Schmitz, M.L., G. Stelzer, H. Altmann, M. Meisterernst and P.A. Baeuerle (1995). Interaction of the C-terminal transactivation domain of p65 NF–κB with TBP, TFIIB and coactivators. *J. Biol. Chem.* **270**: 7219-7226

86. Los, M., M. van de Craen, L. Penning, H. Schenk, M. Westendorp, P.A. Baeuerle, W. Dröge, P.H. Krammer, W. Fiers and K. Schulze-Osthoff (1995). Requirement of an ICE/CED-3 protease for Fas/APO-1-mediated apoptosis. *Nature* **375**: 81-83

87. Pahl, H.L. and P.A. Baeuerle (1995). A novel signal transduction pathway from the endoplasmatic reticulum to the nucleus is mediated by transcription factor NF–κB. *EMBO J.*, **14**: 2580-2588

88. Traenckner, E.B.-M., H.L. Pahl, K.N. Schmidt, S. Wilk and P.A. Baeuerle (1995). Phosphorylation of human IκB-α on serines 32 and 36 controls IκB-α proteolysis and NF-κB activation in response to diverse stimuli. *EMBO J.* **14**: 2876-2883

89. Tran-Thi, T.A., K. Decker and P.A. Baeuerle (1995). Activation of NF–κB and AP-1 in rat Kupffer cells. In: *Falk Symposium 78: Cytokines and Liver* (K. Decker, W. Gerok, V. Groß, T. Andus, eds.) Kluwer Academic Publishers Dordrecht, pp. 31-36

90. Schmitz, M.L. and Baeuerle, P.A. (1995). Signal transduction from the cytoplasm to the cell nucleus by NF–κB/Rel transcription factors. In: *Signalling Mechanisms - From Transcription Factors to Oxidative Stress*. NATO ASI Series (L. Packer and K. Wirtz, eds.) Springer-Verlag Berlin Heidelberg, pp. 279-303

91. Büning, H., P.A. Baeuerle and H. Zorbas (1995). A new interference footprinting method for analysing simultaneously protein contacts to phosphate and guanine residues on DNA. *Nucl. Acids Res.* **23**: 1443-1444

92. Schmitz, M.L., M.A. dos Santos Silva and P.A. Baeuerle (1995). Transactivation domain 2 (TA_2) of p65 NF–κB: similarity to TA_1 and phorbol ester-stimulated activity and phosphorylation in intact cells. *J. Biol. Chem.* **270**: 15576-15584

93. Schmitz, M.L. and P.A. Baeuerle (1995). Multi-step activation of NF–κB/Rel transcription factors. *Immunobiol.* **193**: 116-127

94. Los, M., H. Schenk, K. Hexel, P.A. Baeuerle, W. Dröge and K. Schulze-Osthoff (1995). IL-2 gene expression and NF–κB activation through CD28 requires reactive oxygen production by 5-lipoxygenase. *EMBO J.* **14**: 3731-3740

95. Tran-Thi, T.A., K. Decker and P.A. Baeuerle (1995). Differential activation of transcription factors NF–κB and AP-1 in rat liver macrophages. *Hepatology* **22**: 613-619

96. Schulze-Osthoff, K., M. Los and P.A. Baeuerle (1995). Redox signaling by transcription factors NF–κB and AP-1 in lymphocytes. *Biochem. Pharmacol.* **50**: 735-741

97. Kaltschmidt, C., B. Kaltschmidt and P.A. Baeuerle (1995). Stimulation of ionotropic glutamate receptors activates transcription factor NF–κB in primary neurons. *Proc. Natl. Acad. Sci. USA* **92**: 9618-9622

98. Schmidt, K.N., E. B.-M. Traenckner, B. Meier and P.A. Baeuerle (1995). Induction of oxidative stress by okadaic acid is required for activation of transcription factor NF–κB. *J. Biol. Chem.* **270**: 27136-27142

99. Bierhaus, A., Y. Zhang, Y. Deng, N. Mackman, P. Quehenberger, M. Haase, T. Luther, M. Müller, H. Böhrer, J. Greten, E. Martin, P.A. Baeuerle, R. Waldherr, W. Kisiel, R. Ziegler, D.M. Stern and P.P. Nawroth (1995). Mechanism of the TNF-α mediated induction of endothelial tissue factor. *J. Biol. Chem.* **270**: 26419-26432

100. Pahl, H.L. and P.A. Baeuerle (1996). Identification of transcription factors and their target genes. In: *Meth. Mol. Genet.* (K.W. Adolph, ed.) Academic Press, San Diego, **8**: 278-297

101. Traenckner, E.B.-M. and P.A. Baeuerle (1995). Appearance of apparently ubiquitin-conjugated forms of IκB–α during its phosphorylation-induced degradation in intact cells. *J. Cell Sci.*, Suppl. **19**: 79-84

102. Rupec, R.A. and P.A. Baeuerle (1995). The genomic response of tumor cells to hypoxia and reoxygenation: differential activation of transcripton factors AP-1 and NF-κB. *Eur. J. Biochem.* **234**: 632-640

103. Schmitz, M.L. and P.A. Baeuerle (1996). Bacterial expression, purification and potential use of His-tagged GAL4 fusion proteins. *Methods Mol. Biol.* **63**: 129-137

104. Schulze-Osthoff, K. and P.A. Baeuerle (1998). Regulation of gene expression by oxidative stress. In *Oxyradicals in Molecular Biology* (J.M. McCord, ed.), JAI Press Inc. Greenwich, *Adv. Mol. Cell Biol.* **25**: 15-44

105. Munroe, D.G., E.Y. Wang, J.P. MacIntyre, S.S.C. Tam, D.H.S. Lee, G.R. Taylor, L. Zhou, R.K. Plante, S.M.I, Kazmi, P.A. Baeuerle and C.Y. Lau (1995). Novel intracellular signaling funtion of prostaglandin H synthase-1 in NF-κB activation. *J. Inflamm.* **45**: 260-268

106. Rein, T., R. Schreck, W. Willenbrink, W.J. Neubert, H. Zorbas and P.A. Baeuerle (1995). A conserved high-affinity NF-κB binding site in the interferon regulatory factor-1 promoter is not occupied by NF-κB in vivo and is transcriptionally inactive. *J. Inflamm.* **45**: 269-282

107. Marok, R., P.G. Winyard, A. Coumbe, M.L. Kus, K. Gaffney, S. Blades, P.I. Mapp, C.J. Morris, D.R. Blake, C. Kaltschmidt and P.A. Baeuerle (1996). Activation of transcription factor NF-κB in human inflamed synovial tissue. *Arthritis & Rheumatism* **39**: 583-591

108. Baeuerle, P.A., R.A. Rupec and H.L. Pahl (1996). Reactive oxygen intermediates as second messengers of a general pathogen response. *Pathologie Biologie* **44**: 29-35

109. Lieb, K., C. Kaltschmidt, B. Kaltschmidt, P.A. Baeuerle, M. Berger, J. Bauer and B.L. Fiebich (1996). IL-1β uses common and distinct signalling pathways for induction of the IL-6 and TNF-α genes in the astrocytoma cell line U373. *J. Neurochem.* **66**: 1496-1503

110. Pahl, H.L., M. Sester, H.-G. Burgert and P.A. Baeuerle (1996). Activation of transcription factor NF-κB by the adenovirus protein E3/19K requires its ER retention. *J. Cell. Biol.* **132**: 511-522

111. Pahl, H.L., B. Krauß, K. Schulze-Osthoff, E. B.-M. Traenckner, T. Parks, C. Myers, P. Waring, A. Muehlbacher, P.A. Czernilofsky and P.A. Baeuerle (1996). The immunosuppressive fungal gliotoxin is a selective inhibitior of transcription factor NF-κB. *J. Exp. Med.* **183**: 1829-1840

112. Brand, K., G. Rogler, A. Bartsch, R. Knuechel, M. Page, C. Kaltschmidt, P.A. Baeuerle and D. Neumeier (1996). Activated transcription factor NF-κB/Rel is present in the atherosclerotic lesion. *J. Clin. Invest.* **97**: 1715-1722

113. Pahl, H.L. and P.A. Baeuerle (1996). Control of gene expression by proteolysis. *Curr. Opin. Cell Biol.* 8: 340-347

114. Guan, E., J. Wang, J. Laborda, M. Norcross, P.A. Baeuerle and T. Hoffmann (1996). T cell leukemia-associated human Notch/translocation-associated Notch homologue has IκB-like activity and physically interacts with nuclear factor-κB proteins in T cells. *J. Exp. Med.* **183**: 2025-2032

115. Carter, B.D., C. Kaltschmidt, B. Kaltschmidt, N. Offenhäuser, R. Böhm-Mattaei, P.A. Baeuerle and Y.-A. Barde (1996). Selective activation of NF-κB by nerve growth factor through the neurotrophin receptor p75. *Science* **272**: 542-545

116. Schmidt, K.N., M. Podda, L. Packer and P.A. Baeuerle (1996). Anti-psoriatic drug anthralin activates transcription factor NF-κB in murine keratinocytes. *J. Immunol.* **156**: 4514-4519

117. Südbeck, P., M.L. Schmitz, P.A. Baeuerle and G. Scherer (1996). Sex reversal by loss of the C-terminal transactivation domain of human SOX9. *Nature Genetics* **13**: 230-232

118. Linker, R., P.A. Baeuerle and C. Kaltschmidt (1996). Cloning of the murine relA (p65 NF-κB) gene and comparison to the human gene reveals a distinct first intron. *Gene* **176**: 119-124

119. Buening, H., U. Gaertner, D. v. Schack, P.A. Baeuerle and H. Zorbas (1996). The histidine tail of recombinant DNA binding proteins may influence the quality of interaction with DNA. *Anal. Biochem.* **234**: 227-230

120. Grimm, S., M. Bauer, P.A. Baeuerle and K. Schulze-Osthoff (1996). Bcl-2 down-regulates the activity of transcription factor NF-κB induced upon apoptosis. *J. Cell. Biol.* **134**: 13-23

121. Mueller, M.J., M.A. Cahill, A. Nordheim, and Baeuerle, P.A. (1996). The transcription factor TCF/Elk-1: a nuclear sensor of changes in the cellular redox status. *Adv. Exp. Med. Biol.* **387**: 77-84

122. Schmidt, K.N., P. Amstad, P. Cerutti, and P.A. Baeuerle (1996). Identification of hydrogen peroxide as the relevant messenger in the activation pathway of transcription factor NF-κB. *Adv. Exp. Med. Biol.* **387**: 63-68

123. Schmitz, M.L., A. Indorf, F.P. Limbourg, H. Städtler, E. B.-M. Traenckner and P.A. Baeuerle (1996). The dual effect of adenovirus 5 E1A 13S protein on NF-κB activation is antagonized by E1B 19 kDa. *Mol. Cell. Biol.* **15**: 4052-4063

124. Feske, S., J.M. Müller, D. Graf, R.A. Kroczek, R. Draeger, C. Niemeyer, P. A. Baeuerle, H.-H. Peter, and M. Schlesier (1997). Severe combined immunodeficiency (SCID) due to defective binding of the nuclear factor of activated T cells in T lymphocytes of two male siblings. *Eur. J. Immunol.* **26**: 2119-2126

125. Limbourg, F.P., H. Staedler, G. Chinnadurai, P.A. Baeuerle, and M. L. Schmitz (1996). A hydrophobic region within the Adenovirus E1B 19 kDa protein is necessary for the transient inhibition of NF-κB activated by different stimuli. *J. Biol. Chem.* **271**: 20392-20398

126. Pahl, H.L. and P.A. Baeuerle (1997). Endoplasmic reticulum-induced signal transduction and gene expression. *Trends Cell. Biol* **7**: 50-55

127. Imbert, V., R.A. Rupec, P. Auberger, H.L. Pahl, E. B.-M. Traenckner, C. Müller-Dieckmann, D. Farahifar, B. Rossi, P.A.Baeuerle and J.-F. Peyron (1996). Tyrosine phosphorylation activates NF-κB without proteolytic degradation of IκB-α. *Cell* **86**: 787-798

128. Pahl, H.L. and P.A. Baeuerle (1996). Activation of NF-κB by ER stress requires both Ca^{2+} and reactive oxygen intermediates as messengers. *FEBS Letters* **392**: 129-136

129. Baeuerle, P.A. and D. Baltimore (1996). NF-κB: ten years after. *Cell* **87**: 13-20

130. Camandola, S., G. Leonarduzzi, T. Musso, L. Varesio, R. Carini, A. Scavazza, E. Chiarpotta, P.A. Baeuerle, and G. Poli (1996). Nuclear factor κB is activated by arachidonic acid but not by eicosapentaenoic acids. *Biochem. Biophys. Res. Comm.* **229**: 643-647

131. Pahl, H.L. and Baeuerle, P.A. (1997). The ER overload response: activation of NF-κB. *Trends Biochem Sci.* **22**: 63-67

132. Baeuerle, P.A. and V. Baichwal (1997). NF-κB as frequent target for immunosuppressive and anti-inflammatory molecules. *Adv. Immunol.* **6**: 111-137

133. Brand, K., S. Page, A.K. Walli, D. Neumeier and P.A. Baeuerle (1997). Role of nuclear factor-κB in atherogenesis. *Experimental Physiol.* **82**: 297-304

134. Mueller, J.M., R.A. Rupec and P.A. Baeuerle (1997). Study of gene regulation by NF-κB and AP-1 in response to reactive oxygen intermediates. In *Methods in Molecular Biology* (B. Demple, ed.) Academic Press, New York, **11**: 301-312

135. Schulze-Osthoff, K., M. Bauer, M. Vogt, S. Wesselborg and P.A. Baeuerle (1998). Reactive oxygen intermediates as primary signals and second messengers in the activation of transcription factors. In: *Oxidative Stress and Signal Transduction* (E. Cadenas and H.J. Forman, eds.), Chapman & Hall, New York, 239-259

136. Müller, J.M., M. Cahill, P.A. Baeuerle and A. Nordheim (1997). Antioxidants as well as oxidants activate *c-fos* via Ras-dependent activation of extracellular-signal-regulated kinase 2 and Elk-1. *Eur. J. Biochem.* **244**: 45-52

137. Baichwal, V.R., and P.A. Baeuerle (1997). Apoptosis: activate NF-κB or die? *Curr. Biol.* **7**: 94-96

138. Paal, K., P.A. Baeuerle, and M. Lienhard Schmitz (1997). Basal transcription factors TBP and TFIIB and the viral coactivator 13S E1A bind with distinct kinetics and affinities to the transactivation domain of NF-κB p65. *Nucl. Acids Res.* **25**: 1050-1055

139. B. Kaltschmidt, B. Volk and P.A. Baeuerle and C. Kaltschmidt (1997). Transcription factor NF-κB is activated in primary neurons by amyloid βA4 and in neurons surrounding early plaques from Alzheimer disease patients. *Proc. Natl. Acad. Sci. USA* **94**: 2642-2647

140. Baier-Bitterlich, G., D. Fuchs, R. Zangerle, P.A. Baeuerle, E.R. Werner, F. Fresser, F. Ueberall, G. Baier and Wachter, H. (1997). Trans-activation of the HIV type 1 promoter by 7,8-dihydroneopterin in vitro. *AIDS Res. Hum. Retroviruses* **13**: 173-178

141. Carini, R., G. Leonarduzzi, S. Camandola, T. Musso, L. Varesio, P.A. Baeuerle, and G. Poli (1997). Activation of human immunodeficiency virus long terminal repeat by arachidonic acid. *Free. Radic. Biol. Med.* **22**: 195-199

142. Wissink, S., E. van Heerde, M.L. Schmitz, E. Kalkhoven, B. van der Burg, P. A. Baeuerle, and P. van der Saag (1997). Distinct domains of the RelA subunit of NF-κB are required for negative crosstalk and interaction with the glucocorticoid receptor. *J. Biol. Chem.* **272**: 22278-22284

143. Baichwal., V.R., M. Rothe, Z. Cao, and P.A. Baeuerle (1997). Pro-inflammatory gene expression pathways with novel targets for anti-inflammatory drug discovery. *Pharmaceutical News* **4**: 17-21

144. Mueller, J.M., B. Krauss, C. Kaltschmidt, P.A. Baeuerle and R. Rupec (1997). Hypoxia induces *c-fos* transcription via a MAPK-dependent pathway. *J. Biol. Chem.* **272**: 23435-23339

145. Brand, K., T. Eisele, U. Kreusel, M. Page, S. Page, M. Haas, A. Gerling, C. Kaltschmidt, F.-J. Neumann, N. Mackman, P.A. Baeuerle, A.K. Walli and D. Neumeier (1997). Dysregulation of monocytic nuclear factor kappaB by oxidized low-density lipoprotein. *Arterioscler. Thromb. Vasc. Biol.* **17**: 1901-1909

146. Muenzenmaier, A., C. Lange, A. Covacci, A. Moran, S. Bereswill, P.A. Baeuerle, M. Kist, and H.L. Pahl (1997). A secreted/shed product of *Helicobacter pylori* activates transcription factor nuclear factor-κB. *J. Immunol.* **159**: 6140-6147

147. Gilston, V., H.W. Jones, C.C. Soo, A. Coumbe, S. Blades, C. Kaltschmidt, P.A. Baeuerle, C.J. Morris, D.R. Blake, and P.G. Winyard (1997). NF-κB activation in human knee-joint synovial tissue during the early stage of joint inflammation. *Biochem. Soc. Trans.* **25**, 158S

148. Baeuerle, P.A. (1998). Pro-inflammatory signaling: last pieces in the NF-κB puzzle? *Curr. Biol.* **8**: R19-R22

149. Baichwal, V.R., and P.A. Baeuerle (1998). Kinases in pro-inflammatory signal transduction pathways: new opportunities for drug discovery. *Annu. Reports Med. Chem.* **33**: 233-242

150. Cohen, L., W.J. Henzel, and P.A. Baeuerle (1998). IKAP is a scaffold protein of the IκB kinase complex. *Nature* **395**: 292-296

151. Rogler, G., K. Brand, D. Vogl, S. Page, R. Hofmeister, T. Andus, R. Knuechel, P.A. Baeuerle, J. Schoelmerich and V. Gross (1998). Nuclear factor kappaB is activated in macrophages and epithelial cells of inflamed intestinal mucosa. *Gastroenterology* **115**: 357-369

152. Los, M., K. Khazaie, K. Schulze-Osthoff, P.A. Baeuerle, V. Schirrmacher, and K. Chlichlia (1998). Human T Cell leukemia Virus-I (HTLV-I) Tax-mediated apoptosis in activated T cells requires an enhanced intracellular prooxidant state. *J. Immunol.* **161**: 3050-3055

153. Baeuerle, P.A. (2000). Reactive oxygen intermediates as costimulatory signals of cytokine-induced NF-κB activation pathways. In: *Antioxidant and Redox Regulation of Genes* (C. Sen, H. Sies, and P.A.Baeuerle, eds.), Academic Press, pp. 181-202

154. Medina, J.C., B. Shan, H. Beckmann, R.P. Farrell, D.L. Clark, M. Learned, D. Roche, A. Li, V. Baichwal, C. Case, P.A. Baeuerle, T. Rosen, and J.C. Jaen (1998). Novel antineoplastic agents with efficacy against multidrug resistant tumor cells. *Bioorg. Med. Chem. Lett.* **8**: 2653-2656

155. Baeuerle, P.A. (1998). IκB--NF-κB structures: at the interface of inflammation control. *Cell* **95**: 729-731

156. Béraud, C., W.J. Henzel, and P.A. Baeuerle (1999). Involvement of regulatory and catalytic subunits of phosphoinositide 3-kinase in NF-kappaB activation. *Proc. Natl. Acad. Sci. USA* **19**: 429-434

157. Janssen-Heininger, Y.M., M.E. Poynter, and P.A. Baeuerle (2000). Recent advantages towards understanding redox mechanisms in the activation of nuclear factor kappa B. *Free Radic. Biol. Med.* **28**: 1317-1327

158. Rupec, R.A., D. Poujol, J. Grosgeorge, G.F. Carle, A. Livolsi, J.-F. Peyron, R.M. Schmid, P.A. Baeuerle and G. Messer (1999). Structural analysis, expression, and chromosomal localization of the mouse ikba gene. *Immunogenetics* **49**: 395-403

159. Krappmann, D., E.N. Hatada, S. Tegethoff, J. Li, A. Klippel, K. Giese, P.A. Baeuerle, and C. Scheidereit (2000). The IκB kinase complex is tripartite and contains IKKγ but not IKAP as regular component. *J. Biol. Chem.* **275**: 29779-29787

160. Zohlnhoefer, D., C.A. Klein, T. Richter, R. Brandl, A. Murr, T. Nuehrenberg, A. Schömig, P.A. Baeuerle, and F.-J. Neumann (2001). Gene expression profiling of human stent-induced neointima by cDNA array analysis of microscopic specimens retrieved by helix cutter atherectomy. *Circulation* **103**: 1396-1402

161. De Baey, A., I. Mende, G. Riethmueller, and P.A. Baeuerle (2001). Phenotype and function of

human dendritic cells derived from M-DC8+ monocytes. *Eur. J. Immunol.* **31**: 1646-1655

162. Zohlnhoefer, D., T. Richter, F.-J. Neumann, R. Wessely, R. Brandl, T. Nuehrenberg, A. Murr, C.A. Klein and P.A. Baeuerle (2001). Transcriptome analysis reveals a role of interferon-γ in human neointima formation. *Mol. Cell* **7**: 1059-1069

163. Klein, C.A., S. Seidl, K. Petat-Dutter, S. Offner, J.B. Geigl, O. Schmidt-Kittler, N. Wendler, B. Passlick, R.M. Huber, G. Schlimok, P.A. Baeuerle, and G. Riethmüller (2002). Combined transcriptome and genome analysis of single micrometastatic cells. *Nature Biotech.* **20**: 387-392

164. Naundorf, S., S. Preithner, P. Mayer, S. Lippold, A. Wolf, F. Hanakam, I. Fichtner, P. Kufer, T. Raum, G. Riethmüller and P.A. Baeuerle, T. Dreier (2002). In-vitro and in-vivo activity of MT201, a fully human monoclonal antibody for pancarcinoma treatment. *Int. J. Cancer.* **100**: 101-110

165. Wolf, E., and P.A. Baeuerle (2002). Micromet: engaging immune cells for life. *Drug Discovery Today*. **6**: S25-S28

166. Dreier, T., G. Lorenczewski, C. Brandl, P. Hoffmann, U. Syring, F. Hanakam, P. Kufer, G. Riethmüller, R. Bargou, and P.A. Baeuerle (2002). Extremely potent, rapid and costimulation-independent cytotoxic T cell response against B lymphoma cells catalyzed by a single-chain bispecific antibody. *Intl. J. Cancer* **100**: 690-697

167. Löffler, A, M. Gruen, C. Wuchter, F. Schriever, P. Kufer, T. Dreier, F. Hanakam, P.A. Baeuerle, K. Bommert, L. Karawajew, B. Dörken, and R.C. Bargou (2003). Efficient elimination of chronic lymphocytic B cells by autologous T cells with a bispecific CD19xCD3 single-chain antibody. *Leukemia* **17**: 900-909

168. Wimberger, P., W. Xiang, D. Mayr, J. Diebold, T. Dreier, P.A. Baeuerle and R. Kimmig (2003). Efficient tumor cell lysis by autologous, tumor-resident T lymphocytes in primary ovarian cancer samples by an EpCAM-/CD3-bispecific antibody. *Int. J. Cancer* **105**: 241-248

169. Dreier, T.*, P.A. Baeuerle*, I. Fichtner, M. Grün, B. Schlereth, G. Lorenczweski, P. Kufer, R. Lutterbüse, G. Riethmüller, P. Gjorstrup and R. Bargou (2003). T cell costimulus-independent and very efficacious inhibition of tumor growth in mice bearing subcutaneous or leukemic human B cell lymphoma xenografts by a CD19-/CD3-bispecific single-chain antibody construct. *J. Immunol.* **170**: 4397-4402 (*Equal first authors)

170. Zocher, M., P.A. Baeuerle, T. Dreier, H. and A. Iglesias (2003). Specific depletion in vitro and in vivo of autoreactive B lymphocytes by a recombinant fusion protein. *Int. Immunol.* **15**: 789-796

171. De Baey, A., I. Mende, G. Baretton, A. Greiner, P.A. Baeuerle, and H.M. Diepolder (2002). A subset of human dendritic cells in the T cell area of mucosa-associated lymphoid tissue with high potential to produce TNF-α (2003). *J. Immunol.* **170**: 5089-5094

172. Xiang, W., P. Wimberger, T. Dreier, J. Diebold, D. Mayr, P.A. Baeuerle and R. Kimmig (2003). Cytotoxic activity of novel monoclonal antibody MT201 against primary ovarian tumor cells. *J. Canc. Res. Clin. Oncol.* **129**: 341-348

173. Zohlnhoefer, D, T.G. Nuehrenberg, F.-J. Neumann, T. Richter, A.E. May, C.A. Klein, M. Clauss, A. Schömig, and P.A. Baeuerle (2004). Rapamycin effects transcriptional programs in smooth muscle cells controlling proliferative and inflammatory properties. *Mol. Pharmacol.* **65**: 880-889

174. Mende, I., P. Hoffmann, A. Wolf, E. Kopp, P.A. Baeuerle, A. de Baey, and P. Kufer (2005). Highly efficient antigen targeting to M-DC8$^+$ dendritic cells via FcγRIII/CD16-specific antibody conjugates. *Int. Immunol.* **15**: 539-547

175. Baeuerle, P.A., P. Kufer, and R. Lutterbüse (2003). Bispecific antibodies for polyclonal T cell engagement. *Curr. Opin. Mol. Therapeutics* **5**: 413-419

176. Kufer, P. R. Lutterbuese, and P.A. Baeuerle (2004). A revival of bispecific antibodies. *Trends Biotechnol.* **22**: 238-244

177. Offner, S., A. Hekele, U. Teichmann, S. Weinberger, S. Gross, P. Kufer, C. Itin, P.A. Baeuerle, and B. Kohleisen (2004). Epithelial tight junction proteins as potential antibody targets for pan-carcinoma therapy. *Cancer Immunol. Immunother.* **54**: 431-445

178. Zocher, M., and P.A. Baeuerle (2004). A bispecific single-chain antibody fusion protein for the targeted depletion of autoreactive B cells via unstimulated human T lymphocytes. *Mol. Immunol.* **41**: 511-518

179. Kufer, P., R. Lutterbüse and P. A. Baeuerle (2004). The promise of bispecific antibodies. *Discovery Medicine* **4**: 325-332

180. Offner, S., R. Hofmeister, A. Romaniuk, P. Kufer, and P.A. Baeuerle (2005). Induction of regular cytolytic T cell synapses by bispecific single-chain antibody constructs. *Mol. Immunol.*, in press

181. Schlereth, B., C. Quadt, T. Dreier, G. Lorenczweski, S. Lippold, S.P. Fargo, K.E. Cobb, E. Leo, P. Kufer, R. Bargou, K. Murthy, and P.A. Baeuerle (2005). T cell activation and B cell depletion in chimpanzees by an anti-CD19/anti-CD3 single-chain bispecific antibody construct. *Cancer Immunol. Immunother.*, in press

182. Prang, N., S. Preithner, S. Naundorf, J. Müller, C. Steiger, M. Peters, P.A. Baeuerle, and A.J. da Silva (2005). Cellular and complement-dependent cytotoxicity of monoclonal antibody MT201 against nine human breast cancer cell lines. *Brit. J. Cancer* **92**: 342-349

183. K. Breuhahn, P.A. Baeuerle, Peters, M., N. Prang, U. Töx, R. Köhne-Volland, V. Dries, P. Schirmacher, and E. Leo (2005). Expression of epithelial cell adhesion molecule (Ep-CAM) in chronic necroinflammatory liver diseases, hepatocellular carcinoma and other liver diseases. Submitted.

184. Hoffmann, P., R. Hofmeister, K. Brischwein, C. Brandl, R. Bargou, C. Itin, S. Crommer, N. Prang, and P.A. Baeuerle (2005). Serial killing of tumor cells by cytotoxic T cells activated through a bispecific single-chain antibody construct. *Intl. J. Cancer* **115**: 98-104.

185. Preithner, S., S. Elm, S, Lippold, M. Locher, A. Wolf, A. J. da Silva, P.A. Baeuerle, and N. Prang (2005). High concentrations of therapeutic antibodies are needed to compensate for inhibition

of antibody-dependent cellular cytotoxicity by excess immunoglobulin G. *Mol. Immunol.*, in press.

186. Nuehrenberg, T.G., R. Voisard, F. Fahlisch, M. Rudelius, J. Braun, J. Gschwend, M. Kountides, T. Herter, R. Bauer, V. Hombach, P.A. Baeuerle, and D. Zohlnhoefer (2005). Rapamycin attenuates vascular wall inflammation and progenitor cell promoters after angioplasty. *FASEB J.* **19**: 246-248.

187. Wolf, E., R. Hofmeister, B. Schlereth, P. Kufer, and P.A. Baeuerle (2005). BiTEs: Bispecific antibody constructs with unique anti-tumor activity. *Drug Discovery Today* **10**: 1237-1244.

188. Schlereth, B., I. Fichtner, G. Lorenczewski, P. Kleindienst, K. Brischwein, P. Kufer, R. Lutterbüse, P. Wimberger, R. Kimmig, and P.A. Baeuerle (2005). Eradication of tumors from a human colon cancer cell line and primary ovarian cancer metastases in immunodeficient mice by a single-chain Ep-CAM-/CD3-bispecific antibody construct. *Cancer Research* **65**: 2882-2889.

189. Zohlnhöfer, D., T. Nuehrenberg, F. Haas, F. Bengel, A. Schömig, P. A. Baeuerle, and M. Schwaiger (2005). Myocardial gene expression in patients with ischemic left ventricular dysfunction: transcriptome comparison of matched hibernating and control myocardial tissue. (Submitted)

190. Brischwein, K., B. Schlereth, B. Guller, C. Steiger, A. Wolf, R. Lutterbuese, S. Offner, M. Locher, T. Urbig, T. Raum, P. Kleindienst, R. Kimmig, I. Fichtner, P. Kufer, A.J. da Silva, and P.A. Baeuerle (2005). MT110: A novel bispecific single-chain antibody construct with high efficacy in eradicating solid tumors. *Mol. Immunol.* **in press**

191. Schlereth, B., P. Kleindienst, I. Fichtner, G. Lorenczewski, K. Brischwein, S. Lippold, A.J. da Silva, M. Locher, R. Kischel, R. Lutterbüse, P. Kufer, and P.A. Baeuerle (2005). Potent inhibition of local and disseminated tumor growth in immunocompetent mice by a bispecific single-chain antibody construct specific for murine CD3. *Cancer Immunol. Immunother.* **in press**

192. Leo, E., R. Oberneder, D. Weckermann, B. Ebner, C. Quadt, P. Kirchinger, F. Schmidt, M. Siebels, K. Rohrmann, K. Lensing, R. Koehne-Volland, K. Witschital, K. Brischwein, G. Riethmuller, T. Raum, P. Kufer, M. Locher, N. Prang, and P.A. Baeuerle. Safety, pharmacokinetics, and biological activity of adecatumumab, a fully human pan-carcinoma antibody, in a phase I study with hormone refractory prostate cancer patients. (Submitted)

193. Schanzer, J., P.A. Baeuerle, T. Dreier, and P. Kufer (2005). A human cytokine/single-chain antibody fusion protein for simultaneous delivery of GM-CSF and IL-2 to Ep-CAM overexpressing tumor cells. (Submitted)

194. Schanzer, J., P.A. Baeuerle, I. Fichtner, and P. Kufer (2005). Anti-tumor activity of a dual cytokine/ single-chain antibody fusion protein for simultaneous delivery of GM-CSF and IL-2 to Ep-CAM expressing tumor cells. (Submitted)

195. Jellinghaus, S., K. Brand, T. Nuehrenberg, S. Massberg, F.-J. Neumann, P.A. Baeuerle, H. Schühlen, A. Schömig, and D. Zohlnhöfer (2005). Activation of NFkappaB and its target genes in acute myocardial infarction sites of ruptured plaques. Transcriptome analysis of human coronary atherosclerotic plaques. (Submitted)

196. Went, P., J. Kononen, R. Simon, G. Sauter, and P.A. Baeuerle (2005). Frequent high-level expression of immunotherapeutic target Ep-CAM in colon, stomach, prostate and lung carcinomas. (Submitted)

197. Krinner, E.-M., J. Hepp, P. Hoffmann, S. Bruckmaier, L. Petersen, S. Mittelstrass, L. Parr, I. Schuster, S. Mangold, S. Buziol, I. Hochheim, M. Molhoi, M. Strasser, A. Wolf, P. Kufer, P.A. Baeuerle, and T. Raum (2005). Generation of a polyethylene glycol-conjugated human single-chain antibody neutralizing the proliferative activity of human granulocyte/macrophage colony-stimulating factor at low nanomolar concentration. (Internal review)

198. Crommer, S., S. Wissing, T. Fisch, C. Brandl, N. Prang, A. Kozhich, J. Suzich, E. Leo, M. Locher, P.A. Baeuerle, and R. Hofmeister (2005). Additive cytotoxic effects of rituximab and MT103, a T cell-recruiting CD19-/CD3-bispecific single-chain antibody construct. (Internal review).

199. Spizzo, G., P. Went, S. Dirnhofer, P. Obrist, H. Moch, P.A. Baeuerle, E. Mueller-Holzner, C. Marth, G. Gastl, and A. Zeimet (2005). Overexpression of epithelial cell adhesion molecule (Ep-CAM) is an independent prognostic marker for reduced survival of patients with epithelial ovarian cancer. (Submitted)

200. Kleindienst, P., R. Hofmeister, G. Lorenczewski, S. Lippold, M. Locher, P.A. Baeuerle, and B. Schlereth (2005). Exchanging human Fcγ1 with murine Fcγ2a highly potentiates anti-tumor activity of anti-Ep-CAM antibody adecatumumab in a syngeneic mouse lung cancer model. (Internal review)

201. Krinner, E.-M., J. Hepp, P. Hoffmann, S. Bruckmaier, L. Petersen, S. Petsch, L. Parr, I. Schuster, S. Mangold, S. Buziol, I. Hochheim, J. Volkland, M. Molhoj, M. Sriskandarajah, M. Strasser, C. Itin, A. Wolf, P. Soerensen, P. Kufer, P.A. Baeuerle, and T. Raum (2006). A highly stable polyethylene glycol-conjugated human single-chain antibody neutralizing granulocyte/macrophage colony stimulating factor at low nanomolar concentrations. (Internal review)

202. Krinner, E.-M., T. Raum, S. Bruckmaier, S. Petsch, R. Cierpka, I. Schuster, L. petersen, D. Abebe, M. Molhoj, A. Wolf, P. Sorensen, M. Locher, P.A. Baeuerle and J. Hepp (2006). MT203: a fully human monoclonal IgG1 potently neutralizing the pro-inflammatory cytokine granulocyte/macrophage colony stimulating factor. (Internal review)

203. Mølhøj, M., S. Crommer, D. Rau, M. Sriskandarajah, P. Kufer, K. Brischwein, R. Hofmeister, and P.A. Baeuerle (2006). CD19/CD3-bispecific Antibody MT103 is far superior to tandem diabody with respect to redirected tumor cell lysis. (Internal review)

Scientific Books

1. Baeuerle, P.A., editor (1998). Inducible Gene Expression Volume 1: Environmental Stress and Nutrients. Birkhäuser, Boston. ISBN 0-8176-3605-6

2. Baeuerle, P.A., editor (1998). Inducible Gene Expression Volume 2: Hormonal Signals. Birk-

häuser, Boston. ISBN 0-8176-3734-6

3. Sen, C.K., H. Sies, and P.A. Baeuerle, editors (2000). Antioxidant and Redox Regulation of Genes. Academic Press, San Diego, CA.

Educational Children Books

1. Baeuerle, P.A., and N. Landa (1997). *Cell works*. Barrons, New York

2. Landa, N. and P.A. Baeuerle (1997). *The body's heroes and villains*. Barrons, New York

3. Baeuerle, P.A., and N. Landa (1997). *Ingenious genes*. Barrons, New York

4. Landa, N. and P.A. Baeuerle (1997). *How the Y makes the guy*. Barrons, New York

Curriculum Vitae

Name	Dr. med. Peter Kufer
Birthdate	July 10, 1965
Place of Birth	Mainburg, Germany
Marital Status	Married to Friederike Kufer, Maiden Name: Wichelhaus, Three children: Maximilian *18.07.1996, Konstantin *21.01.1998 und Julian *08.02.2000
Nationality	German
Parents	Peter Kufer, Christine Kufer, Maiden Name: Unterstöger

Schooling

1971 - 1975	Elementary School Obersüßbach, Germany
1975 - 1977	Junior High School, Großgundertshausen
1977 - 1981	High School Rottenburg a. d. Laaber Dipoloma - 24.07.1981
1981- 1982	Comenius Gymnasium, Deggendorf
1982 - 1984	Gabelsberger Gymnasium, Mainburg Diploma - 29.06.1984 - Associate of Arts equivalent

University Education

1985 – 1991	Medical School for Human Medicine at the Ludwig-Maximilians-University (LMU) Munich, Germany
October 1st, 1991	Diploma - Physician following third state exam
Nov. 1991 – April 1993	Practitioner at the Institute for Immunology of the LMU, Munich
May 1993	License to practice Medicine
January 1994	Promotion as M.D. at the Medical Faculty of the LMU, Munich
April 2003	Habilitation (University teaching license) at the Medical Faculty of the LMU, Munich

Professional Career

Jan. 1994 – March 2003	Scientific Group Leader at the Institute for Immunology of the Ludwig-Maximilians-University Munich
April 1999 - March 2005	C1 position as lecturer and scientific employee at the Institute for Immunology of the LMU
Since January 2001	Vice President Immunotherapy, Micromet AG, Munich (full time as of April 2005)

The Fourteenth International Conference

on

Advances in the Application of Monoclonal Antibodies in Clinical Oncology

5-7 May 1997
Thira, Santorini, Greece

(The Minoan fisherman of Santorini)

Sponsored by:

Antisoma

Purdue Pharma L.P.

BIOMIRA

Bispecific diabody for lysis of human B-lineage leukaemia cells

S.M. Kipriyanov[1], G. Moldenhauer[2], G. Strauss[2], M. Little[1]

[1]Recombinant Antibody Research Group (0445), Diagnostics and Experimental Therapy Programme; [2]Dept. of Molecular Immunology (0740), Tumour Immunology Programme, German Cancer Research Centre (DKFZ), Im Neuenheimer Feld 280, 69120 Heidelberg, Germany

Recombinant antibody fragments directed against cell surface antigens can provide useful components for the development of therapeutic agents. To target cytotoxic effector T-cells to B-lineage leukaemia cells expressing the CD19 differentiation marker, we have constructed anti-human CD3 and anti-human CD19 single-chain antibodies by PCR amplification of immunoglobulin variable domain genes from cDNAs of the hybridomas OKT3 and HD37, respectively. Cloning the correct genes coding for the antibody variable domains (especially V_L kappa) was complicated by the presence of several immunoglobulin transcripts, some of them arising from the myeloma cell line. For the rapid functional evaluation of recombinant antibody fragments against cell surface antigens, we combined a colony screening assay with the analysis of crude periplasmic extracts by flow cytometry. This procedure facilitated the efficient cloning of a functional V_H/V_L combination from the hybridoma cDNA. As a part of the anti-CD3 scFv construction process, the PCR amplfied OKT3 V_H gene was modified to improve its *in vivo* folding. These modifications resulted in a dramatic increase of the yield and stability of soluble scFv. We also found that the addition of the non-metabolised sugar (sucrose) to growth medium after induction appeared to stabilise folding intermediates, leading to a further increase in the amount of soluble and functional scFv.

For the creation of bispecific anti-human CD3-CD19 antibodies, two different strategies were utilised. A single chain $(scFv)_2$ antibody, where the individual scFv regions were joined by a 20 amino acid linker, and a **non-covalent heterodimer diabody** were constructed. The soluble diabody proved to be produced by *E.coli* at a much higher yield than $(scFv)_2$, consisted of only dimers after IMAC purification and specifically interacted with both CD3 and CD19 positive cells. The $(scFv)_2$ construct, however, failed to recognise human CD3. The diabody binds CD3 and CD19 cell surface antigens with affinities close to those of parental scFvs. It was less stable than anti-CD3 scFv but more stable than anti-CD19 scFv when incubated in human serum at 37°C. The diabody is potent in retargeting peripheral blood lymphocytes to lyse tumour cells expressing the CD19 antigen. The cytotoxic activity of the diabody was increased by preincubation with effector cells and costimulation using a bivalent anti-human CD28 antibody.

1. Kipriyanov SM, Kupriyanova OA, Little M, Moldenhauer G (1996) Rapid detection of recombinant antibody fragments directed against cell-surface antigens by flow cytometry. J. Immunol. Methods, 196, 51-62.
2. Kipriyanov SM, Moldenhauer G, Little M (1997) High level production of soluble single chain antibodies in small-scale *Escherichia coli* cultures. J. Immunol. Methods, 200, 69-77.
3. Kipriyanov SM, Moldenhauer G, Martin ACR, Kupriyanova OA, Little M (1997) Two amino acid mutations in an anti-human CD3 single chain Fv antibody fragment that affect the yield on bacterial secretion but not the affinity. Protein Engineering, in press.

Article No. jmbi.1999.3156 available online at http://www.idealibrary.com on IDEAL J. Mol. Biol. (1999) 293, 41–56

JMB

Bispecific Tandem Diabody for Tumor Therapy with Improved Antigen Binding and Pharmacokinetics

Sergey M. Kipriyanov[1]*, Gerhard Moldenhauer[2], Jochen Schuhmacher[3] Björn Cochlovius[1], Claus-Wilhelm Von der Lieth[4], E. Ronald Matys[3] and Melvyn Little[1]

[1]*Recombinant Antibody Research Group (D0500)*

[2]*Department of Molecular Immunology*

[3]*Department of Diagnostic and Therapeutic Radiology and*

[4]*Department of Spectroscopy German Cancer Research Center (DKFZ), Im Neuenheimer Feld 280 D-69120, Heidelberg, Germany*

**Corresponding author*

To increase the valency, stability and therapeutic potential of bispecific antibodies, we designed a novel recombinant molecule that is bispecific and tetravalent. It was constructed by linking four antibody variable domains (V_H and V_L) with specificities for human CD3 (T cell antigen) or CD19 (B cell marker) into a single chain construct. After expression in *Escherichia coli*, intramolecularly folded bivalent bispecific antibodies with a mass of 57 kDa (single chain diabodies) and tetravalent bispecific dimers with a molecular mass of 114 kDa (tandem diabodies) could be isolated from the soluble periplasmic extracts. The relative amount of tandem diabodies proved to be dependent on the length of the linker in the middle of the chain and bacterial growth conditions. Compared to a previously constructed heterodimeric CD3 × CD19 diabody, the tandem diabodies exhibited a higher apparent affinity and slower dissociation from both $CD3^+$ and $CD19^+$ cells. They were also more effective than diabodies in inducing T cell proliferation in the presence of tumor cells and in inducing the lysis of $CD19^+$ cells in the presence of activated human PBL. Incubated in human serum at 37 °C, the tandem diabody retained 90 % of its antigen binding activity after 24 hours and 40 % after one week. *In vivo* experiments indicated a higher stability and longer blood retention of tandem diabodies compared to single chain Fv fragments and diabodies, properties that are particularly important for potential clinical applications.

Keywords: bispecific diabody; tandem diabody; domain swapping; human CD19; human CD3

Introduction

Bispecific antibodies (BsAb) provide an effective means of retargeting cytotoxic effector cells against tumor cells (Fanger *et al.*, 1992). They have mainly been produced using murine hybrid hybridomas (Bohlen *et al.*, 1993) or by chemical cross-linking (Brennan *et al.*, 1985; Glennie *et al.*, 1987). However, the immunogenicity of BsAb derived from rodent monoclonal antibodies is a major drawback for clinical use (Khazaeli *et al.*, 1994). They are also difficult to produce and purify in large quantities. Recent advances in recombinant antibody technology have provided several alternative methods for constructing and producing BsAb molecules (Carter *et al.*, 1995; Plückthun & Pack, 1997). For example, single chain Fv (scFv) fragments have been genetically fused with adhesive polypeptides (de Kruif & Logtenberg, 1996) or protein domains (Müller *et al.*, 1998c) to facilitate the formation of heterodimers. The genetic engineering of scFv-scFv tandems linked with a third polypeptide linker has also been carried out in several laboratories (Gruber *et al.*, 1994; Kurucz *et al.*, 1995). A bispecific diabody was obtained by the non-covalent association of two single chain fusion products consisting of the V_H domain from one antibody connected by a short linker to the V_L domain of another antibody (Holliger *et al.*, 1993, 1996). The two antigen binding domains have been shown by

Abbreviations used: scFv, single chain Fv; sc-diabody, single chain diabody; LL, long linker; SL, short linker; Tandab, tandem diabody; BsAb, bispecific antibody; TCR, T cell receptor; IMAC, immobilized metal affinity chromatography; AUC, area under the curves.

E-mail address of the corresponding author: s.kipriyanov@dkfz-heidelberg.de

0022-2836/99/410041–16 $30.00/0

crystallographic analysis to be on opposite sides of the diabody such that they are able to cross-link two cells (Perisic *et al.*, 1994). In contrast to native antibodies, all of the above mentioned bispecific molecules have only one binding domain for each specificity. However, bivalent binding is an important means of increasing the functional affinity and possibly the selectivity for particular cell types carrying densely clustered antigens.

We recently described the construction and characterization of a bispecific diabody with dual specificity for both the human B cell antigen CD19 and ε chain of the CD3/T cell receptor (TCR) complex designed for the treatment of minimal residual disease in patients with leukemias and malignant lymphomas (Kipriyanov *et al.*, 1998). The CD19 antigen is expressed on virtually all B-lineage malignancies from acute lymphoblastic leukemia (ALL) to non-Hodgkin's lymphoma (NHL) (Uckun & Ledbetter, 1988). Moreover, it is not shed and is absent from hemopoietic stem cells, plasma cells, T cells and other tissues. Bispecific diabodies appear to be quite effective in mediating T cell cytotoxicity (Holliger *et al.*, 1996; Kipriyanov *et al.*, 1998; Zhu *et al.*, 1996). However, the co-secretion of two hybrid scFv fragments can give rise to two types of dimer: active heterodimers and inactive homodimers. A second problem is that the two chains of diabodies are held together by non-covalent associations of the V_H and V_L domains and can diffuse away from one another. Moreover, to ensure the assembly of a functional diabody, both hybrid scFv fragments must be expressed in the same cell in similar amounts. This latter requirement is difficult to uphold in eukaryotic expression systems such as yeast, which are often preferred because high yields of enriched product can be obtained (Ridder *et al.*, 1995; Shusta *et al.*, 1998). Finally, the small size of bispecific diabodies (50-60 kDa) leads to their rapid clearance from the blood stream through the kidneys, thus requiring the application of relatively high doses for therapy.

To circumvent the drawbacks of diabodies and to increase the valency, stability and therapeutic potential of recombinant bispecific antibodies, we have now constructed single chain molecules comprising four antibody variable domains (V_H and V_L) of two different specificities in an orientation preventing Fv formation. They can either form bivalent bispecific antibodies by diabody-like folding (sc-diabodies) or dimerize with the formation of tetravalent bispecific antibodies (tandem diabodies). The efficacy of tandem diabody (Tandab) formation is dependent on the length of the linker between two halves of the molecule. Here we show that Tandabs are bispecific and have higher avidity resulting from the bivalency for each specificity. CD3 × CD19 Tandabs were more potent than the diabody for inducing human T cell proliferation in the presence of irradiated $CD19^+$ B cells. In cytotoxic assays, Tandabs were able to retarget human T lymphocytes to malignant B cells. The efficiency of Tandab-mediated cell lysis also compared favorably to that obtained with a diabody of the same dual specificity. *In vivo* studies demonstrated that tetravalent Tandabs were more stable and were retained longer in the blood of normal mice compared to scFv and diabodies. This bispecific antibody format could therefore prove to be particularly advantageous for cancer immunotherapy.

Results

Design of single chain molecules comprising four antibody variable domains

The concept of dimerizing scFv fragments having a short peptide linker between the two domains to create two antigen-binding sites pointing in opposite directions (Holliger *et al.*, 1993) was extended to single chain molecules containing four antibody variable domains. We previously constructed a CD3 × CD19 bispecific diabody comprising two hybrid scFv fragments: an anti-human CD3 V_H domain joined to an anti-human CD19 V_L domain by a short linker peptide and an anti-CD19 V_H connected to an anti-CD3 V_L by a similar linker (Kipriyanov *et al.*, 1998). We have now fused these hybrid scFvs into a single chain polypeptide using either a long (20 amino acid residues) $(Gly_4\text{-}Ser)_4$ or short (five amino acid residues) Gly-Gly-Pro-Gly-Ser linker (Figure 1(a)). The short linker design was based on our experience with the generation of stable mono- and bispecific diabodies using a linker mainly derived from the N-terminal part of a murine C_H1 domain that contained a proline residue (Arndt *et al.*, 1999; Kipriyanov *et al.*, 1998; Le Gall *et al.*, 1999). We therefore modified the traditional Gly_4-Ser motif (Holliger *et al.*, 1993; Huston *et al.*, 1988) to include a proline residue. However, the actual linker length is larger because we originally cloned the antibody V_κ domains using an anti-sense primer complementary to the 5'-region of the C_κ domain gene (Kipriyanov *et al.*, 1996a). Therefore, seven additional amino acid residues introduced by this primer are part of the long (LL) and short (SL) linkers (27 and 12 residues, respectively; Figure 1(a)). The long linker was designed to span the distance between the carboxy terminus of the first pair of V-domains and the amino terminus of the second pair to form a sc-diabody (Figure 1(b)). In contrast, the short linker should prevent intramolecular V_H-V_L pairing and force the four domains to interact with complementary ones of another molecule with the formation of an eight-domain Tandab (Figure 1(c)). It should not be too short, however, since the antigen-binding sites in the middle of the molecule might then be sterically hindered. We therefore chose a 12 residue linker to satisfy these two criteria.

Bacterial expression and purification

The four-domain single chain molecules were expressed as soluble secreted proteins in *Escherichia*

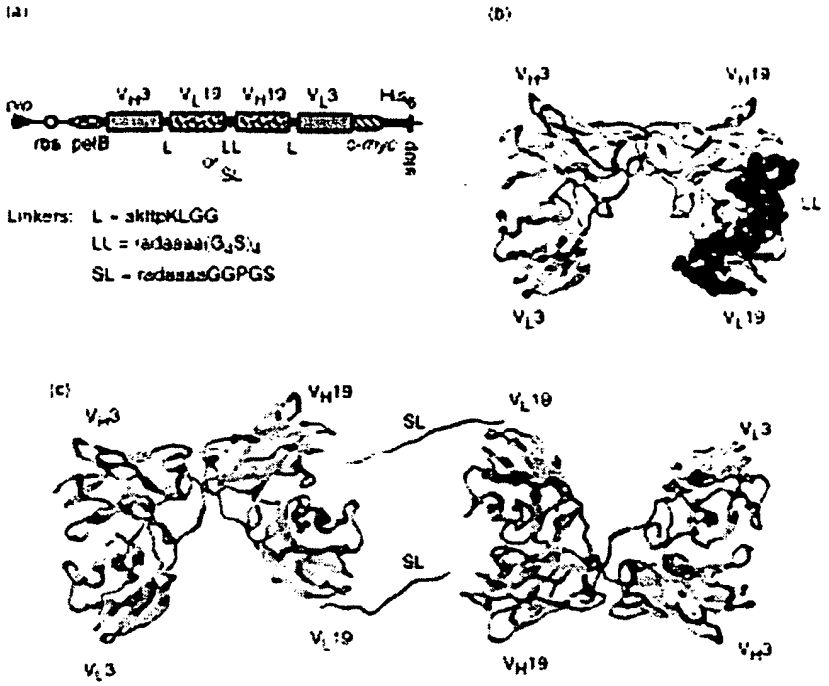

Figure 1. (a) Schematic representation of operons and structural models of (b) sc-diabody and (c) tandem diabody. The locations of promoter/operator (*p/o*), ribosome-binding site (rbs), *pel*B leader (pelB), *c-myc* epitope (*c-myc*), hexahistidine tag (his_6) and stop codon (stop) are indicated. The atoms of the long flexible linker (LL) are represented as filled spheres. Beta-sheets are shown in yellow, beta-turns in blue and irregular peptide sequences in green. The positions of anti-CD3 and anti-CD19 variable domains are indicated.

coli. They were isolated from crude periplasmic fractions by immobilized metal affinity chromatography (IMAC). In contrast to IMAC-purified preparations of well-expressed bispecific CD3 × CD19 diabody (Kipriyanov *et al.*, 1998), those of the four-domain single chain molecules contained large amounts of impurities (Figure 2(a), lane 1). Fortuitously, we found that by exchanging the buffer after IMAC for 50 mM imidazole-HCl (pH 6.4-6.7), most of the contaminating bacterial proteins precipitated while the recombinant antibody fragments remained soluble (Figure 2(a), lane 2). In a final step using the cation-exchange chromatography, recombinant single chain molecules were obtained with a purity greater than 95% (Figure 2(b)). On SDS-PAGE, single bands were observed with mobilities quite close to those expected (calculated $M_r = 57.1$ and 56.2 kDa for single chain molecules with LL and SL, respectively). The corresponding CD3 × CD19 diabody migrated as two closely spaced protein bands with M_r~30 kDa (Figure 2(b), lane 1).

Effect of different expression methods on the formation of tandem diabodies

An analysis of the dimerization behavior of four domain single chain molecules was performed by size-exclusion FPLC on a Superdex 200 column in PBSI buffer (PBS with 50 mM imidazole (pH 7.0)). This buffer was used because, in our experience, PBS alone appeared to be unfavorable for the stability of some antibody fragments, regardless as to whether they had been isolated from inclusion bodies or from soluble periplasmic extracts. For example, buffer exchange for PBS resulted in the aggregation of anti-CD19 scFv and, to a lower extent, of the bispecific CD3 × CD19 diabody (Kipriyanov *et al.*, 1998). Hydrophobic amino acids from either the V_H/V_L or variable/constant domain interfaces, which are normally buried in the Fab fragment but become exposed to solvent in recombinant scFv (Nieba *et al.*, 1997), might be the cause of aggregation. The use of Tris-HCl or Hepes buffers with high salt concentrations (e.g. 1 M NaCl) can help to solve this problem. Alternatively, the presence of imidazole can stabilize scFv fragments and diabodies (our observation) as well as scFv-RNAse fusion proteins (Dr Dianne Newton, personal communication). Empirically, we have determined that PBS with 50 mM imidazole (pH 7.0-7.5), is a suitable buffer for various antibody fragments kept at relatively high concentrations (2-3 mg/ml). Moreover, this buffer did not interfere with antigen binding and did not show any toxic effects after incubation with cultured cells or after injection into mice (intravenous injection of 200 µl).

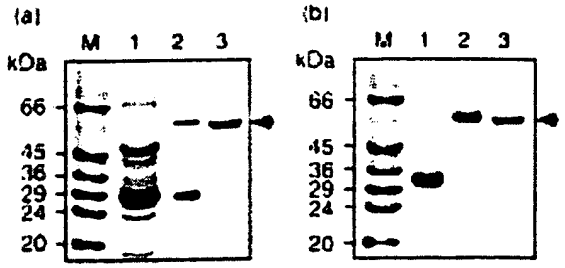

Figure 2. Analyses of bispecific antibody fragments by 12% SDS gel electrophoresis under reducing conditions. (a) SDS-PAGE of the purification of SL-product. Lanes: M, MW markers; 1, sample from IMAC; 2, sample after buffer exchange for 50 mM imidazole-HCl (pH 6.4) and centrifugation; 3, sample eluted from Mono S column. (b) SDS-PAGE of purified bispecific antibody fragments. Lanes: M, markers; 1, diabody; 2, LL product; 3, SL product. The gels were stained with Coomassie brilliant blue. The positions of four domain single chain molecules are indicated.

Size-exclusion chromatography of the LL product purified from bacteria induced in the presence of 0.4 M sucrose (Kipriyanov *et al.*, 1997a) revealed the presence of the monomeric sc-diabody ($M_r \sim 55$ kDa) as well as the homodimer (Tandab) with an apparent $M_r \sim 115$ kDa (Figure 3(b)). We therefore investigated whether the amount of Tandab may depend on the folding history of the protein, and thus on the expression method. The LL and SL products were isolated from periplasmic extracts of *E. coli* cells induced either in normal rich medium or under osmotic stress in the presence of non-metabolized additives such as sucrose (Kipriyanov *et al.*, 1997a) or sorbitol and glycine betaine (Blackwell & Horgan, 1991). As shown in Figure 3, significant increases of the dimeric fractions were obtained using bacteria grown in modified media. As expected, the amount of homodimers was dependent on the linker length. While the LL product comprised almost no dimers using normal medium and about 50% dimers using sorbitol/betaine medium, 80-100% of the SL product was in a dimeric form (Figure 3). In contrast, isolation from inclusion bodies and refolding *in vitro* led exclusively to monomeric LL molecules and predominantly monomeric SL molecules with only 20-30% dimer formation (data not shown). Rechromatography of the first and second peak fractions for both the LL and SL products isolated either from soluble periplasmic extracts or from inclusion bodies yielded only a single species, Tandab or sc-diabody, respectively (data not shown).

The yields of four-domain single chain molecules with LL and SL after expression in *E. coli* shake flask cultures in sorbitol/betaine medium and purification were 0.48(±0.14) mg/l per $A_{600\,nm}$ ($n = 5$) and 0.60(±0.11) mg/l per $A_{600\,nm}$ ($n = 4$), respectively. These values were three- to fourfold higher than those obtained for material isolated both from inclusion bodies and the soluble periplasmic fraction after expression in normal medium (data not shown). For further analyses, homogeneous preparations of the sc-diabody with the long linker and Tandabs with both the long and short linkers were obtained by isolating the respective peaks after size-exclusion chromatography.

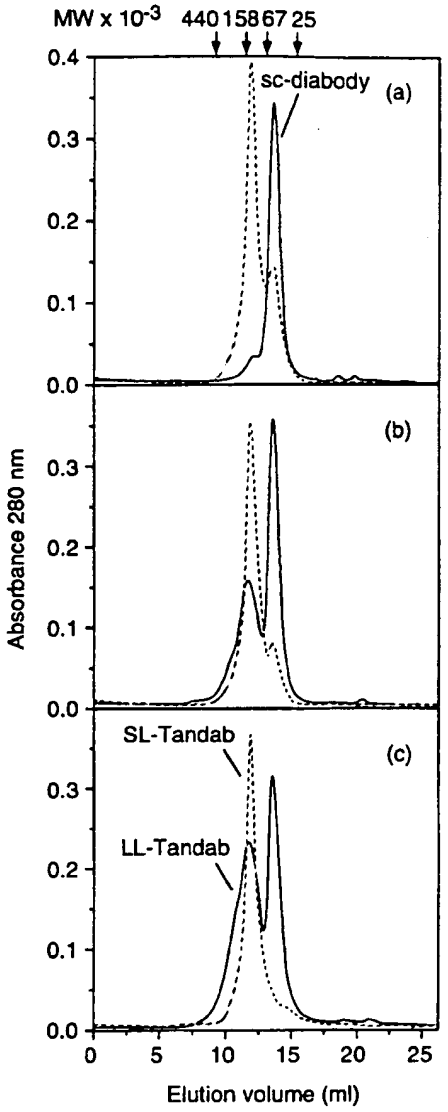

Figure 3. Elution profiles of purified LL product (continuous lines) and SL product (dotted lines) from calibrated Superdex 200 gel filtration column. Antibody fragments isolated from bacteria induced in (a) normal 2 × YT medium, (b) medium with sucrose and (c) medium with sorbitol and betaine were analyzed. The peaks taken for further *in vitro* and *in vivo* analyses are indicated.

Antigen binding activity

Flow cytometry experiments demonstrated specific interactions with both human CD19$^+$ JOK-1 and CD3$^+$ Jurkat cells for all the recombinant bispecific antibodies (Figure 4). On a weight basis, the diabody showed the highest fluorescence intensities when interacting with JOK-1 cells and Tandabs gave the highest signals for binding to Jurkat cells. Surprisingly, the sc-diabodies showed higher fluorescence intensities for binding to Jurkat cells, even though they contained only one c-*myc* epitope for immunodetection in contrast to the two peptide tags of the diabodies (Kipriyanov *et al.*, 1998) (Figure 4(b) and (d)).

The CD19 and CD3 binding affinities were estimated by competitive binding to human JOK-1 and Jurkat cells in the presence of either FITC-labeled anti-CD19 MAb HD37 (Pezzutto *et al.*, 1987) or anti-CD3 MAb OKT3 (Kung *et al.*, 1979) (Figure 5(a) and (b)). The relative affinities were calculated from the corresponding IC_{50} values. Compared to the diabody, the sc-diabody bound CD19 with an almost identical affinity, while the SL and LL-Tandab had affinities that were approximately 1.5 and threefold higher, respectively. Even higher increases in affinity were found for binding to CD3$^+$ cells. The sc-diabody, SL and LL-Tandab, respectively, bound CD3 1.5, three- and eightfold more efficiently than the diabody (Table 1).

To investigate the biological relevance of the differences in affinity values of the bispecific molecules, their *in vitro* retention on the surface of both CD3 and CD19-positive cells at 37 °C was determined by flow cytometry (Figure 5(c) and (d)). The sc-diabody had a relatively short retention half-life ($t_{1/2}$) on CD19$^+$ JOK-1 cells, almost identical with the $t_{1/2}$ of the diabody (Table 1). In contrast, both the tandem diabodies were retained significantly longer on the surface of JOK-1 cells (Table 1). The half-lives of all the bispecific antibodies on the surface of CD3$^+$ Jurkat cells were relatively short (Figure 5(d) and Table 1), reflecting the lower CD3 binding affinities deduced from inhibition experiments (Figure 5(b)). In contrast to the diabody and sc-diabody, both tandem diabo-

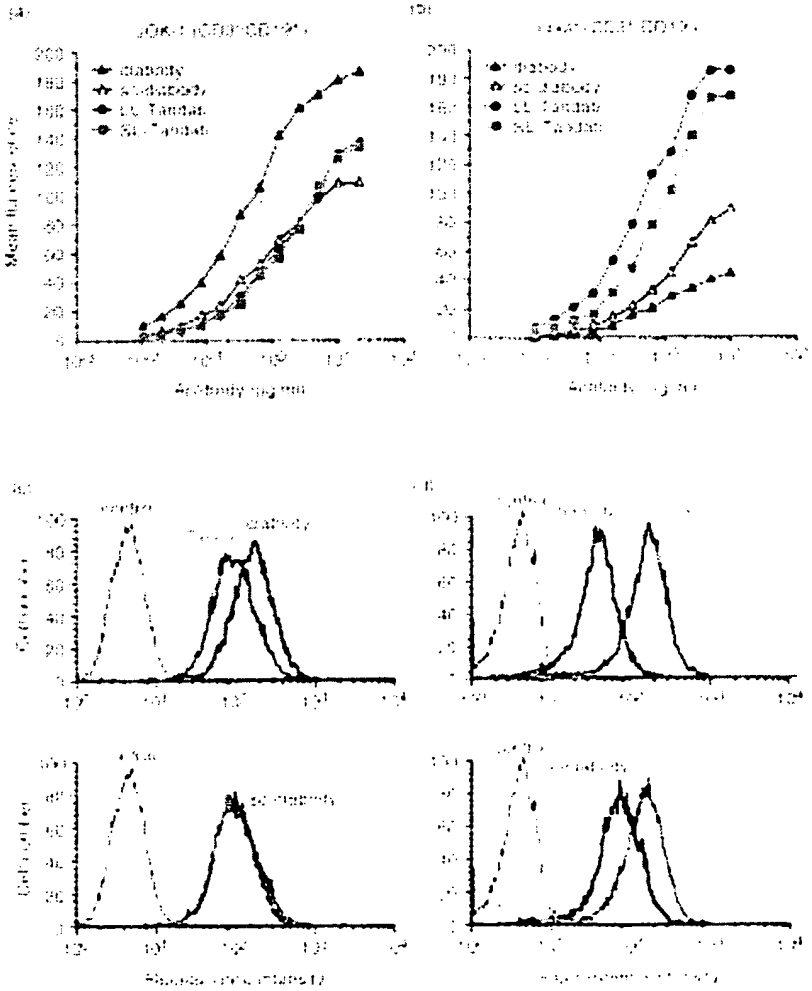

Figure 4. Flow cytometric analysis of antibody fragments binding to (a), (c) CD19$^+$/CD3$^-$ JOK-1 cells and (b), (d) CD3$^+$/CD19$^-$ Jurkat cells. (a) and (b) Fluorescence dependence on antibody concentration. (c) and (d) Overlay plots obtained for antibodies at 10 μg/ml concentration.

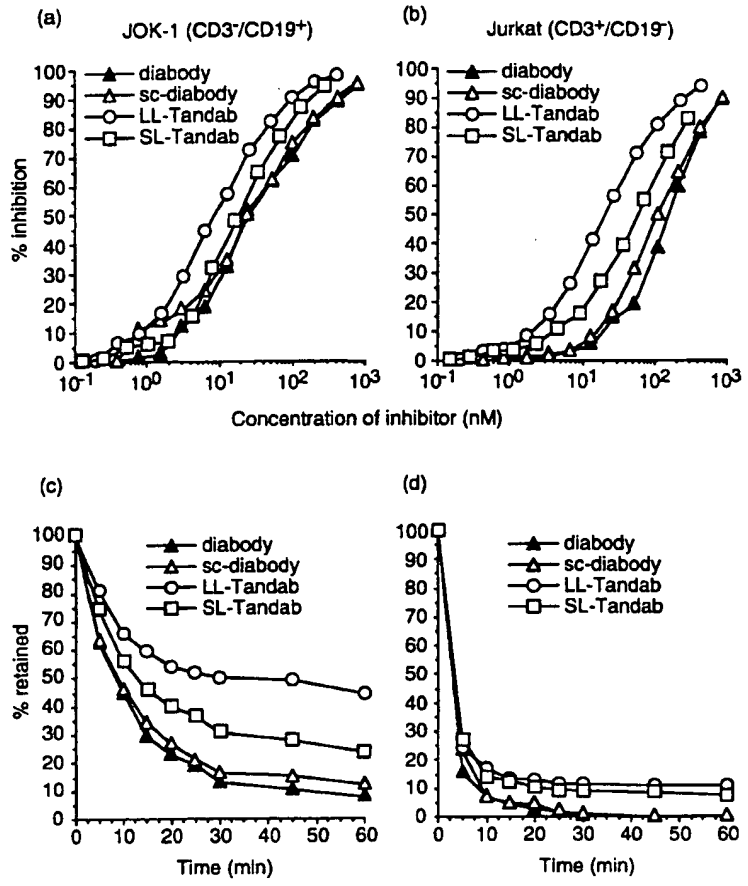

Figure 5. Analyses of apparent affinities by (a), (b) flow cytometry and (c), (d) by cell surface retention *in vitro*. Inhibition of binding of (a) FITC-labeled MAb HD37 to JOK-1 cells and (b) FITC-labeled MAb OKT3 to Jurkat cells in the presence of bispecific antibody fragments are shown. Analogously, cell surface retention profiles were determined either with JOK-1 or (d) Jurkat cells.

dies demonstrated a biphasic decay of fluorescence intensity associated with Jurkat cells (Figure 5(d)). The fast half-life ($t_{1/2}\alpha$) of both Tandabs was nearly identical with the $t_{1/2}$ of the sc-diabody, while the slow half-life ($t_{1/2}\beta$) was almost threefold longer than $t_{1/2}\alpha$ (Table 1). This biphasic dissociation of the Tandabs may indicate the presence of subpopulations of Jurkat cells with different densities of the CD3ε epitope on their surface.

Biological activity

Two *in vitro* tests were used for comparing the biological activity of the bispecific antibodies. First, their ability to stimulate T cell proliferation when bound to the surface of tumor cells was determined. Irradiated CD19⁺ Raji cells were treated with different concentrations of each bispecific antibody and subsequently incubated in the presence of human PBL prestimulated with a low-dose of IL-2. As shown in Figure 6(a), diabody treatment resulted in a strong dose-dependent increase in T cell proliferation. In comparison, the SL-Tandab performed significantly better and the LL-Tandab showed the highest stimulatory effect.

The second test measured the ability of the bispecific molecules to induce tumor cell lysis by redirecting T cell cytotoxicity. At a concentration of 10 μg/ml, the sc-diabody was as potent as the diabody in mediating tumor cell killing by activated human PBL but was slightly less potent than both of the Tandabs (Figure 6(b)). Comparisons of cell apoptosis efficiency at various molar concentrations of the bispecific antibodies demonstrated a consistently better performance of the Tandabs (Figure 6(c) and (d)).

Stability *in vitro*

One of the most important applications of BsAbs is in cancer therapy where factors such as plasma half-life and tumor penetration play an important role. The BsAb should also be stable at 37 °C in human serum to have a significant anti-tumor effect. We therefore analyzed the antigen-binding activity of the recombinant BsAb molecules when stored at a fairly low concentration in human serum at 37 °C for prolonged periods of time. A concentration of 15 μg/ml was chosen in order to avoid the fluorescence plateau in FACScan analysis (Figure 4). The residual activity was estimated by flow cytometry with CD3⁺ Jurkat cells, since the CD3-binding activity of the diabody was previously shown to be less stable than the CD19-

Table 1. Affinity and binding kinetics of recombinant bispecific molecules

Antibody	Valency[a]	IC_{50}^{b} (nM)	K_D^{b} (nM)	k_{off} fast[c] ($s^{-1}/10^{-3}$)	$t_{1/2}\alpha^{c}$ (minutes)	k_{off} slow[c] ($s^{-1}/10^{-3}$)	$t_{1/2}\beta^{c}$ (minutes)
A. *JOK-1 cells ($CD3^-/CD19^+$)*							
Diabody	M	25.25	1.29	1.16 ± 0.28	10.0	N.D.	N.D.
sc-diabody	M	26.61	1.36	1.05 ± 0.30	11.0	N.D.	N.D.
LL-Tandab	B	9.19	0.47	0.48 ± 0.18	24.3	N.D.	N.D.
SL-Tandab	B	20.45	1.05	0.74 ± 0.22	15.7	N.D.	N.D.
B. *Jurkat cells ($CD3^+/CD19^-$)*							
Diabody	M	154.58	15.46	3.97 ± 1.42	2.9	N.D.	N.D.
sc-diabody	M	108.18	10.82	3.44 ± 1.02	3.4	N.D.	N.D.
LL-Tandab	B	20.04	2.00	3.30 ± 1.27	3.5	1.04 ± 0.50	11.2
SL-Tandab	B	57.80	5.78	3.31 ± 0.99	3.5	1.17 ± 0.53	9.8

N.D., not determined.
[a] Putative valency for each specificity. M, monovalent; B, bivalent.
[b] Deduced from inhibition experiments.
[c] Deduced from cell surface retention assays.

binding activity (Kipriyanov *et al.*, 1998). We found that all of the bispecific molecules retained 80-90% of their antigen binding activity after 24 hours incubation at 37 °C in human serum (Figure 7(a)). Prolonged incubation demonstrated that single chain molecules appeared to be more stable than the non-covalent dimer diabody with 1.5 to 2.5-fold increased half-lives (Table 2). For example, even after incubation for one week at 37 °C, the LL-Tandab retained 40% of its activity (data not shown). Western blot analyses of the samples of bispecific molecules showed no proteolytic degradation for any of them after 81 hours of incubation in human serum at 37 °C (data not shown).

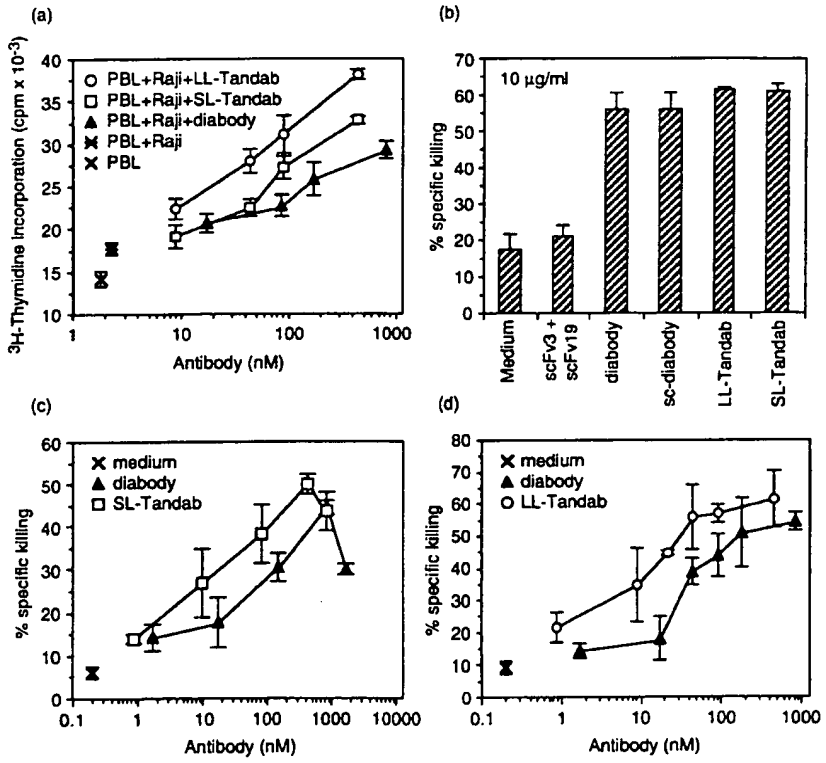

Figure 6. Biological activity of diabodies and tandem diabodies. (a) BsAb stimulation of activated human T cell proliferation in the presence of irradiated $CD19^+$ Raji cells. (b)-(d) BsAb mediated killing of Raji cells by activated human PBL as determined by a JAM test. Effector:tumor cell ratio was 25:1. (b) Antibody fragments were used at concentration of 10 µg/ml. Mean values ± SE are plotted.

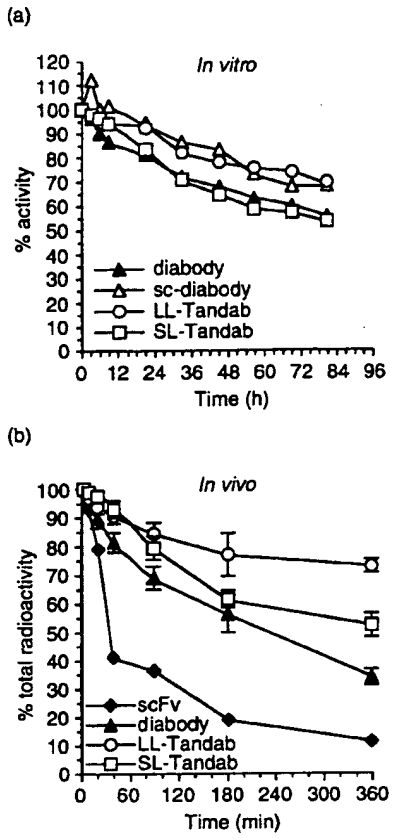

Figure 7. *In vitro* and *in vivo* stability of bispecific antibody fragments. (a) Stability in human serum at 37 °C as determined by flow cytometry using $CD3^+$ Jurkat cells. Activities of the samples at point zero were taken as 100 %. (b) *In vivo* stability of ^{125}I-labeled antibody fragments. Protein-bound radioactivity in TCA precipitated plasma samples were calculated as percentages of the total radioactivity (TCA-pellet and supernatant) at specific time points. The values up to six hours after administration of the labeled compounds are plotted as mean values ± SE.

Blood clearance and stability *in vivo*

To compare the plasma clearance pharmacokinetics of Tandabs and smaller antibody fragments, we administered preparations of ^{125}I-labeled anti-human CD3 scFv monomer (30 kDa) (Kipriyanov *et al.*, 1997b), CD3 × CD19 diabody (58 kDa) (Kipriyanov *et al.*, 1998), LL-Tandab (114 kDa) and SL-Tandab (113 kDa) intravenously to mice. Blood samples were taken at various time points. To exclude errors in calculating plasma half-lives due to free radioiodine resulting from cellular, metabolic degradation of labeled protein, we first determined the proportion of protein-bound radioactivity for each plasma sample by TCA precipitation. As can be seen in Figure 7(b), TCA-precipitable radioactivities of scFv decreased rapidly in the blood over time, only 50 % of the radioactivity were bound to protein 30 minutes after the intravenous injection. In contrast, the diabody lost its label much more slowly, more than 50 % of its radioactivity could be precipitated three hours after injection. The Tandabs were even more stable: 72 and 52 % of the radioactivity was found to be associated with protein six hours after administration of the LL and SL-Tandab, respectively (Figure 7(b)). The estimated half-lives of the diabody and the Tandabs exceeded that of the scFv three- and sixfold, respectively (Table 2). SDS-PAGE analysis followed by autoradiography showed no degradation of either Tandab 1.5 hours after injection (data not shown).

Analyses of blood samples at different time points demonstrated an extremely rapid clearance of scFv from plasma, with an alpha-phase (extravasation and renal clearance) half-life ($t_{1/2}\alpha$) of 3.5 minutes and a beta-phase (catabolism) ($t_{1/2}\beta$) of 74.6 minutes (Figure 8). The diabody had an approximately twofold slower first-pass clearance and a somewhat slower catabolism (Figure 8 and Table 2). Even slower plasma clearance rates were observed for the larger Tandabs (Figure 8). Alpha-phase half-lives were estimated to be four- and eightfold higher for the SL and LL-Tandabs, respectively, in comparison to that of scFv (Table 2). The pharmacokinetic areas under the curves (AUC) were calculated for all of the antibody fragments to provide a means of estimating the total relative dose that would be delivered in a therapeutic application. Tandem diabodies demonstrated the best pharmacokinetic performance, their AUC values were two- and fivefold higher than AUC values calculated for the diabody and scFv, respectively (Table 2). The differences in the pharmacokinetic properties of these constructs correlate quite well with their size.

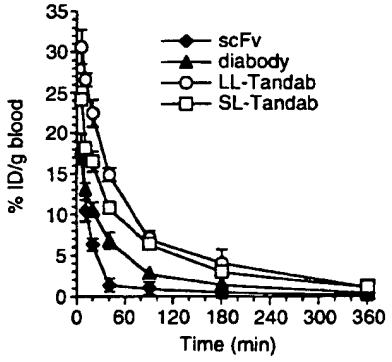

Figure 8. Pharmacokinetics of plasma retention of ^{125}I-labeled antibody fragments in mice. Blood samples were obtained at the times indicated. Data were corrected for non-TCA-precipitable radioactivity. The values up to six hours after administration of the labeled compounds are plotted as mean values ± SE.

Table 2. *In vitro* and *in vivo* stability and pharmacokinetic parameters for scFv and bispecific antibody fragments

Antibody fragment	Stability[a]		Pharmacokinetics[b]		
	in Vitro $t_{1/2}$ (hours)	*in Vivo* $t_{1/2}$ (hours)	Blood clearance $t_{1/2}\alpha$ (minutes)	$t_{1/2}\beta$ (minutes)	AUC %ID/g per minute
scFv	N.D.	1.2	3.5	74.6	422.4
Diabody	63.0	3.1	8.4	91.9	1123
sc-diabody	157.7	N.D.	N.D.	N.D.	N.D.
LL-Tandab	126.2	7.3	28.5	119.7	2919
SL-Tandab	87.3	6.8	11.9	92.5	2234

N.D., not determined.

[a] The half-life values for stability measurements were deduced from the one phase exponential decay fit of experimental data presented in Figure 7 and were calculated as $\ln 2/k$.

[b] To estimate the blood retention half-lives, a bi-exponential function was fitted to each blood clearance curve (Figure 8) after correcting for metabolic degradation of labeled protein. The therapeutic effectiveness of the analyzed antibody fragments was also compared by integration of the blood retention curves. The areas under the curve (AUC) were measured to infinite time with each curve being represented as a bi-exponential function.

Discussion

We have constructed novel recombinant bispecific tetravalent antibody fragments that we have named "tandem diabodies", since their design is based on the intermolecular pairing of V_H and V_L domains as described for diabodies (Holliger *et al.*, 1993). Although the non-covalent forces holding the V_H and V_L domains together are fairly weak, often resulting in Fv dissociation (Glockshuber *et al.*, 1990), the association of two V_H/V_L pairs in a dimer of V_H-V_L fusion proteins (diabody) provides a relatively stable structure (Holliger *et al.*, 1993; Kipriyanov *et al.*, 1998). This observation prompted us to consider whether single chain molecules consisting of four variable domains of two different specificities would form a stable homodimer with four antigen-binding sites. In contrast to previously described bivalent and bispecific scFv-scFv tandems (Gruber *et al.*, 1994; Kurucz *et al.*, 1995), this new class of tandem diabodies are tetravalent. The results presented here demonstrate that such Tandabs can be obtained in a functional form from *E. coli* by fusing two hybrid variable domain pairs in a single polypeptide. The order of V-domains and the linker peptides between them were designed such that each domain pairs with a complementary domain in another molecule (Tandab) or in the other half of the same molecule (single chain diabody).

Since our antibody fragments have genetically fused hexahistidine tags, we used immobilized metal affinity chromatography for the isolation of recombinant products from crude bacterial periplasmic extracts. If the His-tagged protein is highly over-expressed in *E. coli*, a one-step IMAC purification can result in sufficiently pure material for most applications (Casey *et al.*, 1995; Kipriyanov *et al.*, 1998). However, if the protein of interest is present only as a small fraction, several contaminating bacterial proteins can bind to the IMAC column under the purification conditions and co-elute (for a list of histidine-rich *E. coli* proteins, see Müller *et al.*, 1998a). For further purification of antibody fragments from IMAC-eluted material, either antigen-affinity chromatography (Kipriyanov *et al.*, 1994), thiophilic adsorption chromatography (Müller *et al.*, 1998b; Schulze *et al.*, 1994) or immunoaffinity purification using immobilized anti-His-tag monoclonal antibodies (Müller *et al.*, 1998a) have been used. Here, we describe a relatively simple alternative procedure based on the separation of proteins according to their solubility in imidazole-HCl buffer. We found that poorly expressed antibody fragments eluted from IMAC columns can be further enriched by buffer exchange with 50 mM imidazole-HCl (pH 6.4), and subsequently purified to homogeneity by ion-exchange chromatography in the same buffer. This approach was tested for a number of scFv-based recombinant proteins and seems to be generally applicable.

The dimerization of the four-domain single chain molecules proved to be dependent on the expression method. Dimers were probably a product of domain swapping (Bennett *et al.*, 1994) when obtained from soluble periplasmic extracts, whereas predominantly monomers were isolated from inclusion bodies after refolding. Similar observations on the formation of scFv dimers were made by Arndt *et al.* (1998). Major differences between periplasmic folding and refolding *in vitro* include high protein concentrations in the periplasm and the presence of bacterial chaperones. A rough estimation of the concentration of recombinant antibody during folding in the periplasmic space of bacteria indicated a 500-fold difference to the low concentrations employed for folding *in vitro* (Arndt *et al.*, 1998). The domain-swapped dimer is increasingly favored when the concentration of the protein increases (Schlunegger *et al.*, 1997). Some other unknown factors in the periplasm might also influence dimerization. Here, we demonstrate for the first time that inducing synthesis of recombinant antibody fragments in bacteria under osmotic stress promotes the formation of domain-swapped dimers. We tested the effect of adding non-metabolized low molecular mass compounds to the normal growth medium. These were 0.4 M sucrose and 1 M sorbitol in combination with 2.5 mM gly-

cine betaine, both of which were previously shown to inhibit aggregation and encourage correct folding of recombinant proteins in *E. coli* (Blackwell & Horgan, 1991; Bowden & Georgiou, 1990; Kipriyanov *et al.*, 1997a; Sawyer *et al.*, 1994). Although little is known about the mechanism of action of sucrose, sorbitol, or betaine on protein folding *in vivo*, these compounds appear to stabilize protein structures *in vitro* (Arakawa & Timasheff, 1985; Lee & Timasheff, 1981; Xie & Timasheff, 1997).

Dimers of the four-domain single chain molecules probably take the form of domain-swapped tandem diabody (Figure 1(c)). It is very likely that a high-energy barrier must be overcome for sc-diabody to open up and dimerize, as illustrated in Figure 9. To pass from a closed monomer (Figure 9(a)) to a domain-swapped dimer (Figure 9(f)), the sc-diabody must first pass through the open monomer form in which non-covalent bonds of the V_H/V_L interface are broken (Figure 9(b)). The sc-diabody is a functional four-domain protein stabilized by the non-covalent association of two V_H/V_L pairs (Figure 9(a)). These interactions can be substantial since the dissociation constants for Fv fragments can be in the range of 1-100 nM (Givol, 1991; Mallender *et al.*, 1996; Polymenis & Stollar, 1995). The energy barrier would probably be much higher than that required for the formation of Fv dimers (Arndt *et al.*, 1998), since a double open monomer is needed for swapping each domain (Figure 9(c)). The latter requirement can probably only be achieved under denaturing conditions. The same forces that stabilize the association of domains in the monomer must stabilize the dimer. Accordingly, the transition from a closed Tandab (Figure 9(e) and (f)) to the double open monomer (Figure 9(c)) requires the consecutive dissociation of four V_H/V_L complexes. This could explain why we did not see any interconversion between the sc-diabody and the Tandab *in vitro*, for example, under conditions of constitutive dilution during the re-chromatography of Tandabs, as was previously observed for non-covalent scFv dimers (Kipriyanov *et al.*, 1994), or during the concentration of the sc-diabody (data not shown). The incubation of Tandabs at 37°C for prolonged periods of time also did not cause any large decreases in antigen binding as would be expected for a dimer-monomer transition (Figures 4 and 7). It is therefore quite probable that the four-domain single chain molecules undergo dimerization during folding *in vivo*. This would occur if the association of folded domains is slow relative to domain folding. When closed monomer-stabilizing conditions are provided, the open monomers (Figure 9(c)) may either fold "head-to-tail" (Figure 9(b)) or swap domains with complementary ones of another molecule (Figure 9(d)). The solvent additives such as sucrose, sorbitol and betaine might affect the rate of intramolecular and intermolecular domain pairing and thus shift the monomer/dimer balance. For example, it was previously shown that the protein structure stabilizing properties of sucrose, sorbitol and betaine reflect their stronger exclusion from the unfolded protein than from the native structure (Arakawa & Timasheff, 1985; Lee & Timasheff, 1981; Xie & Timasheff, 1997). This interaction makes it thermodynamically unfavorable for proteins to unfold. An additional possibility is that the stabilizers influence periplasmic factors involved in protein folding.

We propose that both the diabody and the sc-diabody have fairly similar structures (Figure 1(b)), which appear to be reflected in their very close antigen-binding and biological characteristics. However, the linker of the sc-diabody may give rise to conformational changes in the V_H/V_L interface, since the sc-diabody bound with

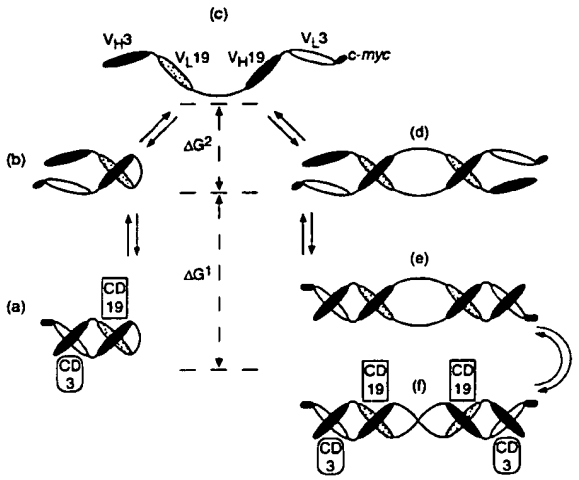

Figure 9. Model of putative pathways leading to sc-diabodies and domain-swapped dimers. The model describes the monomeric and dimeric species in three different forms, an open, a double open and a closed form. (a), (f) The closed form represents the stable bispecific molecule with intact V_H/V_L interfaces that is able to bind both antigens and cross-link two cells. (b), (d) In the open form, only half of the V_H/V_L complexes are formed, the two complementary domains can separate but are not able to change the oligomerization state. (c) The double open form represents the conformation of a monomer with no paired V-domains, which can adopt either the mono- or dimeric conformation. The V_H and V_L domains of both specificities as well as the C-terminal c-*myc* epitope are indicated. The filled arrows indicate possible transition pathways. The broken arrows illustrate putative free energy relationships between different monomeric and dimeric forms and indicate the presence of two transition steps. Depending on experimental conditions, either the monomer or the dimer can be the more stable molecular form. Tandabs shown in (e) and (f) illustrate different conformational states of the closed dimer. It is quite probable that after the first binding event to a cell surface the conformation of the dimer adjusts to enable bivalent binding to the same cell and the cross-linking of two cells.

somewhat higher affinity to $CD3^+$ cells than the diabody (Figure 4 and Table 1). Surprisingly, the diabody showed the highest fluorescence intensities on a weight basis among all examined antibodies when interacting with JOK-1 cells (Figure 4(a) and (c)). However, competition binding assays and cell-surface retention experiments demonstrated that the enhanced fluorescence signals of the diabody were not caused by enhanced affinity (Table 1); they are probably due to the smaller size of the diabody thus facilitating its binding to less accessible cell-anchored CD19 antigens or better presentation of the two c-*myc* epitopes for immunodetection.

Compared with the CD3 × CD19 diabody, the Tandabs exhibited a higher apparent affinity of antigen binding and slower dissociation from both $CD3^+$ and $CD19^+$ cells. *A priori*, it was unclear to what extent an affinity increase would occur with a Tandab that is potentially bivalent for each antigen. For example, the distance between the antigen-binding sites of the same specificity was expected to be shorter in the Tandab than in the IgG molecule. Furthermore, unlike the flexible Fab arms of an IgG that freely rotate on the hinge, the Tandab seemed to have a fairly rigid configuration (Figure 1(c)). If antigen-binding sites of the same specificity occurred only on different sides of the diabody tandem, bivalent cell binding would not have been possible. However, the cell surface retention assay clearly demonstrated bivalent cell binding for both of the Tandabs. A closer examination of the SL-Tandab model from a different perspective (top view) showed a boomerang-shaped symmetric structure with the two halves oriented at an angle of about 165° and separated by the two crossed linkers (Figure 10). The CDR loops of both CD19-binding sites appear to project in one direction, just opposite to the orientation of the anti-CD3 parts of the molecule. The distances between the CD19-binding sites in the SL and LL-Tandab were estimated to be 55 and 110 Å, respectively. Moreover, the CD3-binding sites, even in the SL-Tandab, can span a distance of up to 150 Å, which is similar to the stretch of Fab arms in an IgG molecule (Harris *et al.*, 1998). The molecular model was thus consistent with our experimental findings.

The length of the linker appeared to have some influence on antigen binding, since the LL-Tandab showed a significantly lower K_D and slower k_{off} from CD19-positive cells than the SL-Tandab (Table 1). This could be due to the larger distance between CD19-binding sites in the LL molecule and/or the higher flexibility and freedom of rotation that facilitate bivalent interaction with the cell. In contrast to their dissociation from $CD19^+$ cells, we did not observe any difference in k_{off} between LL and SL-Tandabs for dissociation from $CD3^+$ cells (Figure 4 and Table 1). This may indicate that the distance between the CD3-binding sites is sufficient in both molecules to achieve bivalent binding. In addition, the linker may affect the globular structure of Tandabs, which could account for the observed differences in their pharmacokinetic parameters.

The Tandabs were consistently more effective than the diabody for inducing T cell proliferation in the presence of tumor cells and in effector cell retargeting. As expected, both Tandabs had lower clearance rates compared to smaller antibody fragments such as the scFv and the diabody. The pharmacokinetic parameters ($t_{1/2}$ and AUC) of Tandabs proved to be quite similar to those of 100 kDa $F(ab')_2$ fragments and exceeded those of the smaller $(scFv')_2$ and Fab fragments (for a review, see Adams, 1998). We have shown here that both the sc-diabody and the Tandab are significantly more stable than the diabody *in vitro* and *in vivo* (Figure 7 and Table 2). They might therefore be

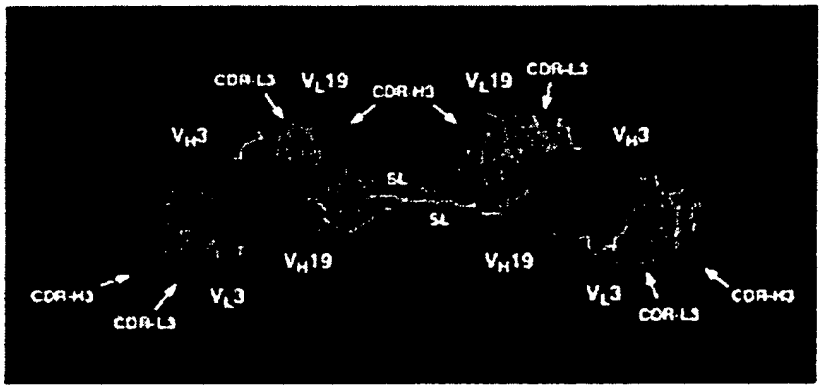

Figure 10. Structural model of SL-Tandab (top view). Anti-CD3 V_H and V_L domains are shown in red and green, anti-CD19 V_H and V_L in magenta and cyan, respectively. The linkers between V-domains and the SL-linkers are shown in yellow and white, respectively. To indicate the antigen-binding sites, the residues of the most hypervariable CDR-3 loops of either V-domain are shown in a spacefill mode. The Figure was generated using a molecular visualization program RasMol v2.5 (Roger Sayle, Biomolecular Structure, Glaxo Research and Development, Greenford, Middlesex, UK).

more useful than the smaller monovalent or bivalent antibody fragments for clinical applications where longer serum performance times are desirable. A further advantage of Tandabs is that they are homodimers stabilized by four interdomain pairings that assemble from a single homogeneous expression product. The bispecific diabody preparations, on the other hand, usually contain a significant proportion of non-functional homodimers (Zhu *et al.*, 1996, 1997), which makes it difficult to obtain a pure homogeneous product. If the Tandab dissociates, it can still form a functional single chain diabody. The construction of a sc-diabody is an alternative way to stabilize a bivalent bispecific diabody in addition to the incorporation of an intermolecular disulfide bridge or a knob-into-hole approach (FitzGerald *et al.*, 1997; Zhu *et al.*, 1997).

The novel bispecific recombinant molecules described here are potential immunotherapeutic agents for treating B cell leukemias and malignant lymphomas, since they bind to the human B cell surface antigen CD19 and the CD3ε chain of the human CD3/TCR complex. Two different approaches have been used previously to generate tetravalent bispecific antibodies: scFv fusion to whole IgG (Coloma & Morrison, 1997) and dimerization of scFv-scFv tandems *via* a linker containing a helix-loop-helix motif (Müller *et al.*, 1998b). In contrast, tandem diabodies comprise only antibody variable domains without the need of extra self-associating structures. To reduce the risk of an immune reaction, appropriate V_H and V_L fragments could be selected from a human antibody library. The linkers can also be easily replaced with ones of human origin. Tandem diabodies are therefore an attractive alternative to existing antibody-derived therapeutics for clinical applications.

Materials and Methods

Molecular modeling

A 3D model of the CD3 × CD19 diabody was generated using the Internet-based homology modeling software (WHATIF) of the EMBL BioComputing unit (http://swift.embl-heidelberg.de/servers/) (Rodriguez *et al.*, 1998). The experimentally solved structure of a bivalent diabody (PDB-entry 1LMK) (Perisic *et al.*, 1994) and a model of the OKT3 derived Fv fragment (Kipriyanov *et al.*, 1997b) were used as templates. The model optimization was performed using the Biopolymer option of Insight II (Molecular Simulations, San Diego, CA). A preliminary 3D structure of the 27 residue long linker was constructed by hand using the Protein option of the Insight II. This model was attached to the diabody structure to link the C terminus of V_L19 with the N terminus of V_H19. The linker was allowed to equilibrate and fit smoothly to the surface of the diabody by running molecular dynamic simulations at 300 K for 100 ps. During the simulation, only the atoms of the constructed linker were allowed to move. The model of the tandem diabody was constructed in a similar way with the exception that no molecular dynamic simulations were performed because of the large computational power required for molecules of such a size.

Plasmid construction

For all the cloning steps and DNA isolation, the *E. coli* K12 strain XL1-Blue (Stratagene, La Jolla, CA) was used. Plasmids pHOG3-19 and pHOG19-3 coding for hybrid V_H3-V_L19 and V_H19-V_L3 scFvs (Kipriyanov *et al.*, 1998) were used for assembly of sc-diabody and Tandab genes. The gene encoding scFv3-19 was amplified by PCR with the primers Bi3sk, 5'-CAG CCG GCC ATG GCG CAG GTG CAA CTG CAG CAG and either Li-1, 5'-TAT ATA CTG CAG CTG CAC CTG GCT ACC ACC ACC ACC GGA GCC GCC ACC ACC GCT ACC ACC GCC GCC AGA ACC ACC ACC ACC AGC GGC CGC AGC ATC AGC CCG to generate a long flexible $(Gly_4\text{-}Ser)_4$ intramolecular linker (PCR fragment 1) or Li-2, 5'-TAT ATA CTG CAG CTG CAC CTG CGA CCC TGG GCC ACC AGC GGC CGC AGC ATC AGC CCG to generate a short rigid Gly-Gly-Pro-Gly-Ser linker (PCR fragment 2). The expression plasmids pDISC1-LL and pDISC2-SL were constructed by ligation of the *NcoI*/*PvuII* restriction fragment from pHOG19-3 comprising the vector backbone and the *NcoI*/*PvuII* digested PCR fragments 1 and 2, respectively.

The improved expression vectors were constructed to include the *hok/sok* plasmid-free cell suicide system (Thisted *et al.*, 1994) and a gene encoding the Skp/OmpH periplasmic factor for higher recombinant antibody production (Bothmann & Plückthun, 1998). The *skp* gene was amplified by PCR with primers skp-1, 5'-CGA ATT CTT AAG ATA AGA AGG AGT TTA TTG TGA AAA AGT GGT TAT TAG CTG CAG G and skp-2, 5'-CGA ATT AAG CTT CAT TAT TTA ACC TGT TTC AGT ACG TCG G using as a template the plasmid pGAH317 (Holck & Kleppe, 1988) kindly provided by Dr R. Chen (Max-Plank Institute for Biology, Tübingen, Germany). The resulting PCR fragment was digested with *AflII* and *HindIII* and cloned into the *AflII*/*HindIII* linearized plasmid pHKK (Horn *et al.*, 1996) (kind gift of Dr D. Riesenberg, NKI, Jena, Germany) generating the vector pSKK1. The genes coding for four domain single chain molecules in plasmids pDISC1-LL and pDISC2-SL were amplified by PCR with primers fe-1, 5'-CGA ATT TCT AGA TAA GAA GGA GAA ATT AAC CAT GAA ATA CC and fe-2, 5'-CGA ATT CTT AAG CTA TTA GTG ATG GTG ATG GTG ATG TGA G. The *XbaI*/*AflII* digested PCR fragments were cloned into pSKK in front of the *skp* insert resulting in expression plasmids pDISC5-LL and pDISC6-SL containing tri-cistronic operons (*lacZ'*, gene encoding the four domain single chain molecule, *skp*) under the control of the *lac* promoter/operator system.

For expression of four-domain single chain molecules as periplasmic inclusion bodies, the *EcoRI*/*XbaI* fragments of plasmids pDISC1-LL and pDISC2-SL comprising antibody genes preceded by a PelB leader sequence were cloned into pOPE51 (Kipriyanov *et al.*, 1994) generating the expression vectors pOPE-LL and pOPE-SL, respectively. The sequences of all newly constructed genes and plasmids were verified by restriction digests and dideoxy sequencing (Sanger *et al.*, 1977).

Protein expression and purification

For functional expression of recombinant antibodies in the bacterial periplasm, the plasmids pDISC5-LL and pDISC6-SL were transformed into *E. coli* K12 strain RV308 (Δ*lac*χ74 *gal*ISII::OP308*strA*) (Maurer *et al.*, 1980)

kindly provided by Dr A. Plückthun (University of Zürich, Zürich, Switzerland). Transformed bacteria were grown overnight in shake flasks containing 2 × YT medium with 0.1 g/l ampicillin and 100 mM glucose (2 × YT_{GA}) at 26 °C. Dilutions (1:50) of the overnight cultures in 2 × YT_{GA} were grown as flask cultures at 25 °C with shaking at 200 rpm. When cultures reached $A_{600\,nm} = 0.6$, bacteria either were induced by adding IPTG to a final concentration of 0.2 mM or were harvested by centrifugation at 20 °C. The pelleted bacteria were resuspended in the same volume of either fresh 2 × YT_{SA} (2 × YT containing 0.1 g/l ampicillin and 0.4 M sucrose; Kipriyanov *et al.*, 1997a) or YTBS medium (2 × YT containing 1 M sorbitol and 2.5 mM glycine betaine; Blackwell & Horgan, 1991). IPTG was added to a final concentration of 0.2 mM and growth was continued at 24 °C for 14-16 hours. The bacterial cells were then harvested by centrifugation and periplasmic extracts were isolated as previously described (Kipriyanov *et al.*, 1997a,b). The periplasmic fractions were dialyzed against start buffer (50 mM Tris-HCl, 1 M NaCl, pH 7.0) at 4 °C. The four-domain single chain molecules were purified by IMAC using Ni-NTA-Superflow resin (Qiagen, Hilden, Germany). After washing with start buffer containing 20 mM imidazole (pH 7.0), the absorbed protein was eluted with 0.3 M imidazole in start buffer (pH 7.0). The elution fractions containing recombinant antibodies were identified by Western blot analysis using anti-c-*myc* MAb 9E10 (IC Chemikalien, Ismaning, Germany) performed as previously described (Kipriyanov *et al.*, 1994). Positive Western blot fractions were pooled and subjected to buffer exchange for 50 mM imidazole-HCl (pH 6.4) using pre-packed PD-10 columns (Pharmacia Biotech, Freiburg, Germany). The turbidity of protein solution was removed by centrifugation. The final purification of four domain single chain molecules was achieved by ion-exchange chromatography on a Mono S HR5/5 column (Pharmacia) in 50 mM imidazole-HCl (pH 6.4), with a linear 0-1 M NaCl gradient. The purified antibody preparations were concentrated and resolved by size-exclusion FPLC on a Superdex 200 HR10/30 column (Pharmacia) in PBSI (15 mM sodium phosphate, 0.15 M NaCl, 50 mM imidazole, pH 7.0). Sample volumes for analytical and preparative chromatographies were 50 and 500 µl, respectively. The column was calibrated with high and low molecular mass gel filtration calibration kits (Pharmacia). All purification procedures were performed at 4 °C. Isolation of the anti-CD3 scFv and CD3 × CD19 diabody was performed as described (Kipriyanov *et al.*, 1997b, 1998).

Growth and induction of *E. coli* XL1-Blue cells (Stratagene) transformed either with pOPE-LL or pOPE-SL plasmids as well as isolation of periplasmic inclusion bodies and purification of recombinant protein by IMAC under denaturing conditions were performed essentially as described (Kipriyanov *et al.*, 1996b). After IMAC, the eluted protein was reduced with 0.3 M DTE for two hours at ambient temperature and the four-domain single chain molecules were refolded by step-wise dialysis in presence of oxidized glutathione as described (Tsumoto *et al.*, 1998).

For long-time storage, antibody preparations were frozen in the presence of 2% human serum albumin (Immuno GmbH, Heidelberg, Germany) and stored at −80 °C.

Measurement of protein concentration

The concentrations of purified scFv, diabody, sc-diabody and SL-Tandab were determined from the $A_{280\,nm}$ values using the extinction coefficients $\varepsilon^{1\,mg/ml} = 1.84$, 1.89, 1.93 and 1.96, respectively, calculated as described by Gill & von Hippel (1989).

Flow cytometry

The human $CD3^+/CD19^-$ acute T cell leukemia line Jurkat and the $CD19^+/CD3^-$ B cell line JOK-1 were used for flow cytometry as described (Kipriyanov *et al.*, 1998).

Affinity determination

The apparent affinities of the bispecific molecules were determined from competitive inhibition assays as previously described (Kipriyanov *et al.*, 1997b, 1998). Briefly, increasing concentrations of purified antibody fragment were added to a subsaturating concentration of FITC-labeled MAb OKT3 (anti-CD3) or HD37 (anti-CD19) and were incubated with Jurkat or JOK-1 cells, respectively. Fluorescence intensities of stained cells were measured using a FACScan flow cytometer (Becton Dickinson, Mountain View, CA). Binding affinities were calculated according to the following equation (Schodin & Kranz, 1993): $K_{D(I)} = IC_{50}/(1 + [\text{FITC-MAb}]/K_{D(MAb)})$, where I is the unlabeled inhibitor (diabody, sc-diabody or Tandab), [FITC-MAb] is the concentration of FITC-labeled MAb, $K_{D(MAb)}$ is the binding affinity of MAb and IC_{50} is the concentration of inhibitor that yields 50% inhibition of binding. Affinity constant (K_D) values of 0.8 and 0.4 nM were assigned to MAb OKT3 (Adair *et al.*, 1994) and HD37 (Kipriyanov *et al.*, 1998), respectively.

In vitro cell surface retention

Cell surface retention assays were performed at 37 °C essentially as described (Adams *et al.*, 1998) except that the detection of the retained antibody fragments was performed using anti-c-*myc* MAb 9E10 (IC Chemikalien) followed by FITC-labeled anti-mouse IgG. Kinetic dissociation constants (k_{off}) were calculated using a first order equation $F_t = F_0 e^{-kt}$, where F_t is a fluorescence at time t, F_0 is a fluorescence at time 0 and k is k_{off}. The half-life ($t_{1/2}$) for dissociation of antibody fragments was calculated from the equation $t_{1/2} = \ln 2/k_{off}$.

Cell proliferation assay

Human PBL (1×10^4/well) were cultured together with irradiated (120 rad) $CD19^+$ Burkitt's lymphoma Raji cells (2.5×10^5/well) in 96-well plate for five days in IMEM (Sigma, Deisenhofen, Germany) supplemented with 10% human AB serum (Sigma), 25 units/ml of recombinant human IL-2 (Chiron Corp., Emeryville, CA) and varying amounts of antibody fragments. ^{3}H-thymidine (0.5 µCi/well) was added 12 hours prior to harvesting. The cells were harvested and ^{3}H-thymidine incorporation was measured with a liquid scintillation beta-counter (Beckman, Palo Alto, CA).

Cytotoxicity assay

The efficacy of the BsAbs for mediating tumor cell lysis by activated human PBLs was determined using the JAM test (Matzinger, 1991). Briefly, 2.5×10^5

activated human PBLs prepared as described (Kipriyanov *et al.*, 1998), were mixed in round-bottomed microtiter plates with 1×10^4 of Raji cells labeled with [^{3}H]-thymidine (effector:target ratio = 25:1) in 100 µl medium plus 50 µl of antibody sample. After incubating the plate at 37 °C, 5 % CO_2 for four hours, the cells were harvested and radioactivity was measured with a liquid scintillation beta counter. Each experiment was carried out in triplicate. Specific killing (%) was calculated as (Matzinger, 1991): $(S\text{-}E)/S \times 100$, where E is experimentally retained labeled DNA in the presence of killers (in cpm) and S is retained DNA in the absence of killers (spontaneous).

Analyses of antibody stability *in vitro*

The antibody fragments were diluted (at least 20-fold) in human serum (Sigma) to a concentration of 15 µg/ml and sterilized by filtration through a Membrex 4CA filter with a void volume of 50 µl and a pore size 0.2 µm (MembraPure, Lörzweiler, Germany). Aliquots (100 µl) were prepared at once under sterile conditions and stored at 37 °C. At given time points, the aliquots were frozen and kept at −80 °C. Activities of the samples after storage were determined by flow cytometry using CD3$^+$ Jurkat cells. Protein degradation in each sample was determined by SDS-12 % PAGE followed by Western blot analysis using anti-c-*myc* MAb 9E10 as described (Kipriyanov *et al.*, 1994).

Radioiodination

Antibody solutions (1 mg/ml in 50 mM Tris-HCl, 1 M NaCl, pH 7.0) were placed in glass tubes coated with 20 µg of IODO-Gen (Pierce, Rockford, IL) per mg of protein. After adding 3 mCi of [^{125}I]iodide (Amersham Buchler, Braunschweig, Germany), the resulting mixture was incubated for ten minutes at room temperature. Unincorporated radioiodine was separated from the labeled protein by size-exclusion chromatography using Bio-Gel P6 (Bio-Rad, Munich, Germany) and PBSI as the elution buffer. The final specific activities of scFv, diabody, LL and SL-Tandab were 2.4, 6.6, 4.0 and 3.8 mCi/mg, respectively.

Pharmacokinetic studies

Male NMRI mice each weighing approximately 40 g (24-27 animals for each labeled protein) were injected into the tail vein with 200 µl of PBSI containing 10 µg of human serum albumin and 5 µg of labeled antibody fragments. At the indicated time points, animals in triplicates were anaesthetized, bled and sacrificed in accordance with local animal protection laws. For scFv, the blood samples were obtained at 5, 10, 20, 40, 90, 180, 360 and 1080 minutes after injection. The time points for the diabody and tandem diabodies were the same, except that the last animal groups were sacrificed 24 hours after injection of the labeled compounds. Blood samples were counted using a gamma counter. Blood content was corrected for protein bound radioactivity (see below) and expressed as a percentage of injected dose per gram of blood (%ID/g). AUC was calculated using GraphPad Prism (GraphPad Software, San Diego, CA) and expressed as %ID/g per minute. The $t_{1/2}\alpha$ was defined by time points 5, 10, 20 and 40 minutes, while the $t_{1/2}\beta$ was defined by time points from 1.5 to 24 hours.

Analyses of antibody stability *in vivo*

A 200 µl sample of blood from each sacrificed animal mixed with 10 µl of heparin (5000 units/ml; Braun Melsungen AG, Melsungen, Germany) followed by sedimentation of cellular material and TCA precipitation of the supernatant. Radioactivity associated with pellets and supernatants was counted and expressed as a percentage of total radioactivity (cpm) for each specific time point. Pooled plasma samples from the earlier time points (up to 1.5 hours) were also analyzed by SDS-12 % PAGE followed by autoradiography.

References

Adair, J. R., Athwal, D. S., Bodmer, M., Bright, S. M., Collins, A., Pulito, V. L., Rao, P. E., Reedman, R., Rothermel, A. L., Xu, D., Zivin, R. A. & Jolliffe, L. K. (1994). Humanization of the murine anti-human CD3 monoclonal antibody OKT3. *Human Antibodies Hybrid.* **5**, 41-47.

Adams, G. P. (1998). Improving the tumor specificity and retention of antibody-based molecules. *In Vivo,* **12**, 11-21.

Adams, G. P., Schier, R., Marshall, K., Wolf, E. J., McCall, A. M., Marks, J. D. & Weiner, L. M. (1998). Increased affinity leads to improved selective tumor delivery of single-chain Fv antibodies. *Cancer Res.* **58**, 485-490.

Arakawa, T. & Timasheff, S. N. (1985). The stabilization of proteins by osmolytes. *Biophys. J.* **47**, 411-414.

Arndt, K. M., Müller, K. M. & Plückthun, A. (1998). Factors influencing the dimer to monomer transition of an antibody single-chain Fv fragment. *Biochemistry,* **37**, 12918-12926.

Arndt, M., Krauss, J., Kipriyanov, S. M., Pfreundschuh, M. & Little, M. (1999). A bispecific diabody that mediates natural killer cell cytotoxicity against xenotransplanted human Hodgkin's tumors. *Blood,* **94**, 2562-2568.

Bennett, M. J., Choe, S. & Eisenberg, D. (1994). Domain swapping: entangling alliances between proteins. *Proc. Natl Acad. Sci. USA,* **91**, 3127-3131.

Blackwell, J. R. & Horgan, R. (1991). A novel strategy for production of a highly expressed recombinant protein in an active form. *FEBS Letters,* **295**, 10-12.

Bohlen, H., Hopff, T., Manzke, O., Engert, A., Kube, D., Wickramanayake, P. D., Diehl, V. & Tesch, H. (1993). Lysis of malignant B cells from patients with B-chronic lymphocytic leukemia by autologous T cells activated with CD3 x CD19 bispecific antibodies in combination with bivalent CD28 antibodies. *Blood,* **82**, 1803-1812.

Bothmann, H. & Plückthun, A. (1998). Selection for a periplasmic factor improving phage display and functional periplasmic expression. *Nature Biotechnol.* **16**, 376-380.

Bowden, G. A. & Georgiou, G. (1990). Folding and aggregation of beta-lactamase in the periplasmic space of *Escherichia coli*. *J. Biol. Chem.* **265**, 16760-16766.

Brennan, M., Davidson, P. F. & Paulus, H. (1985). Preparation of bispecific antibodies by chemical recombination of monoclonal immunoglobulin G1 fragments. *Science,* **229**, 81-83.

Carter, P., Ridgway, J. & Zhu, Z. (1995). Toward the production of bispecific antibody fragments for clinical applications. *J. Hematother.* **4**, 463-470.

Casey, J. L., Keep, P. A., Chester, K. A., Robson, L., Hawkins, R. E. & Begent, R. H. (1995). Purification of bacterially expressed single chain Fv antibodies for clinical applications using metal chelate chromatography. *J. Immunol. Methods*, **179**, 105-116.

Coloma, M. J. & Morrison, S. L. (1997). Design and production of novel tetravalent bispecific antibodies. *Nature Biotechnol.* **15**, 159-163.

de Kruif, J. & Logtenberg, T. (1996). Leucine zipper dimerized bivalent and bispecific scFv antibodies from a semi-synthetic antibody phage display library. *J. Biol. Chem.* **271**, 7630-7634.

Fanger, M. W., Morganelli, P. M. & Guyre, P. M. (1992). Bispecific antibodies. *Crit. Rev. Immunol.* **12**, 101-124.

FitzGerald, K., Holliger, P. & Winter, G. (1997). Improved tumour targeting by disulphide stabilized diabodies expressed in *Pichia pastoris*. *Protein Eng.* **10**, 1221-1225.

Gill, S. C. & von Hippel, P. H. (1989). Calculation of protein extinction coefficients from amino acid sequence data. *Anal. Biochem.* **182**, 319-326.

Givol, D. (1991). The minimal antigen-binding fragment of antibodies-Fv fragment. *Mol. Immunol.* **28**, 1379-1386.

Glennie, M. J., McBride, H. M., Worth, A. T. & Stevenson, G. T. (1987). Preparation and performance of bispecific $F(ab'\gamma)_2$ antibody containing thioether-linked $Fab'\gamma$ fragments. *J. Immunol.* **139**, 2367-2375.

Glockshuber, R., Malia, M., Pfitzinger, I. & Plückthun, A. (1990). A comparison of strategies to stabilize immunoglobulin Fv-fragments. *Biochemistry*, **29**, 1362-1367.

Gruber, M., Schodin, B. A., Wilson, E. R. & Kranz, D. M. (1994). Efficient tumor cell lysis mediated by a bispecific single chain antibody expressed in *Escherichia coli*. *J. Immunol.* **152**, 5368-5374.

Harris, L. J., Skaletsky, E. & McPherson, A. (1998). Crystallographic structure of an intact IgG1 monoclonal antibody. *J. Mol. Biol.* **275**, 861-872.

Holck, A. & Kleppe, K. (1988). Cloning and sequencing of the gene for the DNA-binding 17 K protein of *Escherichia coli*. *Gene*, **67**, 117-124.

Holliger, P., Prospero, T. & Winter, G. (1993). "Diabodies": small bivalent and bispecific antibody fragments. *Proc. Natl Acad. Sci. USA*, **90**, 6444-6448.

Holliger, P., Brissinck, J., Williams, R. L., Thielemans, K. & Winter, G. (1996). Specific killing of lymphoma cells by cytotoxic T-cells mediated by a bispecific diabody. *Protein Eng.* **9**, 299-305.

Horn, U., Strittmatter, W., Krebber, A., Knupfer, U., Kujau, M., Wenderoth, R., Müller, K., Matzku, S., Plückthun, A. & Riesenberg, D. (1996). High volumetric yields of functional dimeric miniantibodies in *Escherichia coli*, using an optimized expression vector and high-cell-density fermentation under non-limited growth conditions. *Appl. Microbiol. Biotechnol.* **46**, 524-532.

Huston, J. S., Levinson, D., Mudgett, Hunter M., Tai, M. S., Novotny, J., Margolies, M. N., Ridge, R. J., Bruccoleri, R. E., Haber, E., Crea, R. & Oppermann, H. (1988). Protein engineering of antibody binding sites: recovery of specific activity in an anti-digoxin single-chain Fv analogue produced in *Escherichia coli*. *Proc. Natl Acad. Sci. USA*, **85**, 5879-5883.

Khazaeli, M. B., Conry, R. M. & LoBuglio, A. F. (1994). Human immune response to monoclonal antibodies. *J. Immunother.* **15**, 42-52.

Kipriyanov, S. M., Dübel, S., Breitling, F., Kontermann, R. E. & Little, M. (1994). Recombinant single-chain Fv fragments carrying C-terminal cysteine residues: production of bivalent and biotinylated miniantibodies. *Mol. Immunol.* **31**, 1047-1058.

Kipriyanov, S. M., Kupriyanova, O. A., Little, M. & Moldenhauer, G. (1996a). Rapid detection of recombinant antibody fragments directed against cell-surface antigens by flow cytometry. *J. Immunol. Methods*, **196**, 51-62.

Kipriyanov, S. M., Little, M., Kropshofer, H., Breitling, F., Gotter, S. & Dübel, S. (1996b). Affinity enhancement of a recombinant antibody: formation of complexes with multiple valency by a single-chain Fv fragment-core streptavidin fusion. *Protein Eng.* **9**, 203-211.

Kipriyanov, S. M., Moldenhauer, G. & Little, M. (1997a). High level production of soluble single chain antibodies in small-scale *Escherichia coli* cultures. *J. Immunol. Methods*, **200**, 69-77.

Kipriyanov, S. M., Moldenhauer, G., Martin, A. C., Kupriyanova, O. A. & Little, M. (1997b). Two amino acid mutations in an anti-human CD3 single chain Fv antibody fragment that affect the yield on bacterial secretion but not the affinity. *Protein Eng.* **10**, 445-453.

Kipriyanov, S. M., Moldenhauer, G., Strauss, G. & Little, M. (1998). Bispecific CD3 x CD19 diabody for T cell-mediated lysis of malignant human B cells. *Int. J. Cancer*, **77**, 763-772.

Kung, P. C., Golstein, G., Reinherz, E. L. & Schlossman, S. F. (1979). Monoclonal antibodies defining distinctive human T cell surface antigens. *Science*, **206**, 347-349.

Kurucz, I., Titus, J. A., Jost, C. R., Jacobus, C. M. & Segal, D. M. (1995). Retargeting of CTL by an efficiently refolded bispecific single-chain Fv dimer produced in bacteria. *J. Immunol.* **154**, 4576-4582.

Lee, J. C. & Timasheff, S. N. (1981). The stabilization of proteins by sucrose. *J. Biol. Chem.* **256**, 7193-7201.

Le, Gall F., Kipriyanov, S. M., Moldenhauer, G. & Little, M. (1999). Di-, tri- and tetrameric single chain Fv antibody fragments against human CD19: effect of valency on cell binding. *FEBS Letters*, **453**, 164-168.

Mallender, W. D., Carrero, J. & Voss, E. (1996). Comparative properties of the single chain antibody and Fv derivatives of mAb 4-4-20. Relationship between interdomain interactions and the high affinity for fluorescein ligand. *J. Biol. Chem.* **271**, 5338-5346.

Matzinger, P. (1991). The JAM test. A simple assay for DNA fragmentation and cell death. *J. Immunol. Methods*, **145**, 185-192.

Maurer, R., Meyer, B. & Ptashne, M. (1980). Gene regulation at the right operator (O_R) bacteriophage λ. I. O_R3 and autogenous negative control by repressor. *J. Mol. Biol.* **139**, 147-161.

Müller, K. M., Arndt, K. M., Bauer, K. & Plückthun, A. (1998a). Tandem immobilized metal-ion affinity chromatography/immunoaffinity purification of His-tagged proteins-evaluation of two anti-His-tag monoclonal antibodies. *Anal. Biochem.* **259**, 54-61.

Müller, K. M., Arndt, K. M. & Plückthun, A. (1998b). A dimeric bispecific miniantibody combines two specificities with avidity. *FEBS Letters*, **432**, 45-49.

Müller, K. M., Arndt, K. M., Strittmatter, W. & Plückthun, A. (1998c). The first constant domain (C_H1 and C_L) of an antibody used as heterodimerization domain for bispecific miniantibodies. *FEBS Letters*, **422**, 259-264.

Nieba, L., Honegger, A., Krebber, C. & Pluckthun, A. (1997). Disrupting the hydrophobic patches at the antibody variable/constant domain interface: improved *in vivo* folding and physical characterization of an engineered scFv fragment. *Protein Eng.* **10**, 435-444.

Perisic, O., Webb, P. A., Holliger, P., Winter, G. & Williams, R. L. (1994). Crystal structure of a diabody, a bivalent antibody fragment. *Structure*, **2**, 1217-1226.

Pezzutto, A., Dörken, B., Rabinovitch, P. S., Ledbetter, J. A., Moldenhauer, G. & Clark, E. A. (1987). CD19 monoclonal antibody HD37 inhibits anti-immunoglobulin-induced B cell activation and proliferation. *J. Immunol.* **138**, 2793-2799.

Plückthun, A. & Pack, P. (1997). New protein engineering approaches to multivalent and bispecific antibody fragments. *Immunotechnology*, **3**, 83-105.

Polymenis, M. & Stollar, B. D. (1995). Domain interactions and antigen binding of recombinant anti-Z-DNA antibody variable domains. The role of heavy and light chains measured by surface plasmon resonance. *J. Immunol.* **154**, 2198-2208.

Ridder, R., Schmitz, R., Legay, F. & Gram, H. (1995). Generation of rabbit monoclonal antibody fragments from a combinatorial phage display library and their production in the yeast *Pichia pastoris*. *Bio/Technology*, **13**, 255-260.

Rodriguez, R., Chinea, G., Lopez, N., Pons, T. & Vriend, G. (1998). Homology modeling, model and software evaluation: three related resources. *Bioinformatics*, **14**, 523-528.

Sanger, F., Nicklen, S. & Coulson, A. R. (1977). DNA sequencing with chain-terminating inhibitors. *Proc. Natl Acad. Sci. USA*, **74**, 5463-5467.

Sawyer, J. R., Schlom, J. & Kashmiri, S. V. S. (1994). The effect of induction conditions on production of a soluble anti-tumor sFv in *Escherichia coli*. *Protein Eng.* **7**, 1401-1406.

Schlunegger, M. P., Bennett, M. J. & Eisenberg, D. (1997). Oligomer formation by 3D domain swapping: a model for protein assembly and misassembly. *Advan. Protein Chem.* **50**, 61-122.

Schodin, B. A. & Kranz, D. M. (1993). Binding affinity and inhibitory properties of a single-chain anti-T cell receptor antibody. *J. Biol. Chem.* **268**, 25722-25727.

Schulze, R. A., Kontermann, R. E., Queitsch, I., Dübel, S. & Bautz, E. K. (1994). Thiophilic adsorption chromatography of recombinant single-chain antibody fragments. *Anal. Biochem.* **220**, 212-214.

Shusta, E. V., Raines, R. T., Plückthun, A. & Wittrup, K. D. (1998). Increasing the secretory capacity of *Saccharomyces cerevisiae* for production of single-chain antibody fragments. *Nature Biotechnol.* **16**, 773-777.

Thisted, T., Sorensen, N. S., Wagner, E. G. & Gerdes, K. (1994). Mechanism of post-segregational killing: Sok antisense RNA interacts with Hok mRNA via its 5'-end single-stranded leader and competes with the 3'-end of Hok mRNA for binding to the mok translational initiation region. *EMBO J.* **13**, 1960-1968.

Tsumoto, K., Shinoki, K., Kondo, H., Uchikawa, M., Juji, T. & Kumagai, I. (1998). Highly efficient recovery of functional single-chain Fv fragments from inclusion bodies overexpressed in *Escherichia coli* by controlled introduction of oxidizing reagent-application to a human single-chain Fv fragment. *J. Immunol. Methods*, **219**, 119-129.

Uckun, F. M. & Ledbetter, J. A. (1988). Immunobiologic differences between normal and leukemic human B-cell precursors. *Proc. Natl Acad. Sci. USA*, **85**, 8603-8607.

Xie, G. & Timasheff, S. N. (1997). Mechanism of the stabilization of ribonuclease A by sorbitol: preferential hydration is greater for the denatured then for the native protein. *Protein Sci.* **6**, 211-221.

Zhu, Z., Zapata, G., Shalaby, R., Snedecor, B., Chen, H. & Carter, P. (1996). High level secretion of a humanized bispecific diabody from *Escherichia coli*. *Bio/Technology*, **14**, 192-196.

Zhu, Z., Presta, L. G., Zapata, G. & Carter, P. (1997). Remodeling domain interfaces to enhance heterodimer formation. *Protein Sci.* **6**, 781-788.

Edited by J. Karn

(Received 8 June 1999; received in revised form 1 September 1999; accepted 1 September 1999)

Int. J. Cancer: 77, 763–772 (1998)

Publication of the International Union Against Cancer
Publication de l'Union Internationale Contre le Cancer

BISPECIFIC CD3 × CD19 DIABODY FOR T CELL-MEDIATED LYSIS OF MALIGNANT HUMAN B CELLS

Sergey M. KIPRIYANOV[1], Gerhard MOLDENHAUER[2], Gudrun STRAUSS[2] and Melvyn LITTLE[1]*

[1]*Recombinant Antibody Research Group, Diagnostics and Experimental Therapy Program, German Cancer Research Center (DKFZ), Heidelberg, Germany*

[2]*Department of Molecular Immunology, Tumor Immunology Program, DKFZ, Heidelberg, Germany*

For the treatment of minimal residual disease in patients with leukemias and malignant lymphomas, we constructed a heterodimeric diabody specific for human CD19 on B cells and CD3ε chain of the T cell receptor complex. The bispecific diabody was expressed in *Escherichia coli* using a vector containing a dicistronic operon for co-secretion of V_H3-V_L19 and V_H19-V_L3 single-chain Fv fragments (scFv). It was purified in one step by immobilized metal affinity chromatography (IMAC) from the periplasmic extract and culture medium. Flow cytometry experiments revealed specific interactions of the diabody with both CD3 and CD19 positive cells, to which it bound with affinities close to those of the parental scFvs. It was less stable than anti-CD3 scFv but more stable than anti-CD19 scFv when incubated in human serum at 37°C. In cytotoxicity tests, the diabody proved to be a potent agent for retargeting peripheral blood lymphocytes to lyse tumor cells expressing the CD19 antigen. The efficiency of cell lysis compared favorably with that obtained with a bispecific antibody (BsAb) of the same dual specificity that was prepared by the quadroma technique. *Int. J. Cancer* 77:763–772, 1998.
© *1998 Wiley-Liss, Inc.*

B cell leukemias and malignant lymphomas represent a heterogeneous group of hematological malignancies occurring in blood, lymph nodes and bone marrow, which frequently disseminate throughout the body. The most common forms of non-Hodgkin's ymphoma (NHL) are derived from the B cell lineage. The incidence of NHL (6–17/100,000) continues to increase worldwide at about 4% a year. Although NHL can be treated with reasonable success at early and intermediate stages, the results of conventional chemotherapy and radiation in advanced stages remain disappointing. This holds particularly true for the prevalent low-grade lymphomas. A fairly large number of patients relapse, and most remissions cannot be extended beyond minimal residual disease. In this case, high-dose chemotherapy combined with total body irradiation together with the support of an autologous bone marrow transplantation (BMT) or peripheral blood stem cell transplantation (PBSCT) offers an alternative means of curing the disease. However, an important issue still to be solved concerns the presence of residual tumor cells in the patient that give rise to a recurrence of the leukemia or lymphoma.

To eradicate residual tumor cells, BsAbs have been proposed as a means of recruiting cytotoxic T cells for killing tumor cells (Fanger *et al.*, 1992). For example, clinical studies have shown tumor regression in patients treated with BsAb directed against tumor antigens and the CD3 component of the T cell receptor complex, respectively (Canevari *et al.*, 1995; Nitta *et al.*, 1990). One of the best targets for bispecific antibodies on malignant human B cells is CD19 (Grossbard *et al.*, 1992). This antigen is expressed on virtually all B-lineage malignancies from acute lymphoblastic leukemia (ALL) to NHL. Moreover, it is not shed and is absent from hemopoietic stem cells, plasma cells, T cells and other tissues. A potential disadvantage is that normal B cells may also be killed by CD3 × CD19 BsAb treatment. However, these cells are rapidly replaced by differentiation from the stem cell pool.

Various strategies have been utilized for the creation of BsAbs. Heteroconjugates have been produced by chemical cross-linking of 2 monoclonal antibodies (MAb) (Anderson *et al.*, 1992) or Fab' fragments (Brennan *et al.*, 1985). Alternatively, BsAbs were produced using hybrid hybridoma (quadroma) technology (Bohlen *et al.*, 1993; Csóka *et al.*, 1996). A major limitation of this procedure is the production of inactive antibodies due to the random L-H and H-H associations. Only about 15% of the antibody produced by the quadroma is of the desired specificity (Milstein and Cuello, 1983). The correct BsAb must then be purified in a costly procedure from a large quantity of other very similar molecules. A further limitation of the quadroma BsAb from rodent cell lines is their immunogenicity. Repeated doses of rodent antibodies elicit an anti-immunoglobulin response, referred to as HAMA (human anti-murine antibody).

Some of the limitations of MAbs as therapeutic agents have recently been addressed by genetic engineering (Winter and Milstein, 1991) including a few methods for BsAb fragment production (Carter *et al.*, 1995). Bispecific $F(ab')_2$ have been created either by chemical coupling from Fab' fragments expressed in *E. coli* (Shalaby *et al.*, 1992) or by heterodimerization through leucine zippers (Kostelny *et al.*, 1992). Even smaller BsAb fragments have been constructed based on scFv: the association of V_H and V_L domains is stabilized by a flexible polypeptide linker (Bird *et al.*, 1988). The genetic engineering of 2 scFvs linked with a third polypeptide linker, as initially suggested by Huston *et al.*, (1991), has now been carried out in several laboratories for the production of bispecific single-chain antibody segments $(scFv)_2$ with a potential anti-tumor activity (Gruber *et al.*, 1994; Mack *et al.*, 1995).

An alternative BsAb fragment is the scFv heterodimer diabody (Holliger *et al.*, 1993). It is formed by the non-covalent association of 2 single-chain fusion products consisting of the V_H domain from one antibody connected by a short linker to the V_L domain of another antibody (Atwell *et al.*, 1996; Holliger *et al.*, 1996; Zhu *et al.*, 1996). The 2 antigen binding domains have been shown by crystallographic analysis to be on opposite sides of the complex such that they are able to cross-link 2 cells (Perisic *et al.*, 1994).

Starting with the mRNA of hybridoma cells HD37 (Pezzutto *et al.*, 1987) and OKT3 (Kung *et al.*, 1979), we previously constructed recombinant scFv antibody fragments specific for the human B cell antigen CD19 (Kipriyanov *et al.*, 1996) and the CD3ε chain of the human CD3/T cell receptor complex (Kipriyanov *et al.*, 1997*b*). Here, we describe the construction and production of a bispecific diabody in bacteria with dual specificity for both the human B cell antigen CD19 and CD3/TCR. The diabody has been compared with parental scFvs with respect to its stability in human serum at 37°C and binding affinity to both CD19-positive human B cells and CD3-positive human T cells. In cytotoxic assays, the CD3 × CD19 diabody was able to retarget human PBL to malignant B cells. The efficiency of cell lysis compared favorably with that obtained with a BsAb of the same dual specificity prepared by the quadroma technique.

Grant sponsor: Deutsche Krebshilfe/Mildred Scheel Stiftung.

*Correspondence to: Recombinant Antibody Research Group (D0500), German Cancer Research Center, Im Neuenheimer Feld 280, D-69120 Heidelberg, Germany. Fax: (49)6221-423-462.
E-mail: m.little@dkfz-heidelberg.de

Received 23 January 1998; Revised 6 March 1998

MATERIAL AND METHODS

Monoclonal antibodies

The CD3 ϵ-chain-specific hybridoma cell line OKT3 secreting an IgG_{2a} MAb (Kung *et al.*, 1979) was obtained from the ATCC (Rockville, MD). The HD37 cell line produces a MAb (IgG_1) reactive with the human CD19 molecule and has been described in detail (Pezzutto *et al.*, 1987). Monoclonal antibodies were produced in a miniPERM bioreactor (Heraeus, Osterode, Germany) and purified by affinity chromatography on a Protein-A Sepharose CL-4B column (Pharmacia, Uppsala, Sweden). Isolation and characterization of hybrid hybridoma OKT3 × HD37 has been described (Csóka *et al.*, 1996).

Vector construction

The *E. coli* K12 strain XL1-Blue (Stratagene, La Jolla, CA) was used as the cloning and expression host. Plasmids pHOG-αCD19 and pHOG-dmOKT3 encoding the scFv fragments derived from hybridoma HD37 specific for human CD19 (Kipriyanov *et al.*, 1996) and OKT3 specific for human CD3 (Kipriyanov *et al.*, 1997*b*), respectively, were used for assembly of the diabody to create the expression plasmid pKID3 × 19. Briefly, a PCR fragment of the V_H domain of anti-CD19 preceded by a *Bgl*II site and followed by a segment coding for a LysLeuGlyGly linker was generated using the primers DP1, 5′-TCACACAGAATTCTT AGATCTATTAAAGAGGAGAAATTAACC and DP2, 5′-AGCA-CACGATATCACCGCCAAGCTTGGGTGTTGTTTTGGC (Fig. 1). The PCR fragment was digested with EcoRI and EcoRV and ligated with the EcoRI/EcoRV linearized plasmid pHOG-dmOKT3, generating the vector pHOG19-3. The PCR fragment of the V_L domain of anti-CD19 followed by a segment coding for a c-myc epitope and a hexahistidinyl tail was generated using the primers DP3, 5′-AGCACACAAGCTTGGCGGTGATATCTTGCTCACCCAAA-CTCCA plus DP4, 5′-AGCACACTCTAGAGACACACAGATCT-TTAGTGATGGTGATGGTGATGTGAGTTTAGG. The PCR frag-

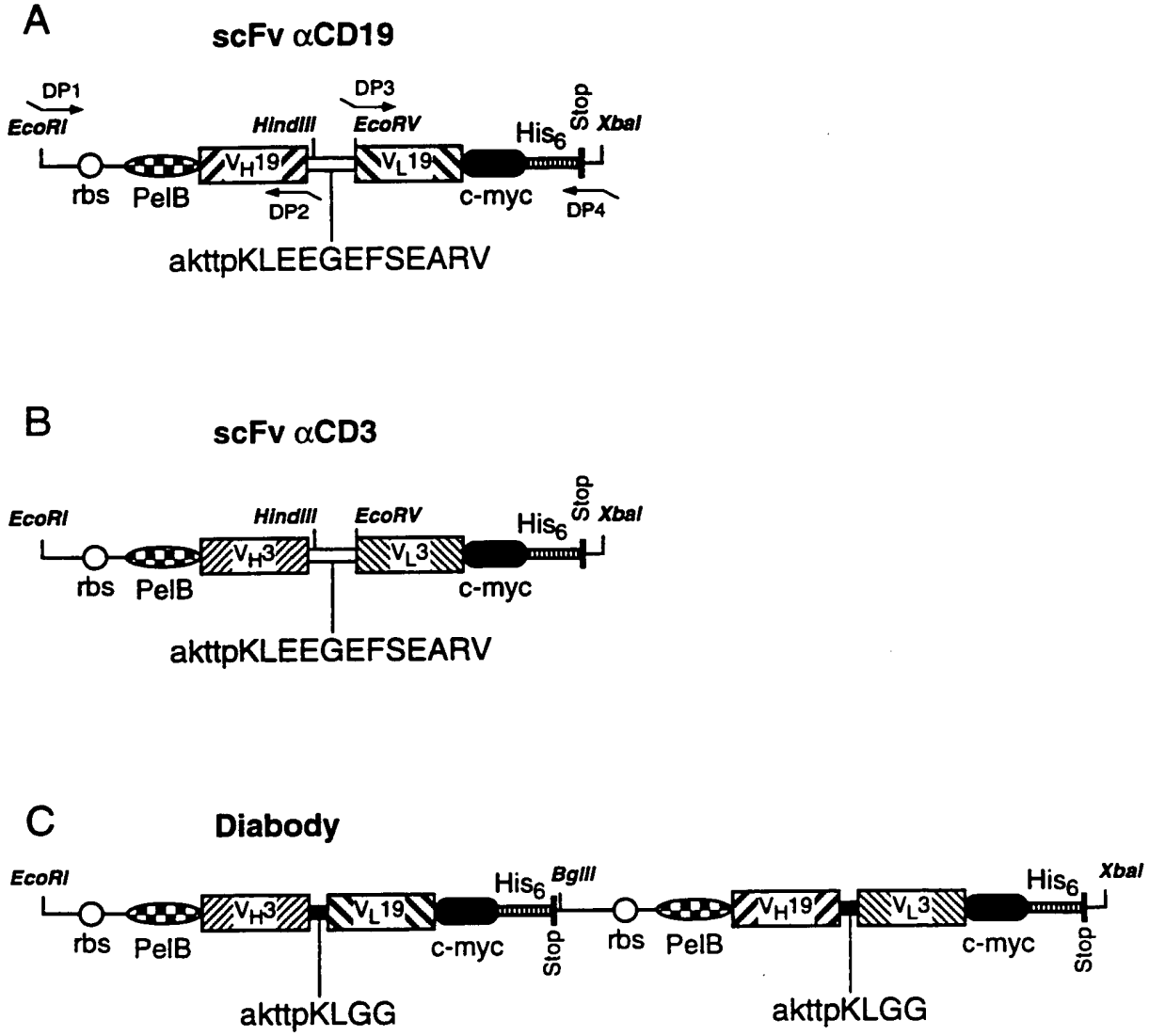

FIGURE 1 – Schematic representation of operons encoding anti-CD19 and anti-CD3 scFvs in plasmid pHOG21 (Kipriyanov *et al.*, 1997*a*) (*a* and *b*, respectively) and dicistronic operon encoding the bispecific anti-human CD3 × CD19 diabody in plasmid pKID3 × 19 (*c*). The positions of primers and most important restriction sites used for constructing the plasmids are shown. The locations of ribosome binding sites (rbs), pelB leader sequences (pelB), c-myc epitopes (c-myc), hexahistidinyl tags (His_6) and stop codons (Stop) are indicated. Amino acid sequences of linkers connecting V-domains are shown below each drawing. In the linker, amino acids derived from the C_H1 domain are indicated by small letters and residues introduced artificially are shown in block letters.

ment of the V_L domain of anti-CD19 contained a *BglII* site near the 3′ end of the coding strand. It was digested with HindIII and XbaI and ligated with the HindIII/XbaI linearized plasmid pHOG-dmOKT3, generating the vectors pHOG3-19. The expression plasmid pKID3 × 19 for cosecretion of the two hybrid scFvs was constructed by ligation of the *BglII/XbaI* restriction fragment from pHOG3-19 comprising the vector backbone and the *BglII/XbaI* fragment from pHOG19-3. All sequences encoding hybrid scFv fragments were verified by the dideoxynucleotide method (Sanger *et al.*, 1977).

ScFv and diabody expression and purification

Bacterial growth, induction and isolation of periplasmic extracts was performed as previously described (Kipriyanov *et al.*, 1996, 1997*a, b*). For isolation of anti-CD3 and anti-CD19 scFv, the culture supernatant and the soluble periplasmic extract were combined and concentrated using Amicon YM10 membranes with a 10 kDa cut-off (Amicon, Witten, Germany) followed by thorough dialysis against 50 mM Tris-HCl, 1 M NaCl, pH 7.0. The diabody was concentrated by ammonium sulfate precipitation (final concentration 70% of saturation) as recommended (Atwell *et al.*, 1996). The protein precipitate was collected by centrifugation (30,000*g*, 4°C, 30 min) and dissolved in 1/10 of the initial volume of 50 mM Tris-HCl, 1 M NaCl, pH 7.0. Purification was achieved by IMAC as previously described (Kipriyanov *et al.*, 1997*a*). The final purification of scFv-αCD3 (Ia = 7.52) and scFv-αCD19 (Ia = 6.19) was achieved by ion-exchange chromatography on a MonoS HR5/5 column (Pharmacia) in 50 mM MES, pH 6.0, or on a MonoQ HR5/5 column (Pharmacia) in 20 mM Tris-HCl, pH 8.0, respectively, with a linear 0–1 M NaCl gradient. The purified antibody preparations were dialyzed against PBS (15 mM Na-phosphate, 0.15 M NaCl, pH 7.0). All purification procedures were performed at 4°C. For long-time storage, diabody and scFv were frozen in the presence of BSA (final concentration 10 mg/ml) or 10% FCS and stored at −80°C.

Measurement of protein concentration

Protein concentrations were determined by the Bradford (1976) dye-binding assay, using the Bio-Rad (Munich, Germany) protein assay kit. The concentrations of purified diabody, scFv-αCD3 and scFv-αCD19 were determined from the A_{280} values using the extinction coefficients $\epsilon^{1mg/ml}$ = 1.89, 1.84 and 1.82, respectively, calculated according to Gill and von Hippel (1989).

SDS-PAGE and size-exclusion chromatography

SDS-PAGE was performed according to Laemmli (1970) under reducing conditions. Western blot analyses using either rabbit serum A (Breitling *et al.*, 1991) recognizing the N-terminus of the processed antibody fragment (without a pelB leader) or mouse MAb 9E10 (IC Chemikalien, Ismaning, Germany) specific for a peptide of the c-myc oncoprotein were performed as previously described (Kipriyanov *et al.*, 1994). Analytical gel filtration of the diabody and scFv preparations was performed in PBS using a Superdex 75 HR10/30 column (Pharmacia). Sample volume and flow rate were 200 µl and 0.5 ml/min, respectively. The column was calibrated with a low molecular weight gel filtration calibration kit (Pharmacia).

Flow cytometry

The human $CD3^+/CD19^-$ acute T cell leukemia line Jurkat and the $CD19^+/CD3^-$ B cell line JOK-1 were used for flow cytometry, performed as previously described (Kipriyanov *et al.*, 1996). In brief, 5×10^5 cells in 50 µl RPMI 1640 medium (GIBCO BRL, Eggestein, Germany) supplemented with 10% FCS and 0.1% sodium azide (referred to as complete medium) were incubated with 100 µl of a recombinant antibody preparation for 45 min on ice. After washing with complete medium, the cells were incubated with 100 µl of 10 µg/ml anti c-myc MAb 9E10 (IC Chemikalien) in the same buffer for 45 min on ice. After a second washing cycle, the cells were incubated with 100 µl of FITC-labeled goat anti-mouse IgG (GIBCO BRL) under the same conditions as before. The cells were then washed again and resuspended in 100 µl of 1 µg/ml solution of propidium iodide (Sigma, Deisenhofen, Germany) in complete medium to exclude dead cells. The relative fluorescence of stained cells was measured using a FACScan flow cytometer (Becton Dickinson, Mountain View, CA).

Affinity determination

Affinities of MAb HD37 (Pezzutto *et al.*, 1987) and scFv-αCD19 (Kipriyanov *et al.*, 1996) were determined by cellular RIA. Antibody (100 µg) was labeled with 1 mCi [^{125}I]-iodide by the chloramine T method (Greenwood *et al.*, 1963). RIA was performed in a flexible polyvinyl chloride microtiter plate blocked with PBS containing 0.2% (w/v) gelatin at 4°C overnight. After washing, 10^6 JOK-1 cells in 50 µl PBS containing 0.2% gelatin and 5% (v/v) pooled human IgG (Venimmun Behringwerke, Marburg, Germany) were incubated in triplicate with increasing amounts of the radiolabeled antibody preparation for 1 hr at room temperature. The plate was washed and aspirated 3 times using PBS/0.2% gelatin. The dried plate was sliced, and the radioactivity in individual wells was measured using a gamma-counter. Affinity constants were determined by a Scatchard (1949) plot analysis.

Apparent affinities of diabody and scFv were determined from competitive inhibition assays as previously described (Kipriyanov *et al.*, 1997*b*). In brief, increasing concentrations of purified antibody fragment were added to a subsaturating concentration of FITC-labeled MAb OKT3 or HD37 and incubated with Jurkat or JOK-1 cells, respectively, as described above for FACScan analysis. Fluorescence intensities of stained cells were measured as described above. Binding affinities were calculated according to the following equation derived from that of Schodin and Kranz (1993):

$$K_{a(I)} = (1 + [\text{FITC-MAb}] \times K_{a(MAb)})/IC_{50}$$

where I is the unlabeled inhibitor (diabody or scFv), [FITC-MAb] is the concentration of FITC-labeled MAb, $K_{a(MAb)}$ is the binding affinity of MAb and IC_{50} is the concentration of inhibitor that yields 50% inhibition of binding. Affinity constant values of 1.2×10^9 M^{-1} and 2.5×10^9 M^{-1} were taken for MAb OKT3 (Adair *et al.*, 1994) and HD37 (determined by RIA), respectively.

Analyses of diabody and scFv stability

The antibody fragments were stored in freshly prepared human serum from a healthy donor at 37°C at a concentration 20 µg/ml. At given time points, 250 µl aliquots were taken under sterile conditions, frozen and kept at −80°C. Activities of samples after storage were determined by flow cytometry.

Preparation and stimulation of effector cells

Human PBMCs were isolated from the buffy coat of healthy donors by Ficoll/Hypaque (Pharmacia) density gradient centrifugation. The PBMC interphase was washed twice in PBS and used immediately as effector cells. Cultures of PBMC were grown using RPMI 1640 (GIBCO BRL) supplemented with 2% heat inactivated FCS (GIBCO BRL), 2 mM glutamine, 1 mM pyruvate and 0.05 mM 2-ME. To obtain CTLs, PBMCs were cultured at a concentration of 2×10^6 ml in medium containing anti-CD3 MAb OKT3 (5 µg/ml) and recombinant human IL-2 (20 U/ml) (EuroCetus, Amsterdam, The Netherlands). After 4 days, the cells were washed twice to remove remaining antibody and cultured overnight in medium alone. The cytotoxicity assay was performed on day 5.

Cytotoxicity assay

The CD19-expressing Burkitt's lymphoma cell lines Raji and Namalwa were used as target cells. Cells were cultured in RPMI 1640 (GIBCO BRL) supplemented with 10% heat inactivated FCS (GIBCO BRL), 2 mM glutamine and 1 mM pyruvate at 37°C in a humidified atmosphere containing 7.5% CO_2. The cytotoxic T cell assays were carried out in RPMI 1640 medium supplemented with 10% FCS, 10 mM HEPES, 2 mM glutamine, 1 mM pyruvate and 0.05 mM 2-ME. Cytotoxic activity was assessed using a standard

[^{51}Cr]-release assay; 2 × 10^6 target cells were labeled with 200 μCi Na[^{51}Cr]O_4 (Amersham-Buchler, Braunschweig, Germany) followed by 4 washing cycles and resuspended in medium at a concentration 2 × 10^5/ml. Effector cells were adjusted to a concentration of 5 × 10^6 ml. Increasing amounts of CTLs in 100 μl were titrated to 10^4 target cells/well in 50 μl. Antibodies (50 μl) were added to each well. The whole assay was set up in triplicate and incubated for 4 hr at 37°C. Supernatant (100 μl) was harvested and assayed for [^{51}Cr] release in a gamma-counter (Cobra Auto Gamma; Canberra Packard, Dreieich, Germany). Maximum release was determined by incubating the target cells in 10% SDS, and spontaneous release was determined by incubating the cells in medium alone. Specific lysis (%) was calculated as: (experimental release − spontaneous release)/(maximal release − spontaneous release) × 100.

RESULTS

Diabody design and construction

Single-chain Fv fragments derived from the hybridomas HD37 (Pezzutto *et al.*, 1987) and OKT3 (Kung *et al.*, 1979) were used for creating a bispecific CD3 × CD19 diabody. A significant increase in the stability of the OKT3 anti-CD3 scFv was achieved by substituting a serine for cysteine in position 100A of the V_H domain (Kipriyanov *et al.*, 1997*b*). The C-terminus of a V_H domain was connected to the N-terminus of a V_L domain of another specificity using a short rigid linker to restrict intra-chain pairing of V_H and V_L. The linker design was based on our strategy of cloning antibody V_H domains using an anti-sense primer complementary to the 5′-region of the γ chain C_H1 domain gene (Kipriyanov *et al.*, 1996, 1997*b*). Seven amino acids introduced by this primer formed a major part of the linker (Fig. 1). The plasmid pKID3 × 19 was constructed to express the CD3 × CD19 diabody by co-secretion of the 2 hybrid scFvs V_H3-V_L19 and V_H19-V_L3 from a dicistronic operon (Fig. 1). The operon is under the transcriptional control of the wt lac promoter/operator, which is inducible with IPTG. Each hybrid scFv is preceded by a pelB leader sequence to direct secretion to the periplasmic space of *E. coli*. Both hybrid *scFv* genes are followed by nucleotide sequences coding for a c-myc tag for immunodetection and a hexahistidinyl tail for purification of recombinant product using IMAC (Fig. 1).

Diabody expression and purification

The CD3 × CD19 diabody was secreted from *E. coli* cells transformed with the pKID3 × 19 plasmid. Relatively equal amounts of soluble hybrid scFv V_H3-V_L19 and V_H19-V_L3 were detected in crude periplasmic extracts by Western blot analysis using either MAb 9E10 specific to the C-terminal c-myc epitope or by serum A specific for the N-terminus of processed (without pelB leader) antibody fragment (data not shown). FACScan analyses of crude periplasmic extracts demonstrated that the diabody produced by bacteria specifically interacted with both CD3-positive Jurkat cells and CD19-positive JOK-1 cells. In contrast, neither hybrid scFv alone bound these cell lines (data not shown).

To obtain higher yields of soluble antibody fragments, we added 0.4 M sucrose to bacterial cells that had been induced with IPTG. We have shown that under these conditions the yield of soluble scFv can be increased up to 150-fold (Kipriyanov *et al.*, 1997*a*). The diabody was found to accumulate in the *E. coli* periplasm and was also released into the culture medium (data not shown). After concentrating by ammonium sulfate precipitation and purification by IMAC, yields of 2.0–2.5 mg/l with a purity greater than 95% were achieved (Fig. 2*a*). In contrast, ammonium sulfate was shown to be rather ineffective for precipitating monospecific anti-CD19 and anti-CD3 single chain Fv fragments that were isolated in parallel. Much higher yields of the purified scFv antibody fragments were obtained by concentrating by ultrafiltration prior to IMAC (data not shown).

Analyses of diabody and scFv by SDS-PAGE and size-exclusion FPLC

Purified antibody fragments were analyzed by electrophoresis on 12% SDS polyacrylamide gels. Under these conditions, the diabody was resolved into 2 protein bands corresponding to the calculated M_r of 28,900 for scFv V_H19-V_L3 and 29,300 for scFvs V_H3-V_L19 (Fig. 2*a*). Anti-CD3 and anti-CD19 scFvs appeared as single bands (calculated M_r are 29,800 and 30,400, respectively).

An analysis of antibody fragments by gel-filtration on a Superdex 75 column is shown in Figure 2*b*. The scFv-αCD3 consisted only of monomers, the scFv-αCD19 of monomers, dimers and a multimeric form and the bispecific diabody only of dimers. The apparent m.w. of the diabody deduced from its chromatographic mobility was lower than its actual m.w., reflecting its compact structure (Perisic *et al.*, 1994).

Antigen binding specificity and affinity of diabody and scFv

Flow cytometry experiments demonstrated a specific interaction of the diabody with both human CD19-positive JOK-1 and CD3-positive Jurkat cells. The fluorescence intensities were fairly comparable to those obtained using the parental monospecific scFvs at similar concentrations (Fig. 3).

The CD19 and CD3 binding affinities of the diabody were estimated by competitive binding to human JOK-1 and Jurkat cells in the presence of either FITC-labeled MAb HD37 (anti-CD19) or OKT3 (anti-CD3). The IC_{50} value of diabody competing with FITC-OKT3 for binding T-cells was similar to that of scFv-αCD3 (Fig. 4*b*; Table I). In contrast, scFv anti-CD19 competed with FITC-HD37 more effectively than the bispecific diabody (Fig. 4*a*). probably because a significant amount of this scFv fragment was in a dimeric and multimeric form (Fig. 2*b*). Direct affinity measurements of radio-iodinated anti-CD19 MAb HD37 and scFv demonstrated that both have very similar affinity constants in the sub-nanomolar range (Table I), reflecting the bivalent nature of the scFv anti-CD19.

Table I summarizes the results of affinity measurements. The similarity in affinities of the bispecific diabody with the parental scFvs suggests that all the non-covalent heterodimers (diabody) are correctly formed by specific V_H-V_L interactions. The affinity of the diabody for CD19-positive target B cells was 10-fold higher than its affinity for CD3 positive effector T cells.

Stability of bispecific diabody in human serum

One might expect that the bispecific diabody would be rather labile, as it was formed by non-covalent interactions of 2 hybrid scFv molecules. We therefore investigated the stability of the diabody and both parental anti-CD3 and anti-CD19 scFvs when stored at a fairly low concentration in human serum at 37°C for prolonged periods of time. A concentration of 20 μg/ml was chosen to avoid the fluorescence plateau in FACSscan analysis (Kipriyanov *et al.*, 1997*b*). The residual antigen binding activity was estimated by flow cytometry. We found that the anti-CD3 scFv, which retained 70% of activity after 5 days of incubation, appeared to be significantly more stable than anti-CD19 scFv, which lost 50% of its activity after 36 hr of incubation and 95% after 4 days (Fig. 5). The diabody had an intermediate stability. It was less stable than the anti-CD3 scFv but slightly more stable than the anti-CD19 scFv (Fig. 5). The loss of both CD3 and CD19 binding had similar time kinetics, indicating an interdependent denaturation of the 2 binding domains.

Induction of specific cytotoxicity by diabody

The ability of the bispecific diabody to induce tumor cell lysis by redirecting T cell-mediated cytotoxicity was investigated using PBMC from healthy donors as effector cells. After stimulating with soluble MAb OKT3 and IL-2 for 4 days, the cells were washed to remove remaining antibody and cultured in medium alone overnight. Human B cell lines Raji and Namalwa expressing CD19 were used as target cells. The effect of the bispecific diabody was measured using a standard [^{51}Cr]-release assay with increasing

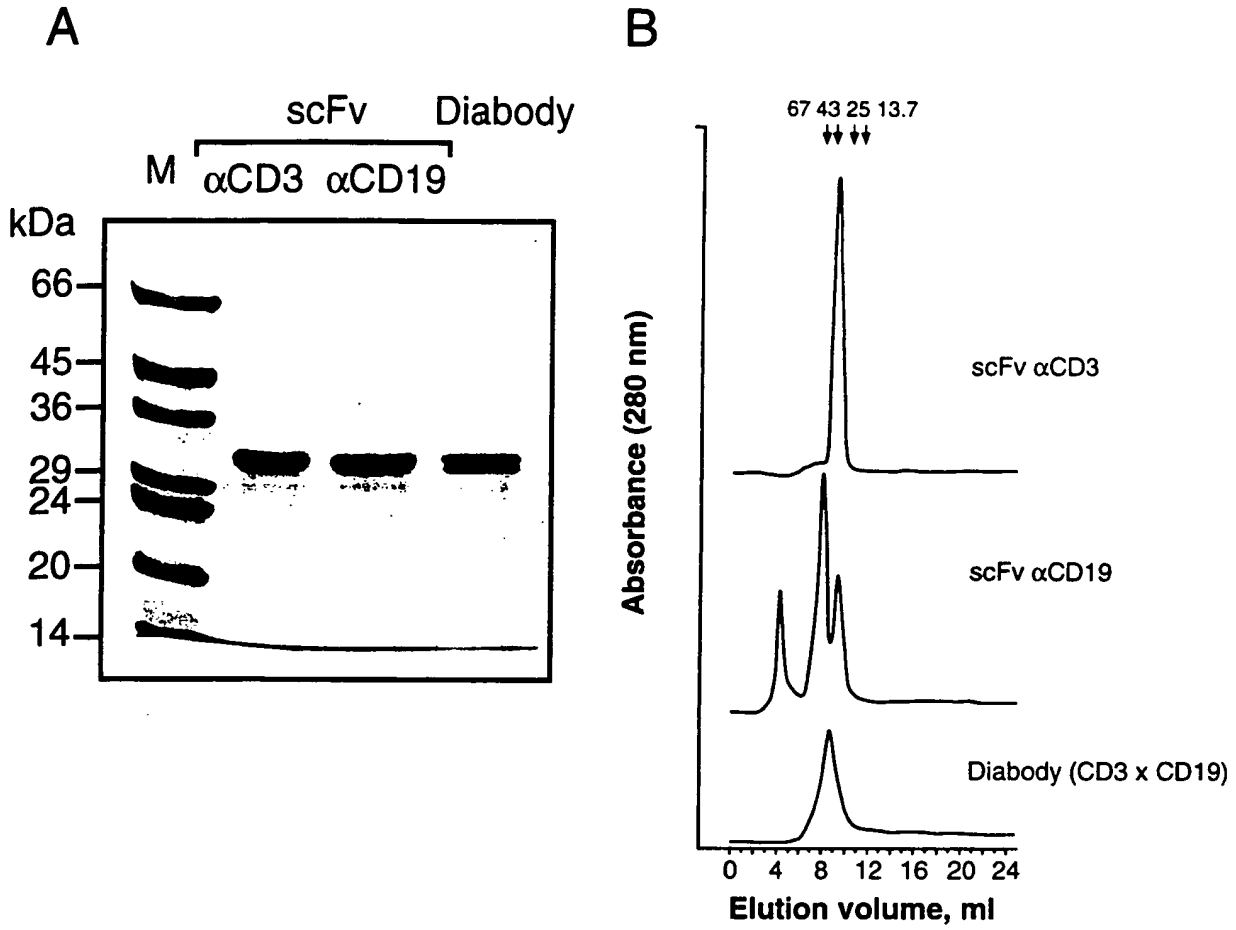

FIGURE 2 – Analyses of purified scFv anti-CD3, scFv anti-CD19 and bispecific diabody. (*a*) 12% SDS-PAGE under reducing conditions. The gel was stained with Coomassie brilliant blue. (*b*) Analytical gel filtration on a Superdex 75 column. The elution buffer was PBS, pH 7.0. Sample volume and flow rate were 200 µl and 0.5 ml/min, respectively. Molecular masses were calibrated with BSA (67 kDa), ovalbumin (43 kDa), chymotrypsinogen A (25 kDa) and ribonuclease A (13.7 kDa).

effector to target cell ratios. A mixture of both parental scFv fragments (anti-CD3 and anti-CD19) served as a negative control for determining the background lysis. Although the observed background lysis was different in different experiments, the diabody appeared to be quite potent in retargeting activated PBMC to lyse both target cell lines in a concentration-dependent manner (Fig. 6).

The CD3 × CD19 diabody was compared with a BsAb of the same specificity isolated from a hybrid-hybridoma OKT3 × HD37 (Csóka *et al.*, 1996). Bispecific diabody proved to be 10-fold more potent over the BsAb on a weight basis (3-fold on a molar basis) (Fig. 6*a*). Moreover, the increased cytotoxicity of the diabody was independent of the effector:target ratio (Fig. 6).

DISCUSSION

The 95 kDa CD19 antigen represents the broadest lineage-specific marker expressed on human B cells: it is present on the surface of virtually all B lymphocytes, including early B progenitor cells. CD19 is lost during the terminal stages of B cell differentiation but is exposed on the vast majority of B cell tumors (Uckun and Ledbetter, 1988). We therefore chose this antigen as the target molecule for BsAb-mediated cytotoxicity and constructed an anti-human CD19 scFv (Kipriyanov *et al.*, 1996).

Although different BsAb cross-linking NK cells (De Palazzo *et al.*, 1992) or activated neutrophils (Michon *et al.*, 1995) to tumor cells have been described, the most effective approach for tumor rejection appears to be targeting via the CD3 molecule on cytotoxic T cells. The feasibility and effectiveness of this immunotherapeutic concept has been studied extensively in pre-clinical models, as well as in phase I clinical trials (Bolhuis *et al.*, 1996).

For the generation of a bispecific antibody suitable for therapy of human B cell malignancies, we aimed to construct a small recombinant molecule with dual specificity for both the human B cell surface antigen CD19 and the signal-transducing CD3ε chain of the human TCR/CD3 complex. Although numerous anti-human CD3 MAbs have been used to study the T cell activation (Schwinzer *et al.*, 1992) and to create BsAb either by chemical conjugation (Anderson *et al.*, 1992; Nitta *et al.*, 1990) or by the quadroma technique (Bohlen *et al.*, 1993; Jacobs *et al.*, 1997), only 2 different anti-human CD3 antibody fragments have been used to date for the creation of recombinant BsAb. Variable domains derived from the hybridoma TR66 were used for constructing CD4-FvCD3 bispecific single chain molecules Janusins (Traunecker *et al.*, 1991) and later for the creation of $(scFv)_2$ specific for both the epithelial 17-1A antigen and human CD3 (Mack *et al.*, 1995). In the second case, humanized V domains originally derived from the murine hybridoma UCHT1 were used for constructing anti-CD3/anti-$p185^{HER2}$ $F(ab')_2$ (Shalaby *et al.*, 1992) and a diabody (Zhu *et al.*, 1996). For constructing the BsAb described here, we used an scFv gene derived from the well-known hybridoma OKT3, which had been modified to improve its stability and folding in bacteria (Kipriyanov *et al.*, 1997*b*).

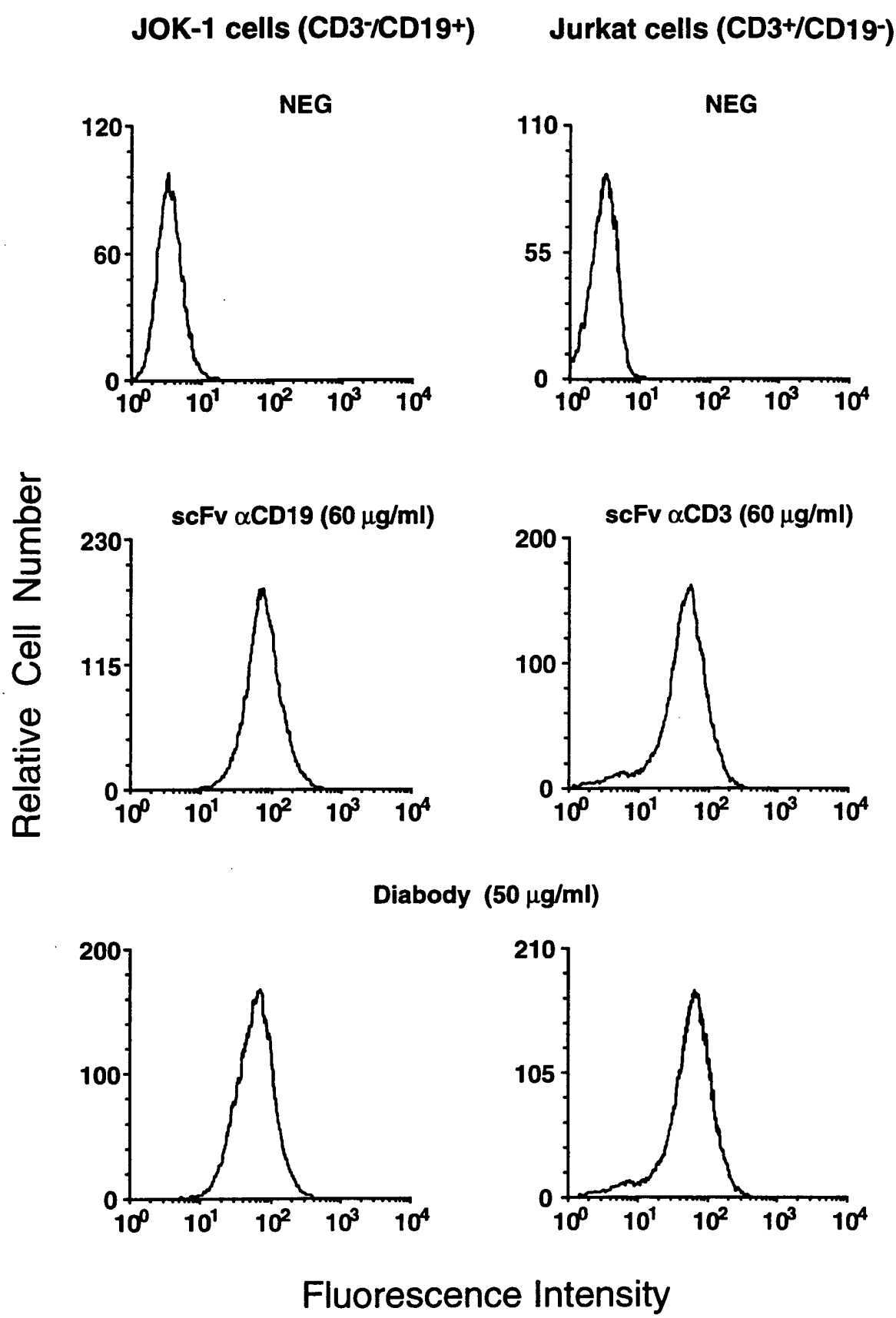

FIGURE 3 – Flow cytometric analysis of scFv and diabody binding to $CD19^+/CD3^-$ JOK-1 cells and $CD3^+/CD19^-$ Jurkat cells. As a negative control, the binding of an irrelevant scFv was used.

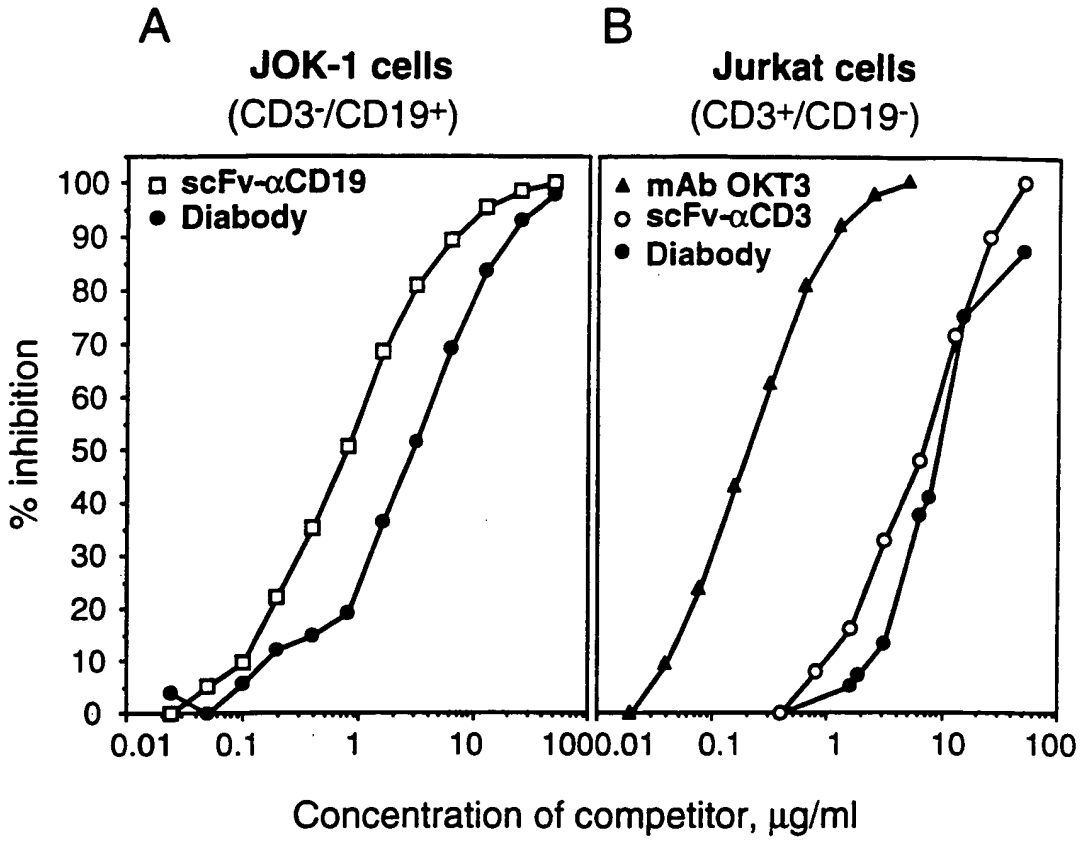

FIGURE 4 – Analyses of apparent affinities by flow cytometry. Inhibition of binding of FITC-labeled MAbs HD37 to JOK-1 cells (*a*) and inhibition of binding of FITC-labeled MAbs OKT3 to Jurkat cells (*b*) in the presence of MAb OKT3, scFv-αCD19, scFv-αCD3 and bispecific diabody are shown.

TABLE I – AFFINITIES OF MAb AND ANTIBODY FRAGMENTS

Antibody	IC_{50} (nM)	K_a (M^{-1})[1]	K_a (M^{-1})[2]
JOK-1 cells			
MAb HD37	n.d.[3]	n.d.	2.5×10^9
scFv-αCD19	24.0	9.7×10^8	2.9×10^9
Diabody	48.8	4.8×10^8	n.d.
Jurkat cells			
MAb OKT3	1.3	7.7×10^8	n.d.
scFv-αCD3	222.2	4.5×10^7	n.d.
Diabody	156.0	6.4×10^7	n.d.

[1]Affinities determined from inhibition experiments.–[2]Affinities determined from Scatchard plots.–[3]Not determined.

Initial attempts to produce bispecific CD3 × CD19 $(scFv)_2$ molecules, as recommended by Gruber *et al.* (1994), were unsatisfactory because of the small yields and low anti-CD3 activity (data not shown). We therefore constructed a more rigid cross-over scFv dimer (diabody). This construct has been shown to have 2 antigen-binding sites at opposite ends of the molecule, separated by 65 Å, which is sufficient to span the distance between 2 cells (Holliger *et al.*, 1996; Perisic *et al.*, 1994). The CD3 × CD19 diabody was produced by bacteria in a soluble functional form and could be retrieved from periplasmic extracts and culture medium in one step with a yield comparable to those obtained for parental scFv fragments.

Structurally, the isolated diabody was a stable compact dimer with an apparent m.w. around 50 kDa. Theoretically, the cosecretion of two hybrid scFv fragments may give rise to 2 types of dimer: active heterodimers and likely inactive homodimers. Affinity measurements indicated that the diabody was mostly, if not completely, in the active heterodimeric form. It bound to human CD3 with an affinity indistinguishable from that of the parental scFv-αCD3 and to human CD19 with an affinity about one half that of scFv-αCD19. This latter scFv has been shown to have a very high affinity in the subnanomolar range, similar to that of the parental MAb. Size-exclusion chromatography demonstrated that a significant part of this scFv was present in the form of non-covalent dimers and even higher oligomers, probably resulting in an enhanced affinity due to the increased avidity. In contrast, the CD19 binding domain of the diabody is only monomeric.

The higher affinity of the anti-CD19 moiety resulted in an almost 10-fold stronger binding of the diabody to the surface of target B cells than to the surface of T cells. Strong binding to a target tumor cell and weaker binding to an effector cell may have certain advantages for cancer therapy. For example, experiments *in vitro* demonstrated that the cytotoxic potential of recombinant BsAb does not depend on the affinity of its CD3-binding domain (Zhu and Carter, 1995). Furthermore, in a model of TCR serial triggering (Valitutti *et al.*, 1995), a high off-rate of the TCR is essential since it allows a single peptide-MHC complex to engage many TCRs in successive rounds of ligation, triggering and dissociation. Therefore, a higher affinity could result in less stimulation because the lower off-rate may prevent TCR reusage. A similar situation may also be present in the case of the surrogate antigenic stimulation of T cells through the anti-CD3 part of BsAb. For example, i.v. administration of a $F(ab')_2$ of OC/TR BsAb, which has a relatively high affinity for human CD3ε (10^8 M^{-1}) (Jacobs *et al.*, 1997), induced a generalized *in vivo* activation with severe side effects (Tibben *et al.*, 1993), which most probably originated from target cell-independent direct activation of T cells and subsequent release of cytokines. Therefore, a recombinant BsAb that binds strongly to

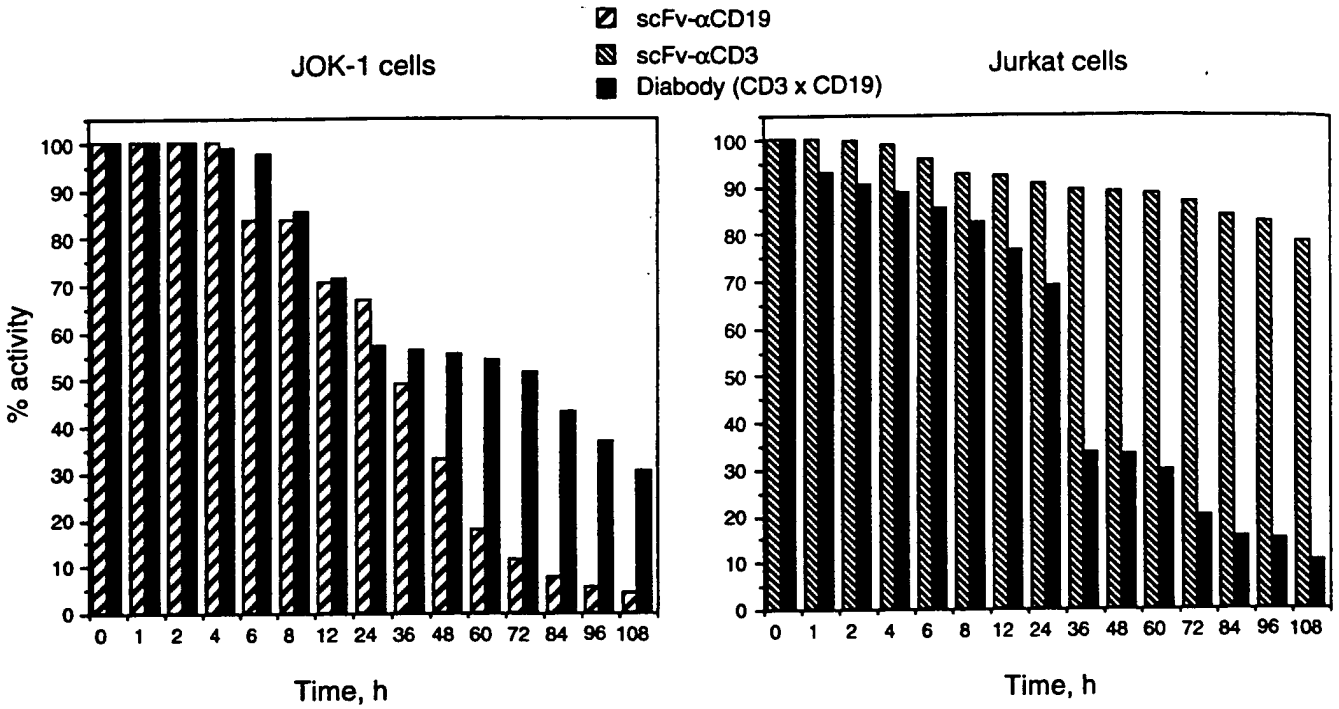

FIGURE 5 – Stability of scFv fragments and diabody in human serum at 37°C. The antibody fragments were incubated at 20 μg/ml in human serum at 37°C for the times shown. The CD19 and CD3 binding activity was assessed by flow cytometry using $CD19^+/CD3^-$ JOK-1 and $CD3^+/CD19^-$ Jurkat cells. Activity of the samples at point zero was taken as 100%.

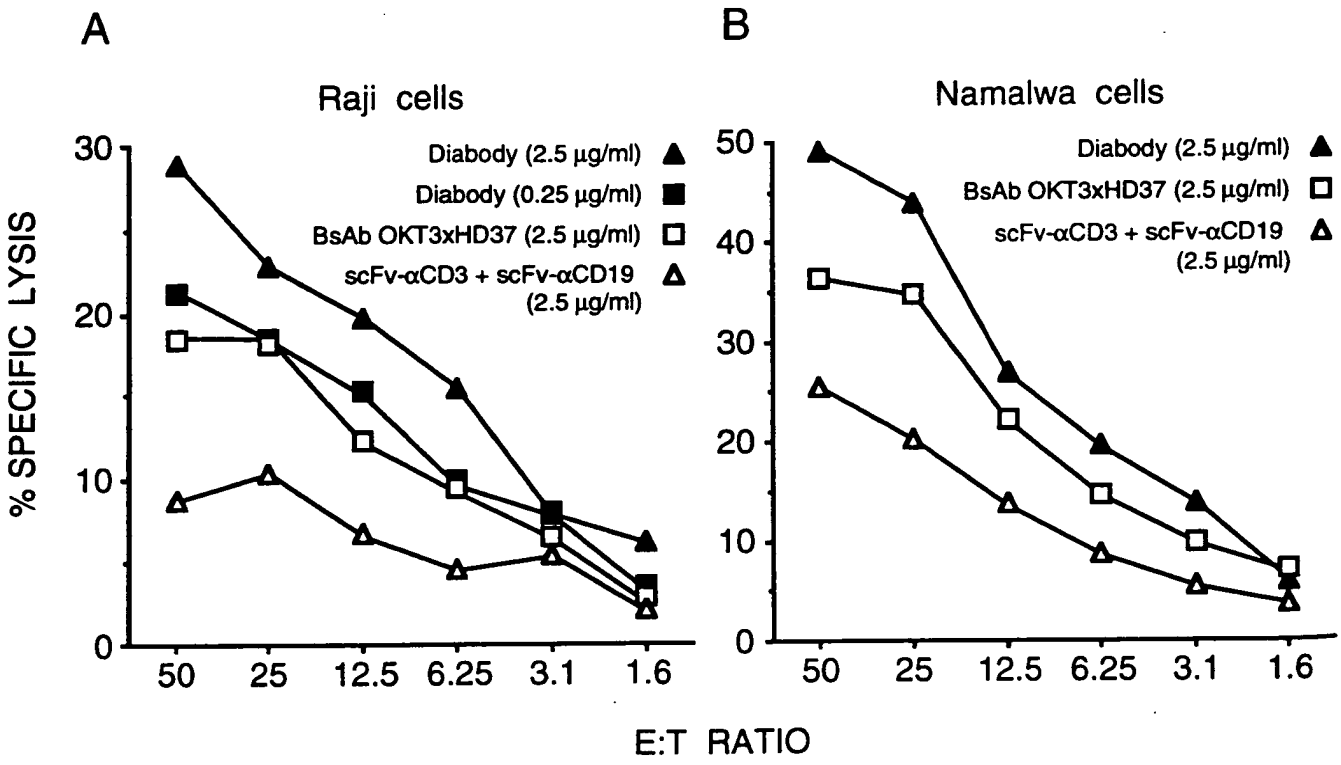

FIGURE 6 – Diabody-mediated lysis of CD19-positive B cells by activated human PBMC. The human CD19 expressing [^{51}Cr]-labeled target cell lines Raji (*a*) and Namalwa (*b*) were co-incubated with effector CTLs at different effector/target ratios for 4 hr. Percent cytotoxicity was calculated based on [^{51}Cr]-release in the presence of 2.5 μg/ml of parental scFvs, 0.25 μg/ml of diabody, 2.5 μg/ml of diabody or 2.5 μg/ml of BsAb OKT3 × HD37.

target tumor cells and significantly more weakly to the signal-transducing CD3ε chain of the TCR/CD3 complex on effector cells may prove to have the most desirable properties.

An analysis of the stability of antibody fragments in human serum demonstrated a significant difference between scFv-αCD19 and scFv-αCD3. The present data confirm our previous observation that scFv derived from the hybridoma OKT3 and containing a Cys/Ser substitution in CDR-H3 has an enhanced stability (Kipriyanov *et al.*, 1997*b*). A comparison of the stabilities of the diabody and the parental scFvs, performed here suggests a stabilizing effect of the anti-CD3 moiety of the diabody on the CD19-specific moiety and also an interdependent denaturation of the 2 binding domains.

The bispecific diabody was able to induce an efficient lysis of the target cells by human CTLs. A comparison with a hybrid-hybridoma BsAb of the same dual specificity (Csóka *et al.*, 1996) indicated that the diabody was even more potent in recruiting activated T cells for cytolysis of the target cells. The increased efficiency of the smaller diabody may be due to the closer proximity of the target cell and T cells connected by the diabody (Holliger *et al.*, 1996; Perisic *et al.*, 1994).

The prohibitive cost of preparing bispecific antibodies with the quadroma technology has made it difficult to start clinical trials. Recombinant antibodies, on the other hand, can be produced cheaply in large quantities using high cell density fermentation of bacterial cultures (Horn *et al.*, 1996; Zhu *et al.*, 1996). Furthermore, these smaller antibodies are less immunogenic due to the absence of constant domains. Consequently, we are now concentrating on the production of larger quantities of the diabody for testing in phase I clinical trials.

ACKNOWLEDGEMENTS

We thank Mr. A. Keller for excellent technical assistance.

REFERENCES

ADAIR, J.R., ATHWAL, D.S., BODMER, M., BRIGHT, S.M., COLLINS, A., PULITO, V.L., RAO, P.E., REEDMAN, R., ROTHERMEL, A.L., XU, D., ZIVIN, R.A. and JOLLIFFE, L.K., Humanization of the murine anti-human CD3 monoclonal antibody OKT3. *Hum. Antibodies Hybridomas*, **5**, 41–47 (1994).

ANDERSON, P.M., CRIST, W., HASZ, D., CARROLL, A.J., MYERS, D.E. and UCKUN, F.M., G19.4(αCD3) × B43(αCD19) monoclonal antibody hetero-conjugate triggers CD19 antigen-specific lysis of t(4;11) acute lymphoblastic leukemia cells by activated CD3 antigen-positive cytotoxic T cells. *Blood*, **80**, 2826–2834 (1992).

ATWELL, J.L., PEARCE, L.A., LAH, M., GRUEN, L.C., KORTT, A. and HUDSON, P., Design and expression of a stable bispecific scFv dimer with affinity for both glycophorin and N9 neurominidase. *Mol. Immunol.*, **33**, 1301–1312 (1996).

BIRD, R.E., HARDMAN, K.D., JACOBSON, J.W., JOHNSON, S., KAUFMAN, B.M., LEE, S.-M., LEE, T., POPE, S.H., RIORDAN, G.S. and WHITLOW, M., Single-chain antigen-binding proteins. *Science*, **242**, 423–426 (1988).

BOHLEN, H., HOPFF, T., MANZKE, O., ENGERT, A., KUBE, D., WICKRAMANAYAKE, P.D., DIEHL, V. and TESCH, H., Lysis of malignant B cells from patients with B-chronic lymphocytic leukemia by autologous T cells activated with CD3 × CD19 bispecific antibodies in combination with bivalent CD28 antibodies. *Blood*, **82**, 1803–1812 (1993).

BOLHUIS, R.L.H., HOOGENBOOM, H.R. and GRATAMA, J.W., Targeting of peripheral blood T lymphocytes. *Springer Semin. Immunopathol.*, **18**, 211–226 (1996).

BRADFORD, M.M., A rapid and sensitive method for the quantitation of microgram quantities of protein utilizing the principle of protein-dye binding. *Anal. Biochem.*, **72**, 248–254 (1976).

BREITLING, F., DÜBEL, S., SEEHAUS, T., KLEWINGHAUS, I. and LITTLE, M., A surface expression vector for antibody screening. *Gene*, **104**, 147–153 (1991).

BRENNAN, M., DAVIDSON, P.F. and PAULUS, H., Preparation of bispecific antibodies by chemical recombination of monoclonal immunoglobulin G1 fragments. *Science*, **229**, 81–83 (1985).

CANEVARI, S. and 17 OTHERS, Regression of advanced ovarian carcinoma by intraperitoneal treatment with autologous T lymphocytes retargeted by a bispecific monoclonal antibody. *J. nat. Cancer Inst.*, **87**, 1463–1469 (1995).

CARTER, P., RIDGWAY, J. and ZHU, Z., Toward the production of bispecific antibody fragments for clinical applications. *J. Hematother.*, **4**, 463–470 (1995).

CSÓKA, M., STRAUSS, G., DEBATIN, K.-M. and MOLDENHAUER, G., Activation of T cell cytotoxicity against autologous common acute lymphoblastic leukemia (cALL) blasts by CD3 × CD19 bispecific antibody. *Leukemia*, **10**, 1765–1772 (1996).

DE PALAZZO, I.G., HOLMES, M., GERCEL-TAYLOR, C. and WEINER, L.M., Antitumor effect of a bispecific antibody targeting CA19-9 antigen and CD16. *Cancer Res.*, **52**, 5713–5719 (1992).

FANGER, M.W., MORGANELLI, P.M. and GUYRE, P.M., Bispecific antibodies. *Crit. Rev. Immunol.*, **12**, 101–124 (1992).

GILL, S.C. and VON HIPPEL, P.H., Calculation of protein extinction coefficients from amino acid sequence data. *Anal. Biochem.*, **182**, 319–326 (1989).

GREENWOOD, F.C., HUNTER, W.M. and GLOVER, J.C., The preparation of ^{131}I-labeled human growth hormone of high specific radioactivity. *J. Biochem.*, **89**, 114–120 (1963).

GROSSBARD, M.L., PRESS, O.W., APPELBAUM, F.R., BERNSTEIN, I.D. and NADLER, L.M., Monoclonal antibody-based therapies of leukemia and lymphoma. *Blood*, **80**, 863–878 (1992).

GRUBER, M., SCHODIN, B.A., WILSON, E.R. and KRANZ, D.M., Efficient tumor cell lysis mediated by a bispecific single chain antibody expressed in *Escherichia coli*. *J. Immunol.*, **152**, 5368–5374 (1994).

HOLLIGER, P., BRISSINCK, J., WILLIAMS, R.L., THIELEMANS, K. and WINTER, G., Specific killing of lymphoma cells by cytotoxic T-cells mediated by a bispecific diabody. *Protein Eng.*, **9**, 299–305 (1996).

HOLLIGER, P., PROSPERO, T. and WINTER, G., "Diabodies": small bivalent and bispecific antibody fragments. *Proc. nat. Acad. Sci. (Wash.)*, **90**, 6444–6448 (1993).

HORN, U., STRITTMATTER, W., KREBBER, A., KNUPFER, U., KUJAU, M., WENDEROTH, R., MÜLLER, K., MATZKU, S., PLÜCKTHUN, A. and RIESENBERG, D., High volumetric yields of functional dimeric miniantibodies in *Escherichia coli*, using an optimized expression vector and high-cell-density fermentation under non-limited growth conditions. *Appl. Microbiol. Biotechnol.*, **46**, 524–532 (1996).

HUSTON, J.S., MUDGETT HUNTER, M., TAI, M.S., MCCARTNEY, J., WARREN, F., HABER, E. and OPPERMANN, H., Protein engineering of single-chain Fv analogs and fusion proteins. *Methods Enzymol.*, **203**, 46–88 (1991).

JACOBS, N., MAZZONI, A., MEZZANZANICA, D., NEGRI, D.R.M., VALOTA, O., COLNAGHI, M.I., MOUTSCHEN, M.P., BONIVER, J. and CANEVARI, S., Efficiency of T cell triggering by anti-CD3 monoclonal antibodies (mAb) with potential usefulness in bispecific mAb generation. *Cancer Immunol. Immunother.*, **44**, 257–264 (1997).

KIPRIYANOV, S.M., DÜBEL, S., BREITLING, F., KONTERMANN, R.E. and LITTLE, M., Recombinant single-chain Fv fragments carrying C-terminal cysteine residues: production of bivalent and biotinylated miniantibodies. *Mol. Immunol.*, **31**, 1047–1158 (1994).

KIPRIYANOV, S.M., KUPRIYANOVA, O.A., LITTLE, M. and MOLDENHAUER, G., Rapid detection of recombinant antibody fragments directed against cell-surface antigens by flow cytometry. *J. Immunol. Methods*, **196**, 51–62 (1996).

KIPRIYANOV, S.M., MOLDENHAUER, G. and LITTLE, M., High level production of soluble single chain antibodies in small-scale *Escherichia coli* cultures. *J. Immunol. Methods*, **200**, 69–77 (1997*a*).

KIPRIYANOV, S.M., MOLDENHAUER, G., MARTIN, A.C., KUPRIYANOVA, O.A. and LITTLE, M., Two amino acid mutations in an anti-human CD3 single chain Fv antibody fragment that affect the yield on bacterial secretion but not the affinity. *Protein Eng.*, **10**, 445–453 (1997*b*).

KOSTELNY, S.A., COLE, M.S. and TSO, J.Y., Formation of a bispecific antibody by the use of leucine zippers. *J. Immunol.*, **148**, 1547–1553 (1992).

KUNG, P.C., GOLSTEIN, G., REINHERZ, E.L. and SCHLOSSMAN, S.F., Monoclonal antibodies defining distinctive human T cell surface antigens. *Science*, **206**, 347–349 (1979).

LAEMMLI, U.K., Cleavage of structural proteins during the assembly of the head of the bacteriophage T4. *Nature (Lond.)*, **227**, 680–685 (1970).

MACK, M., RIETHMÜLLER, G. and KUFER, P., A small bispecific antibody construct expressed as a functional single-chain molecule with high tumor cell cytotoxicity. *Proc. nat. Acad. Sci. (Wash.)*, **92**, 7021–7025 (1995).

MICHON, J., MOUTEL, S., BARBET, J., ROMET-LEMMONNE, J.-L., DEO, Y.D., FRIDMAN, W.H. and TEILLAUD, J.-L., *In vitro* killing of neuroblastoma cells by neutrophils derived from granulocyte colony stimulating factor treated cancer patients using an anti-disialoganglioside/anti-FcγRI bispecific antibody. *Blood*, **86**, 1124–1130 (1995).

MILSTEIN, C. and CUELLO, A.C., Hybrid hybridomas and their use in immunohistochemistry. *Nature (Lond.)*, **305**, 537–540 (1983).

NITTA, T., SATO, K., YAGITA, H., OKUMURA, K. and ISHI, S., Preliminary trial of specific targeting therapy against malignant glioma. *Lancet*, **335**, 368–376 (1990).

PERISIC, O., WEBB, P.A., HOLLIGER, P., WINTER, G. and WILLIAMS, R.L., Crystal structure of a diabody, a bivalent antibody fragment. *Structure*, **2**, 1217–1226 (1994).

PEZZUTTO, A., DÖRKEN, B., RABINOVITCH, P.S., LEDBETTER, J.A., MOLDENHAUER, G. and CLARK, E.A., CD19 monoclonal antibody HD37 inhibits anti-immunoglobulin-induced B cell activation and proliferation. *J. Immunol.*, **138**, 2793–2799 (1987).

SANGER, F., NICKLEN, S. and COULSON, R., DNA sequencing with chain terminating inhibitors. *Proc. nat. Acad. Sci. (Wash.)*, **74**, 5463–5467 (1977).

SCATCHARD, G., The attractions of proteins for small molecules and ions. *Ann. N.Y. Acad. Sci.*, **51**, 660–672 (1949).

SCHODIN, B.A. and KRANZ, D.M., Binding affinity and inhibitory properties of a single-chain anti-T cell receptor antibody. *J. biol. Chem.*, **268**, 25722–25727 (1993).

SCHWINZER, R., FRANKLIN, R.A., DOMENICO, J., RENZ, H. and GELFAND, E.W., Monoclonal antibodies directed to different epitopes in the CD3-TCR complex induce different states of competence in resting human T cells. *J. Immunol.*, **148**, 1322–1328 (1992).

SHALABY, M.R., SHEPARD, H.M., PRESTA, L., RODRIGUES, M.L., BEVERLEY, P.C., FELDMANN, M. and CARTER, P., Development of humanized bispecific antibodies reactive with cytotoxic lymphocytes and tumor cells overexpressing the HER2 protooncogene. *J. exp. Med.*, **175**, 217–225 (1992).

TIBBEN, J.G., BOERMAN, O.C., CLAESSENS, R.A.M.J., CORSTENS, F.H.M., VAN DEUREN, M., DE MULDER, P.H.M., VAN DER MEER, J.W.M., KEUSER, K.G.G. and MASSUGER, L.F.A.G., Cytokine release in an ovarian carcinoma patient following intravenous administration of bispecific antibody OC/TR $F(ab')_2$. *J. nat. Cancer Inst.*, **85**, 1003–1004 (1993).

TRAUNECKER, A., LANZAVECCHIA, A. and KARJALAINEN, K., Bispecific single chain molecules (Janusins) target cytotoxic lymphocytes on HIV infected cells. *EMBO J.*, **10**, 3655–3659 (1991).

UCKUN, F.M. and LEDBETTER, J.A., Immunobiologic differences between normal and leukemic human B-cell precursors. *Proc. nat. Acad. Sci. (Wash.)*, **85**, 8603–8607 (1988).

VALITUTTI, S., MÜLLER, S., CELLA, M., PADOVAN, E. and LANZAVECCHIA, A., Serial triggering of many T-cell receptors by a few peptide-MHC complexes. *Nature (Lond.)*, **375**, 148–151 (1995).

WINTER, G. and MILSTEIN, C., Man-made antibodies. *Nature (Lond.)*, **349**, 293–299 (1991).

ZHU, Z. and CARTER, P., Identification of heavy chain residues in a humanized anti-CD3 antibody important for efficient antigen binding and T cell activation. *J. Immunol.*, **155**, 1903–1910 (1995).

ZHU, Z., ZAPATA, G., SHALABY, R., SNEDECOR, B., CHEN, H. and CARTER, P., High level secretion of a humanized bispecific diabody from *Escherichia coli*. *Bio/Technology*, **14**, 192–196 (1996).

INTERNATIONAL

Journal of Cancer

Int. J. Cancer: **112**, 509–518 (2004)

Publication of the International Union Against Cancer

EFFECT OF TETRAVALENT BISPECIFIC CD19×CD3 RECOMBINANT ANTIBODY CONSTRUCT AND CD28 COSTIMULATION ON LYSIS OF MALIGNANT B CELLS FROM PATIENTS WITH CHRONIC LYMPHOCYTIC LEUKEMIA BY AUTOLOGOUS T CELLS

Uwe REUSCH[1], Fabrice LE GALL[1], Manfred HENSEL[2], Gerhard MOLDENHAUER[3], Anthony D. HO[2], Melvyn LITTLE[1] and Sergey M. KIPRIYANOV[1]*

[1]*Affimed Therapeutics, Heidelberg, Germany*
[2]*Department of Internal Medicine V, University of Heidelberg, Heidelberg, Germany*
[3]*Department of Molecular Immunology, German Cancer Research Center, Heidelberg, Germany*

To develop an effective antitumor immunotherapy for B-lineage non-Hodgkin's lymphoma, we constructed a tetravalent tandem diabody (tanDb) specific for both human CD19 (B-cell marker) and CD3 (T-cell antigen). Here, we report the effective killing of malignant primary B cells from patients with B-cell chronic lymphocytic leukemia (B-CLL) by autologous T cells induced by tanDb at very low E:T ratios. Mononuclear cells from patients with B-CLL were cultured with bispecific antibody fragments in either the presence or absence of monospecific anti-CD28 antibody. Use of tetravalent tanDbs caused almost quantitative elimination of malignant B cells from the blood samples of 19 patients and some cytotoxic activity in 3 of 23 analyzed cases. In contrast, the structurally similar but bivalent diabody and single-chain diabody demonstrated nearly no antitumor activity in an autologous system. tanDb-induced activation and proliferation of T cells occurred only in the presence of CD19$^+$ target cells. Expression of the B7-1 (CD80) and B7-2 (CD86) molecules on the surface of leukemia cells made unnecessary the additional CD28-costimulation of T cells. When only a few tanDb molecules were present, the effect of CD28 costimulation on T-cell activation was more pronounced. Depending on the patient sample, we observed a 10- to 1,000-fold decrease of the half-maximal concentrations of tanDb for cell lysis. Upon CD28 crosslinking by agonistic MAb, specific tumor cell lysis was found at tanDb concentrations as low as 0.5 pM. These data demonstrate that the tetravalent CD19×CD3 tanDb might be a promising tool for the immunotherapy of human B-cell leukemias and lymphomas.

Key words: *tandem diabody; immunotherapy; CD19; CD3; B-cell chronic lymphocytic leukemia*

CLL is the most common leukemia of adults in Western countries. It is a systemic hematologic malignancy that originates from B cells (B-CLL) in 95% of patients, while only a minority of cases are derived through malignant transformation of T cells (T-CLL). Although B-CLL is classified as NHL, several issues make this leukemia a unique entity among malignant lymphomas. B-CLL is an accumulative disease of slowly proliferating CD5$^+$ B lymphocytes that develops in the aging population. Whereas some patients with B-CLL have an indolent course and die after many years from unrelated causes, others progress very rapidly and succumb within a few years from this currently incurable leukemia.[1]

The latest chemotherapeutic approaches for treatment of B-CLL include DNA-damaging agents (chlorambucil) in combination with purine analogues (fludarabine, pentostatin and cladribine) and corticosteroids (prednisone).[2] Although significant improvement in remission rates and survival have been achieved, chemotherapy is quite often associated with myelosuppression and opportunistic infections.[2] Immunotherapy using MAbs directed against surface antigens on CLL cells might be an attractive alternative to conventional chemotherapy because of lack of significant myelotoxicity. Alemtuzumab (Campath-1H), a humanized MAb specific for CD52 on both B and T cells, was the first antibody approved for CLL on the basis of responses in one-third of patients with advanced disease.[3] However, prolonged immunosuppression due to T-cell depletion is a serious side effect of alemtuzumab, leading to severe infectious complications.[4,5] Another approved antibody drug, the chimeric murine/human anti-CD20 MAb rituximab (IDEC-C2B8), has proven efficacy and tolerability in NHL, achieving response rates of 73% and 48% in previously untreated and relapsed/refractory indolent low-grade NHL, respectively. However, the amount of CD20 molecules expressed in B-CLL is lower than in other NHLs. Moreover, significant levels of circulating CD20, which can be detected in the plasma of B-CLL patients, interfere with the binding of rituximab to malignant cells.[6] These factors result in limited activity of rituximab as a single agent in B-CLL patients relapsed or refractory after prior chemotherapy.[7]

One of the alternative immunotherapeutic strategies is based on activation of host immune mechanisms using bispecific antibodies.[8,9] The bispecific antibody makes a bridge between the tumor cell and the immune effector cell, triggering cytotoxic responses. For B-CLL, the B-cell marker CD19 is one of the best targets since it is profusely expressed on leukemic cells and is not shed or internalized by B-CLL cells.[10] One of the best-studied cytotoxic triggering receptors is a multichain TCR/CD3 signaling complex on T cells.[8] To date, different forms of the CD19×CD3 bispecific antibody have been generated and used in a number of *in vitro* and *in vivo* therapeutic studies.[11–18] These bispecific antibodies have been produced using either rodent hybrid hybridomas,[12–14] chemical crosslinking of 2 MAbs[11] or recombinant antibody

Abbreviations: ADCC, antibody-dependent cellular cytotoxicity; BrdU, bromodeoxyuridine; BsDb, bispecific diabody; CD, cluster of differentiation; CLL, chronic lymphocytic leukemia; CTLA-4, cytotoxic T lymphocyte–associated antigen 4; EC_{50}, half-maximal effective concentration; HS, human serum; MAb, monoclonal antibody; NHL, non-Hodgkin's lymphoma; PBL, peripheral blood lymphocyte; PBMC, peripheral blood mononuclear cell; scBsDb, single-chain BsDb; scFv, single-chain variable fragment of antibody; tanDb, tandem diabody; TCR, T-cell receptor; TNF, tumor necrosis factor; TRAIL, TNF-α-related apoptosis-inducing ligand; V_H, variable domain of the heavy chain of an antibody; V_L, variable domain of the light chain of an antibody; WBC, white blood count.

Grant sponsor: German BioRegio Program; Grant number: BEO32/AZ12389.

*Correspondence to: Affimed Therapeutics, Technologiepark, Im Neuenheimer Feld 582, D-69120 Heidelberg, Germany.
Fax: +49-6221-65307-77. E-mail: s.kipriyanov@affimed.com

Received 18 December 2003; Accepted after revision 21 April 2004

DOI 10.1002/ijc.20417
Published online 16 June 2004 in Wiley InterScience (www.interscience.wiley.com).

TABLE 1 - CD19×CD3 TanDb-MEDIATED DEPLETION OF CD19⁺ LEUKEMIA CELLS AND T-CELL PROLIFERATION IN PBMC CULTURES FROM CLL PATIENTS[1]

B-CLL patient	Age (years)/ gender	Binet stage/ therapy number[2]	Days of culture	T-cell prol. factor[3]	Without antibody			TanDb (5 μg/ml)			TanDb (1 μg/ml)			TanDb + MAb 15E8		
					% T cells[4]	% B cells[5]	Total cells[6]	% T cells[4]	% B cells[5]	Total cells[6]	% T cells[4]	% B cells[5]	Total cells[6]	% T cells[4]	% B cells[5]	Total cells[6]
001	57/M	A/0	7	n.d.	9.5	89.2	n.d.	98.8	0.5	n.d.	n.d.	n.d.	n.d.	n.d.	n.d.	n.d.
002	65/M	B/2(2)	7	2.4	8.2	91.8	1.9	98.0	0.8	1.5	14.3	85.6	2.6	99.4	0.5	3.2
003	73/M	B/0	7	21.1	5.3	94.5	3.2	98.6	0.9	3.2	96.5	3.4	3.7	99.8	0.1	2.2
004	61/M	A/1	7	37.8	8.4	91.6	1.4	99.4	0.6	2.8	99.3	0.6	4.5	n.d.	n.d.	n.d.
004	61/M	A/1	7 (HS)	29.1	8.3	91.5	1.1	99.2	0.6	2.0	99.6	0.3	2.7	n.d.	n.d.	n.d.
005	51/M	B/0	6	31.9	3.6	96.6	4.5	99.0	0.1	4.7	94.7	0.6	5.4	n.d.	n.d.	n.d.
005	51/M	B/0	6 (HS)	53.8	5.7	94.2	2.1	99.7	0.3	4.9	96.2	0.6	6.7	99.8	0.1	3.4
006[7]	62/F	A/0	7	38.8	5.8	94.2	2.4	99.5	0.5	5.4	98.2	1.7	5.4	99.7	0.3	2.5
006[7]	63/F	A/0	6	26.6	6.2	93.8	2.9	99.7	0.3	3.0	99.4	0.5	4.8	n.d.	n.d.	n.d.
007	67/M	A/0	6	15.7	19.8	80.2	1.1	94.6	6.0	3.6	84.5	15.4	4.1	99.4	0.2	2.4
008	61/M	A/7(6)	7	64.4	1.7	98.0	3.9	98.3	1.1	2.7	95.5	1.7	4.5	98.9	0.4	3.0
009	75/M	B/4(3)	6	9.6	5.9	94.8	3.4	97.5	1.7	3.1	56.1	43.6	3.4	66.9	33.0	1.8
010	58/F	B/0	5	n.d.	42.6	56.6	1.8	99.2	0.3	3.9	n.d.	n.d.	n.d.	99.8	0.1	4.2
011	59/F	B/0	5	6.8	26.9	73.2	2.3	99.7	0.2	4.4	99.5	0.4	4.2	99.4	0.6	3.8
012	63/M	A/1	6	n.d.	2.9	97.1	3.3	2.8	97.2	5.9	n.d.	n.d.	n.d.	16.3	84.1	6.7
013	58/M	C/4(4)	5	n.d.	3.4	96.5	4.5	2.8	97.1	4.8	n.d.	n.d.	n.d.	n.d.	n.d.	n.d.
014	60/F	B/0	6	4.1	17.4	80.9	1.9	28.9	70.8	4.4	36.9	55.7	3.6	n.d.	n.d.	n.d.
015	63/M	B/0	6	9.1	40.0	59.9	0.9	99.8	0.1	2.3	93.0	0.9	3.5	n.d.	n.d.	n.d.
016	78/F	A/0	6	50.9	4.1	95.9	1.9	98.6	1.3	2.4	96.4	3.5	4.1	n.d.	n.d.	n.d.
017	60/M	A/0	7	1.6	7.7	92.2	2.3	10.7	89.2	3.3	10.4	88.3	2.7	n.d.	n.d.	n.d.
018	67/F	A/0	6	11.5	6.9	92.2	2.6	32.1	65.6	5.2	59.8	40.1	3.5	n.d.	n.d.	n.d.
019[7]	71/M	A/0	5	2.9	17.0	82.9	1.5	n.d.	n.d.	n.d.	41.4	49.3	2.1	79.5	19.4	3.5
019[7]	72/M	A/0	6	5.5	18.2	79.4	1.6	64.7	35.0	2.3	68.2	27.3	2.3	94.3	2.5	2.6
020	61/F	A/0	7	13.7	20.9	74.4	0.7	n.d.	n.d.	n.d.	83.5	16.4	2.4	n.d.	n.d.	n.d.
021	59/M	A/0	6	11.7	9.5	90.4	2.8	58.6	41.3	5.4	43.4	56.5	5.5	26.9	71.0	4.8
021	59/M	A/0	6 (HS)	5.5	19.4	80.5	3.3	98.4	0.3	4.3	98.2	1.7	4.1	95.3	4.2	3.9
022	74/M	A/0	7	3.1	3.1	68.5	3.9	n.d.	n.d.	n.d.	9.1	69.0	4.1	85.9	13.9	4.3
022	74/M	A/0	7 (HS)	1.7	3.3	61.7	5.1	n.d.	n.d.	n.d.	5.0	93.5	5.8	91.8	0.2	5.3
023	73/M	A/1	7	5.6	1.7	97.7	3.9	n.d.	n.d.	n.d.	10.6	88.2	3.5	83.1	20.1	3.4

[1]PBMC cultures were incubated for the indicated time periods either without antibodies, with 5 or 1 μg/ml tanDb alone or with 1 μg/ml tandab in the presence of 1 μg/ml anti-CD28 MAb 15E8. Experiments carried out in autologous HS are indicated.–[2]Quantity of different therapies is shown in the brackets.–[3]T-cell proliferation factor in PBMC cultures incubated in the presence of 1 μg/ml tanDb without costimulation, determined as a ratio of the absolute number of T cells in the treated culture to the absolute number of T cells in the control culture without antibodies.–[4]CD3⁺ cells.–[5]CD19⁺ cells.–[6]Total amount of living cells in millions in PBMC cultures after incubation. Initially, 4×10^6 cells were seeded in 2 ml medium.–[7]Experiments performed with blood samples from the same patient but taken at different time points.

n.d., not determined.

technology.[13,15,16] For example, recombinant bispecific molecules can be formed by noncovalent association of 2 single-chain fusion products consisting of the V_H and V_L domains of different specificity in an orientation preventing intramolecular pairing with the formation of a 4-domain heterodimer, so-called BsDb.[19] We previously demonstrated that CD19×CD3 BsDb is more effective than quadroma-derived bispecific antibody at mediating T-cell cytotoxicity *in vitro* against tumor cells.[13,18] Although BsDb was relatively rapidly cleared from the blood through the kidneys, its antitumor activity in animal tumor models was closely similar to that of the much larger quadroma-derived bispecific antibody.[18,20] However, the BsDb is formed by heterodimerization of 2 different gene products, which must be expressed in the same cell in similar amounts. The problem of quantitative heterodimer formation can be overcome by linking 4 variable domains derived from antibodies of 2 specificities into a single-chain construct, resulting in either an $(scFv)_2$, 2 scFv modules composed of 2 adjacent V_H and V_L domains of the same specificity,[16] or a diabody-like structure, a so-called scBsDb.[15,21]

In contrast to native antibodies, all of the bispecific antibody formats mentioned above have only one binding domain for each specificity. To increase the valence, stability and therapeutic potential of recombinant bispecific antibodies, we constructed a novel tetravalent bispecific molecule with M_r 113 kDa, described by us as a tanDb, that is specific for both human CD19 and CD3 cell surface antigens.[15] The CD19×CD3 tanDb possesses an increased functional affinity to both antigens, improved pharmacokinetics and elevated activity in mediating killing of CD19⁺ tumor cell lines by T cells from healthy donors *in vitro*.[15] Treatment of SCID mice bearing an established Burkitt's lymphoma (5 mm diameter) with human PBLs, CD19×CD3 tanDb and anti-CD28 costimulation resulted in complete elimination of tumors in all animals within 10 days.[17] In contrast, mice receiving human PBLs in combination with either BsDb alone or BsDb plus anti-CD28 MAb showed only partial tumor regression.[17,22]

In the present study, we demonstrate vigorous activation of autologous T cells and killing of malignant cells induced by tetravalent CD19×CD3 tanDb in peripheral blood cultures from CLL patients. In contrast, under the same conditions, bivalent bispecific molecules (BsDb and scBsDb) showed significantly lower T-cell activating and antitumor activities. We provide evidence that tanDb-mediated T-cell activation takes place only in the presence of CD19⁺ cells and clarify the effect of CD28 costimulation on the antitumor activity of autologous T cells recruited by the CD19×CD3 bispecific tanDb.

MATERIAL AND METHODS

Recombinant molecules

Construction and production of bispecific CD19×CD3 diabody, scBsDb and tanDb were previously described.[13,15,18,21] Monospecific anti-CD3 tanDb was assembled from OKT3-derived V_H and V_L domains[23] essentially as described for CD19×CD3 tanDb.[15] Gene constructions were performed according to standard DNA manipulation techniques, and the experimental details are available from the authors upon request. All recombinant proteins were isolated with >95% purity, as judged by reducing SDS-PAGE followed by Coomassie staining.

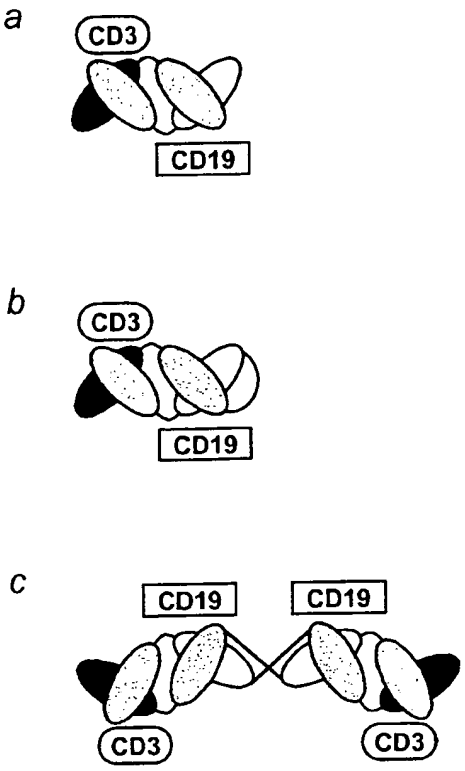

FIGURE 1 – Schematic representation of BsDb *(a)*, scBsDb *(b)* and tanDb *(c)* proteins.

Patient specimens

Twenty-three patients fulfilling the clinical, morphologic and immunophenotypic criteria of B-CLL were selected at the Department of Internal Medicine, University of Heidelberg; and blood samples were obtained after informed consent. Nine of the patients were female and 14, male; ages ranged 51–78 years (median 63). According to the Binet classification,[24] 14 patients were in stage A, 8 in stage B and 1 in stage C. Median WBC was $40 \times 10^3/\mu l$ (range 15 to $211 \times 10^3/\mu l$). At the time of the study, 16 patients had never been treated, 2 had received only chlorambucil therapy, 1 had received only fludarabine therapy, 1 had received chlorambucil and fludarabine therapy and 3 had received chlorambucil, fludarabine and combinations of cyclophosphamide, vincristine and prednisone without or with doxorubicin. After chemotherapy, patients had been off treatment for at least 3 months. Patient data are summarized in Table I.

Isolation of PBLs

Heparinized peripheral blood samples were obtained from patients with leukemia or healthy volunteers. PBMCs were isolated by density gradient centrifugation. Blood samples were twice diluted with PBS (Invitrogen, Breda, the Netherlands), layered on a cushion of Histopaque-1077 (Sigma-Aldrich, Deisenhofen, Germany) and centrifuged at 800*g* for 25 min. PBMCs located in the interface were collected and washed 3 times with PBS before use. For depletion of B cells, PBMCs from a healthy donor were incubated in RPMI medium/10% FCS (Invitrogen) on nylon wool at 37°C for 1 hr. By this method, $CD3^+$ cells were enriched from 52.1% to 77.0% and $CD19^+$ cells reduced from 12.4% to 2.7% in the nonadherent cell fraction.

Antibodies and flow cytometry

Cell surface antigen expression was measured after indirect immunofluorescence staining by flow cytometry. In brief, PBMCs were incubated with murine MAbs OKT3 (anti-CD3[25]), UCHT1 (anti-CD3; Beckman-Coulter, Krefeld, Germany), Edu-2 (anti-CD4; Chemicon, Hofheim, Germany), BL1A (anti-CD5, Beckman-Coulter), UCHT4 (anti-CD8, Chemicon), HD37 (anti-CD19[26]), J4.119 (anti-CD19, Beckman-Coulter), 15E8 (anti-CD28[27]), BB-1 (anti-CD80, Chemicon), MAB104 (anti-CD80, Beckman-Coulter), BU63 (anti-CD86, Chemicon), HA5.2B7 (anti-CD86, Beckman-Coulter) and BNI3 (anti-CD152, BD Pharmingen, Heidelberg, Germany) in the presence of 1 mg/ml human IgG (Sigma-Aldrich) in PBS supplemented with 2% FCS (Invitrogen) and 0.1% sodium azide (Roth, Karlsruhe, Germany) for 45 min on ice. After 3 washing steps, primary antibodies were detected with FITC-conjugated goat antimouse IgG or IgM (Dianova, Hamburg, Germany). Living cells (10^4) were analyzed on a Beckman-Coulter EPICS XL flow cytometer. Dead cells were excluded by staining with 2 μg/ml propidium iodide (Sigma-Aldrich).

Autologous T-cell activation and depletion of leukemia cells

PBMCs from patients with B-CLL were seeded in individual wells of a 12-well plate in 2 ml RPMI medium containing either 10% FCS (Invitrogen) or 10% autologous HS at a density of 2×10^6 cells/ml. Recombinant antibodies were added at the indicated concentrations with or without anti-CD28 MAb 15E8[27] (0.5–2.0 μg/ml). After 5–7 days of incubation, cells were harvested, counted in the presence of trypan blue and stained with anti-CD3 MAb OKT3,[25] anti-CD4 MAb Edu-2 (Chemicon), anti-CD8 MAb UCHT4 (Chemicon) and anti-CD19 MAb HD37[26] for flow cytometry. Living cells (10^4) were analyzed using a flow cytometer and the relative amounts of $CD3^+$, $CD4^+$, $CD8^+$ and $CD19^+$ cells determined. To determine the T-cell proliferation factor in the treated PBMC culture, the absolute number of T cells in the culture was divided by the absolute number of T cells in the control culture. The B-cell depletion factor was calculated as a ratio of the absolute number of malignant $CD19^+$ cells in the control culture to the absolute amount of B cells in the treated culture. For calculation of half-maximal concentrations of tanDb for cell lysis (EC_{50}), sigmoidal dose–response curves were generated for each B-CLL patient using the software program PRISM (GraphPad, San Diego, CA).

Proliferation assay

PBMCs in RPMI-1640 plus 10% FCS were plated at 2×10^5 cells/well in a 96-well flat-bottomed tissue culture plate (Greiner, Frickenhausen, Germany). Antibodies at various concentrations were added and the cells incubated at 37°C in a humidified atmosphere with 5% CO_2 for the indicated time. BrdU was added to a final concentration of 10 μM, and plates were incubated for an additional 18 hr. BrdU incorporation was determined by Cell Proliferation ELISA (Roche, Mannheim, Germany) according to the manufacturer's instructions.

RESULTS

Effect of tetravalence of CD19×CD3 bispecific molecules on autologous T-cell proliferation and depletion of primary leukemia cells

Both bivalent (diabody and single-chain diabody) and tetravalent (tanDb) CD19×CD3 bispecific molecules (schematically shown in Fig. 1) were compared for their capacity to mediate killing of malignant B-CLL cells by nonstimulated autologous T lymphocytes. Freshly isolated PBMCs from patients with B-CLL containing 60–98% $CD19^+/CD5^+$ leukemia cells were incubated in the presence of different concentrations of recombinant antibodies at 37°C for 5–7 days. Bispecific molecules were used with and without anti-CD28 MAb 15E8, which provides a costimulatory signal for T cells, thus leading to their proliferation and increased cytolytic activity.[21] Cells were harvested, counted and stained with MAbs for the following cell differentiation markers: CD19 (B cells, B-CLL cells), CD3 (T cells), CD4 (T-cell subpopulation) and CD8 (T-cell subpopulation). Living cells (10^4)

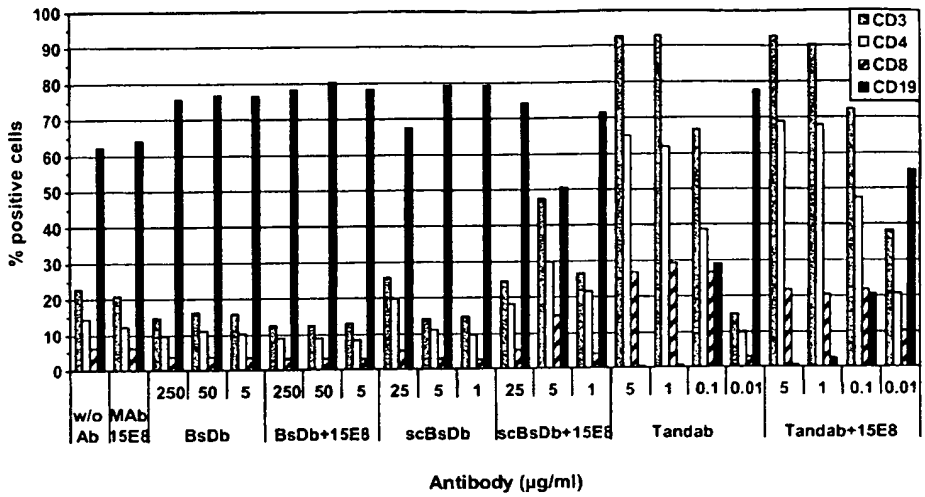

FIGURE 2 – Depletion of primary malignant CD19$^+$ leukemia cells and proliferation of autologous T cells induced by CD19×CD3 bispecific molecules. Freshly isolated PMBCs from B-CLL patient 011 were incubated for 5 days without antibodies (w/o Ab) or in the presence of the indicated concentrations of BsDb, scBsDb or tanDb with or without anti-CD28 MAb 15E8 (0.5 µg/ml) or with MAb 15E8 alone. The relative amounts of CD3$^+$, CD4$^+$, CD8$^+$ and CD19$^+$ cells were determined by flow cytometry and plotted. This experiment is representative of experiments performed with PBMC samples from different B-CLL patients (see Table II).

TABLE II – DEPLETION OF CD19$^+$ LEUKEMIA CELLS AND PROLIFERATION OF AUTOLOGOUS T CELLS INDUCED BY CD19×CD3 BISPECIFIC MOLECULES[1]

B-CLL patient	TanDb		TanDb + MAb 15E8		BsDb		BsDb + MAb 15E8		scBsDb		scBsDb + MAb 15E8	
	T-cell proliferation factor[2]	B-cell depletion factor[3]	T-cell proliferation factor	B-cell depletion factor	T-cell proliferation factor	B-cell depletion factor	T-cell proliferation factor	B-cell depletion factor	T-cell proliferation factor	B-cell depletion factor	T-cell proliferation factor	B-cell depletion factor
002	4.8	301.4	22.5	7.2	0.8	0.8	0.7	0.8	n.d.	n.d.	n.d.	n.d.
003	15.6	119.8	9.9	2140.0	0.9	1.0	0.8	1.1	n.d.	n.d.	n.d.	n.d.
005	27.5	834.7	n.d.	n.d.	0.8	1.3	1.0	1.2	n.d.	n.d.	n.d.	n.d.
006	39.3	79.6	17.4	371.0	2.7	0.6	10.4	0.8	n.d.	n.d.	n.d.	n.d.
007	15.5	4.1	8.3	242.3	1.0	0.6	0.9	0.7	n.d.	n.d.	n.d.	n.d.
008	3.9	127.6	6.2	206.6	1.0	1.0	0.3	0.7	n.d.	n.d.	n.d.	n.d.
009	13.0	71.2	3.8	10.5	1.3	0.8	n.d.	n.d.	n.d.	n.d.	n.d.	n.d.
010	5.5	87.3	5.8	1059.3	1.5	0.4	1.4	0.3	n.d.	n.d.	n.d.	n.d.
011	7.1	135.7	7.1	65.6	0.9	0.6	0.8	0.6	0.8	0.7	4.6	0.5
018	9.3	0.8	n.d.	n.d.	n.d.	n.d.	n.d.	n.d.	4.2	0.6	n.d.	n.d.
019	5.1	1.6	10.3	45.0	n.d.	n.d.	n.d.	n.d.	1.3	0.6	4.1	1.0

[1]PBMC cultures were incubated with the indicated molecules at concentration of 5 µg/ml without or with 1 µg/ml anti-CD28 MAb 15E8.–[2]T-cell proliferation factor determined as a ratio of the absolute number of T cells in the treated culture to the absolute number of T cells in the control culture without antibodies.–[3]B-cell depletion factor determined as a ratio of the absolute number of B cells in the control culture without antibodies to the absolute number of B cells in the treated culture. n.d., not determined.

were analyzed using a Beckman-Coulter flow cytometer and the relative amounts of CD3$^+$, CD4$^+$, CD8$^+$ and CD19$^+$ cells plotted. Table I summarizes the results of the CD3 and CD19 analyses of PBMC cultures incubated in the presence of CD19×CD3 tanDb with and without costimulation.

Unlike the results obtained with human CD19$^+$ cell lines and PBLs isolated from healthy donors,[13,15,18,21] the bivalent diabody and single-chain diabody demonstrated no antitumor effect in a CLL autologous system, even at 5 µM, with or without CD28 costimulation, although slight proliferation of both CD4$^+$ and CD8$^+$ T cells was observed (Fig. 2, Table II). In contrast, the tetravalent CD19×CD3 tanDb demonstrated much higher T-cell proliferation activity with concomitant depletion of malignant CLL cells. At a concentration of 1 µg/ml (10 nM), the tanDb caused nearly quantitative depletion of CD19$^+$ leukemia cells in PBMC samples (Fig. 2). While CD28 costimulation had nearly no effect on T-cell proliferation and antitumor activity of tanDb used at concentrations above 0.1 µg/ml, its influence on the depletion of CLL cells was obvious when tanDb was used at 0.01 µg/ml (0.1 nM).

Target cell–induced T-cell activation and cytotoxicity

Since the tetravalent tanDb can simultaneously bind 2 CD3 molecules on the cell surface,[15] its binding to T cells may potentially cause CD3 crosslinking, leading to MHC-independent T-cell activation and proliferation. To prove that the CD19×CD3 tanDb causes T-cell activation only in the presence of CD19$^+$ tumor cells, we produced monospecific antihuman CD3 tanDb with 4 CD3-binding sites. T-cell proliferation assay was performed using human PBMC cultures isolated from 2 healthy donors. PBMC preparations contained both CD19$^+$ B cells (10–15% of total cell count) and CD3$^+$ T cells (approx. 70%). After incubation of PBMCs in the presence of either monospecific anti-CD3 or bispecific CD19×CD3 tanDbs, T-cell proliferation was colorimetrically measured by incorporation of BrdU into the cellular DNA. During incubation for 72 hr, monospecific anti-CD3 tanDb induced no proliferation of autologous lymphocytes from both donors, even at 10 µg/ml (Fig. 3). In contrast, CD19×CD3 tanDb demonstrated high mitogenic activity for both PBMC cultures, presumably due to CD3 crosslinking *via* CD19-bearing B cells (Fig. 3). T-cell

proliferation induced by CD19×CD3 tanDb was significant even at 10 ng/ml.

To examine whether the presence of $CD19^+$ cells is necessary for T-cell activation mediated by CD19×CD3 tanDb, we performed a T-cell proliferation assay using either the whole PBMC preparation (12.4% $CD19^+$ cells) or PBMCs depleted for B cells (2.7% $CD19^+$ cells). The results shown in Figure 4 clearly demonstrate significantly lower T-cell proliferation in PBMC cultures depleted for $CD19^+$ B cells, thus indicating antigen-specific T-cell activation in the presence of CD19×CD3 tanDb. These experiments exclude the possibility that binding of the tetravalent molecule alone to T cells elicits T-cell activation and cytotoxicity against $CD19^+$ B cells.

Bispecific CD19×CD3 tanDb and a monospecific anti-CD3 tanDb were also compared in autologous PBMC cultures from the B-CLL patient containing >90% leukemia cells (Fig. 5). No T-cell proliferation and no depletion of leukemia cells were observed when anti-CD3 tanDb was used. In contrast, adding CD19×CD3 tanDb to PBMC culture induced vigorous proliferation of both $CD4^+$ and $CD8^+$ T cells as well as killing of tumor cells (Fig. 5).

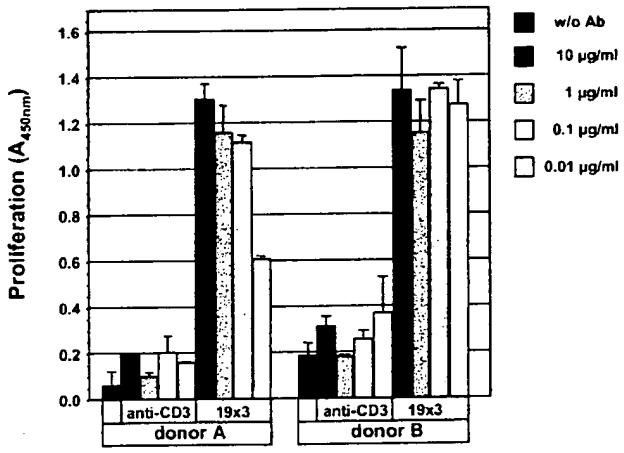

FIGURE 3 – T-cell proliferation in response to either bispecific CD19×CD3 or monospecific anti-CD3 tanDbs. PBMCs from healthy donor A or donor B were incubated either without antibody (w/o Ab) or in the presence of tanDb at 10 ng/ml, 100 ng/ml, 1 µg/ml and 10 µg/ml for 72 hr and pulsed with 10 µM BrdU for an additional 18 hr; incorporation of BrdU was determined by BrdU ELISA. Means and SDs of triplicates are shown.

These data confirm that a T-cell activation signal is provided by bispecific CD19×CD3 tanDb crosslinking the CD3 receptor *via* binding to $CD19^+$ tumor cells.

Effect of CD28 costimulation on the antitumor activity of CD19×CD3 tanDb

It is generally accepted that T-cell activation requires 2 distinct signals. The first depends on the ligation of the TCR/CD3 complex and the CD4 or CD8 coreceptor. The second can be provided by the cell surface molecules that mediate essential costimulatory signals, thereby complementing TCR/CD3-mediated events. CD28 is such a potent costimulatory molecule, and ligation of CD28 with its natural ligands B7-1 (CD80) and B7-2 (CD86) promotes T-cell survival and enhances TCR-mediated signaling to initiate and maintain T-cell responses.[28] Alternatively, the costimulatory signal can be provided by an agonistic anti-CD28 antibody.[29] Our preliminary results demonstrated that adding costimulatory anti-CD28 MAb 15E8 enhanced the antitumor activity of CD19×CD3 bispecific molecules and, in some cases, T-cell proliferation (Fig. 2, Table II). We therefore analyzed the expression patterns of the natural ligands for CD28, B7-1 (CD80) and B7-2 (CD86), on the surface of leukemic cells. Analysis of PBMC samples isolated from 6 CLL patients by flow cytometry demonstrated intermediate to high levels of CD80 expression, whereas CD86 was present at lower levels than CD80 (Fig. 6).

Analysis of the expression of costimulatory molecules on the surface of PBMCs from CLL patients cultured either with or without CD19×CD3 tanDb demonstrated significant upregulation of CD86 expression after tanDb treatment (Fig. 7*c*). Expression of the second CD28 ligand, CD80, was slightly upregulated only on CLL cells cultured without antibodies (Fig. 7*b*). In contrast to the CD19×CD3 tanDb bridging $CD19^+$ malignant B cells with T cells, crosslinking of CD19 on the surface of B-CLL cells using either soluble or immobilized anti-CD19 MAb HD37[26] did not cause any changes in the expression levels of CD80 and CD86 on cultured PBMCs from B-CLL patients and did not influence the survival of B-CLL cells (data not shown). Interestingly, tanDb treatment also caused upregulation of the inhibitory molecule CTLA-4 (CD152) on the surface of PBMCs; higher levels of CD152 expression were observed in cultures with higher cytotoxic activity (Fig. 8).

Although most of the leukemia cells expressed CD80 and CD86 on their surface, analysis of the results of T-cell proliferation and CLL cell killing demonstrated higher T-cell activation and stronger antitumor effects when CD19×CD3 tanDb was used in combination with costimulatory anti-CD28 MAb 15E8 (Fig. 2, Table I). Using CD19×CD3 tanDb, a positive antitumor effect was observed for the vast majority of CLL PBMC samples containing

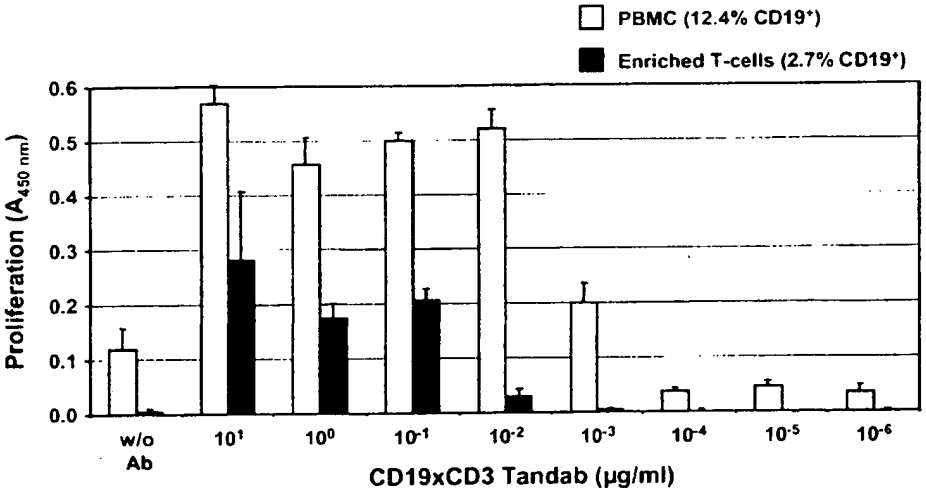

FIGURE 4 – Induction of T-cell proliferation by CD19×CD3 tanDb in normal PBMC culture from a healthy donor and in PBMC culture depleted for B cells. PBMCs were incubated either without antibody (w/o Ab) or in the presence of CD19×CD3 tanDb at concentrations from 1 pg/ml to 1 µg/ml for 72 hr and pulsed with 10 µM BrdU for an additional 18 hr; incorporation of BrdU was determined by BrdU ELISA. Means and SDs of triplicates are shown.

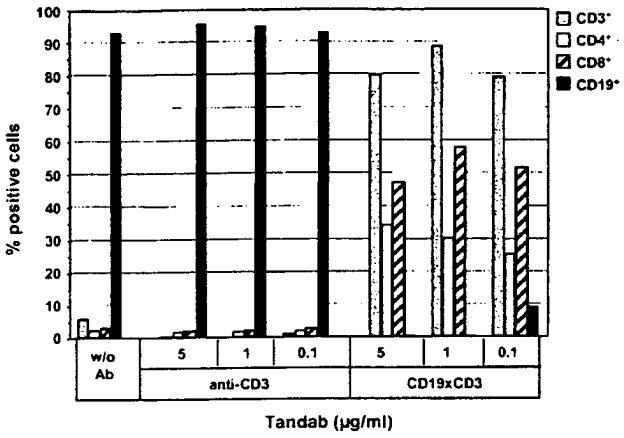

FIGURE 5 – Depletion of primary malignant CD19$^+$ leukemia cells and proliferation of autologous T cells induced either by bispecific CD19×CD3 or by monospecific anti-CD3 tanDbs. Freshly isolated PMBCs from B-CLL patient 006 were incubated for 6 days without antibodies (w/o Ab) or in the presence of the indicated concentrations of monospecific anti-CD3 or bispecific CD19×CD3 tanDb. Relative amounts of CD3$^+$, CD4$^+$, CD8$^+$ and CD19$^+$ cells were determined by flow cytometry and plotted.

as low as 2% T cells. No response was shown only for 2 PBMC samples, though in one case T-cell proliferation was observed when tanDb was used in combination with CD28 costimulation (Table I). Comparison of results of T-cell proliferation and cytotoxicity between PBMC cultures from the same patient incubated either in FCS or in autologous serum demonstrated only marginal 1.5- to 2-fold differences in T-cell proliferation, while showing 10- to 100-fold more efficient depletion of leukemic cells in autologous serum than in FCS (patients 04, 05, 021 and 022, Table I).

Analyses of the CLL cell killing efficacy obtained at different concentrations of CD19×CD3 tanDb used either with or without CD28 costimulation demonstrated that adding anti-CD28 MAb 15E8 caused a 10- to 1,000-fold lowering of the half-maximal concentration of tanDb for cell lysis (EC_{50}). Characteristic dose–response curves obtained for PBMC cultures from 2 CLL patients are shown in Figure 9. This effect was observed for all tested CLL PBMC samples, though EC_{50} values exhibited considerable variation (Table III). Depending on the T-cell response of a particular patient, EC_{50} values ranged from 1 µg/ml to 0.5 ng/ml when using tanDb alone and from 150 ng/ml to as low as 50 pg/ml when tanDb was used with CD28 costimulation (Table III).

DISCUSSION

B-CLL is characterized by abnormal expansion of monoclonal CD5$^+$/CD19$^+$ mature B lymphocytes in the peripheral blood, bone marrow and lymphatic organs.[30] A curative therapy for B-CLL is not yet known, thus stimulating the search for new immunotherapeutic strategies. An emerging approach is the retargeting of cellular effector systems, such as T cells, by bispecific antibodies.[8] However, progress in research and development into the clinical applications of these immunotherapeutic agents has been significantly slowed by problems of manufacturing, immunogenicity of mouse-derived antibodies, lack of therapeutic efficacy, toxicity associated with cytokine storms and unfavorable pharmacokinetics.[9] To improve the therapeutic potential of bispecific antibodies, we constructed a novel recombinant molecule named "tandem diabody" (tanDb), which is bispecific and tetravalent.[15] In the present study, we analyzed the ability of the tetravalent CD19×CD3 tanDb to cause T-cell activation and depletion of malignant leukemia cells in an autologous system derived from patients suffering from B-CLL.

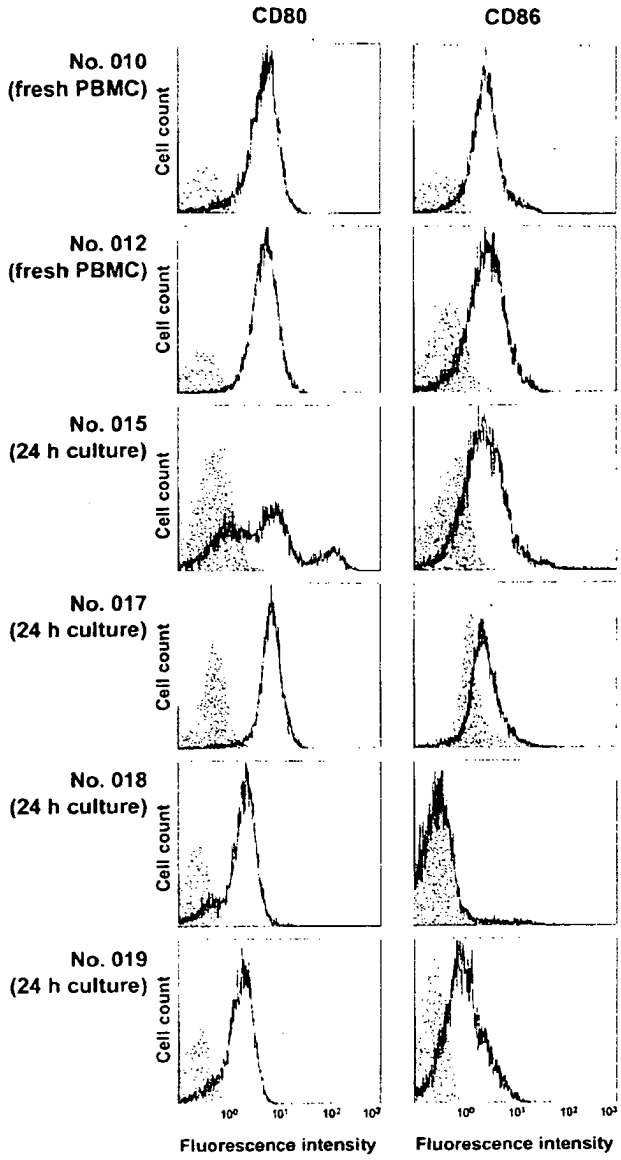

FIGURE 6 – CD80 (B7-1) and CD86 (B7-2) expression on PBMCs from B-CLL patients. Freshly isolated PBMCs or PBMCs cultured for 24 hr without antibodies were stained with anti-CD80 MAb BB-1 or anti-CD86 MAb BU63 followed by FITC- or phycoerythrin-conjugated goat antimouse IgG or IgM, respectively. Stained cells were analyzed by a Beckman-Coulter flow cytometer. Solid gray histograms represent control staining with secondary antibodies alone.

Peripheral T cells, representing a minor population in the peripheral blood of B-CLL patients, are usually in a resting state and need strong signals for activation.[31] Here, we have demonstrated that bispecific CD19×CD3 molecules induced depletion of leukemia cells by nonstimulated autologous T cells in PBMC cultures from patients with B-CLL. No T-cell enrichment was performed, resulting in E:T cell ratios close to those *in vivo*. However, antibody-induced T-cell activation and tumor cell killing were observed only for the tetravalent tanDbs, while structurally similar but bivalent diabody and single-chain diabody demonstrated nearly no antitumor activity. These data indicate the importance of bivalent binding to both T cells and tumor cells for T-cell activation and stimulation of T cell–mediated cytotoxicity under condi-

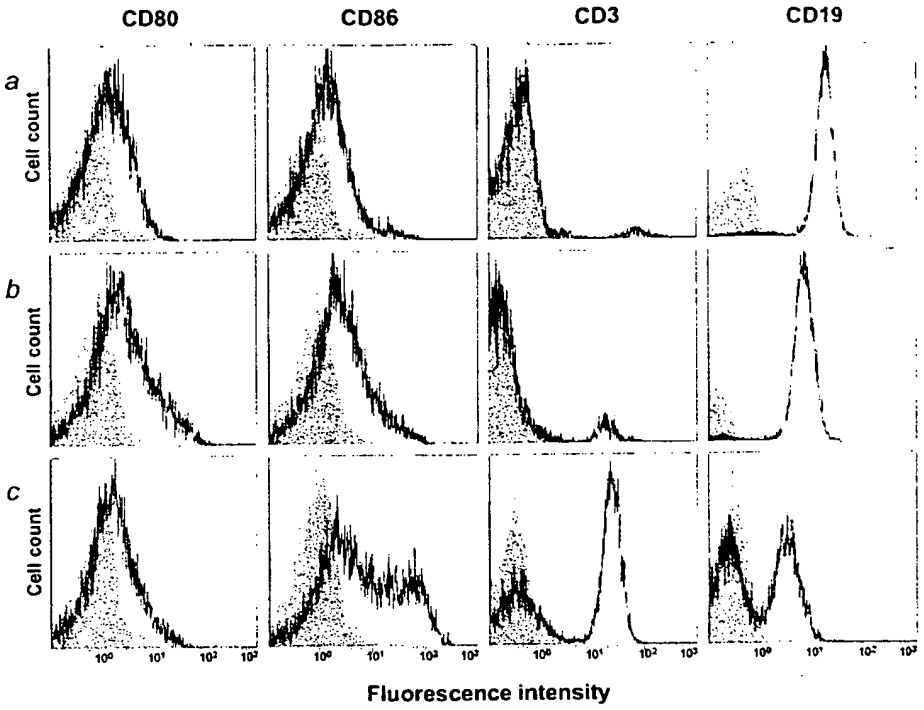

FIGURE 7 – Expression of co-stimulatory molecules on PBMCs from patient 021 with B-CLL, as determined by flow cytometry. Freshly isolated PBMCs *(a)* and PBMCs incubated in medium with FCS for 6 days either without antibodies *(b)* or in the presence of 1 μg/ml CD19×CD3 tanDb *(c)* were stained with FITC-conjugated anti-CD3 MAb UCHT1 or anti-CD19 MAb J4.119 and with phycoerythrin-conjugated anti-CD80 MAb MAB104 or anti-CD86 MAb HA5.2B7 (solid lines). Solid gray histograms represent corresponding isotype controls. All stainings were performed in the presence of 1 mg/ml human IgG. Cells (1×10^4) were analyzed on a Beckman-coulter flow cytometer.

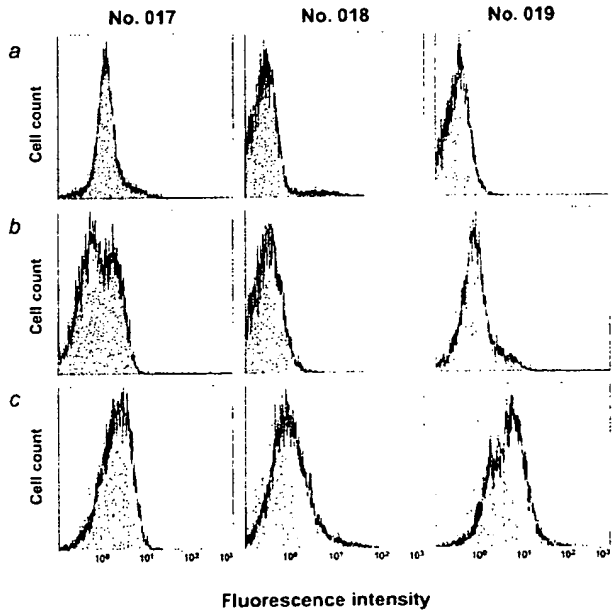

FIGURE 8 – Expression of CTLA-4 (CD152) molecules on PBMCs from B-CLL patients 017, 018 and 019 with low response, medium response and high response to tanDb treatment, respectively, as determined by flow cytometry. Freshly isolated PBMCs *(a)* and PBMCs incubated in medium with FCS for 6 days either without antibodies *(b)* or in the presence of 1 μg/ml CD19×CD3 tanDb *(c)* were stained with anti-CD152 MAb BNI3 (solid lines). Solid gray histograms represent corresponding isotype controls.

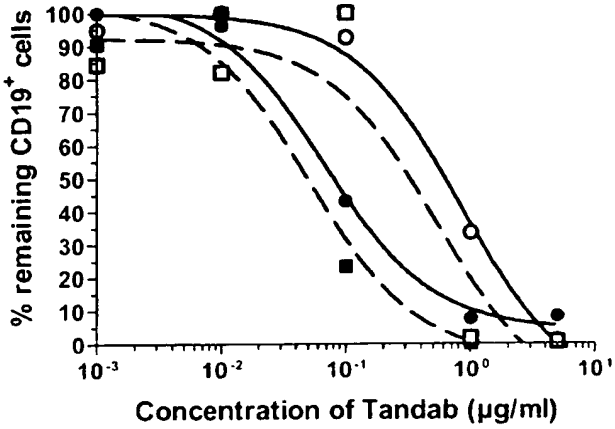

FIGURE 9 – Effect of CD28 costimulation on T-cell cytotoxicity mediated by CD19×CD3 tanDb. The percentage of remaining $CD19^+$ leukemia cells in PBMC samples from B-CLL patients 008 (squares, broken lines) and 009 (circles, solid lines) was plotted against the concentration of tanDb used either with (filled symbols) or without (open symbols) CD28 costimulation.

tions of low E:T ratios. Previously, it was demonstrated that dimerization of a subagonistic antimelanoma/anti-CD28 scFv–scFv fusion [$(scFv)_2$] molecule led to the appearance of supra-agonistic properties of a dimer in inducing vigorous T-cell activation and killing of melanoma cells.[32] Although the tanDb molecule contains 2 CD3-binding sites, our results demonstrated that T-cell activation and proliferation occurred only in the presence of $CD19^+$ target cells. Since no additional stimulus for T-cell activation was provided, the T-cell activation and cytotoxicity resulted from bridging CD3 through $CD19^+$ tumor cells.

Using CD19×CD3 tanDb alone, a very strong antitumor effect leading to almost quantitative elimination of leukemia cells was observed for PBMC samples from 15 of 23 B-CLL patients. In 5 specimens, moderate T-cell stimulation and killing of $CD19^+$ cells was observed, and only 3 PBMC preparations did not respond to tanDb alone. Additional stimulation provided by anti-CD28 MAb significantly increased the cytotoxic effect in moderate responders

TABLE III - EFFECT OF CD28 COSTIMULATION ON T-CELL CYTOTOXICITY MEDIATED BY CD19×CD3 TanDb

B-CLL patient	EC_{50} of tandab (ng/ml)	
	Tandab alone	Tandab + MAb 15E8
002	1200.0 (0.99)[1]	156.5 (0.99)
009	826.7 (0.99)	67.3 (0.99)
008	509.8 (0.87)	51.4 (0.96)
014	428.9 (0.91)	n.d.
016	285.8 (1.00)	n.d.
021 (HS)[2]	157.6 (1.00)	54.3 (0.99)
006[3]	99.8 (1.00)	0.14 (1.00)
011	93.6 (0.98)	53.2 (0.99)
015	67.5 (0.99)	n.d.
007	65.6 (0.99)	36.7 (0.99)
005	51.7 (0.99)	0.05 (1.00)
003	31.3 (1.00)	0.06 (1.00)
018	14.8 (0.95)	n.d.
006[3]	11.4 (1.00)	n.d.
004	0.5 (1.00)	n.d.

[1] R^2, goodness of fit is shown in parentheses.–[2]Experiment carried out in autologous serum.–[3]Experiments performed with blood samples from the same patient but taken at different time points. n.d., not determined.

and even induced T-cell proliferation in 2 nonresponding PBMC samples. Thus, in 22 of 23 patient samples, strong T-cell activation and killing of leukemic B cells were demonstrated after incubation with CD19×CD3 tanDb and anti-CD28 MAb. Seven PBMC samples were obtained from patients who had previously received 1–7 chemotherapy regimens. Four of these cases showed almost quantitative elimination of malignant B cells with CD19×CD3 tanDb alone and 2 showed a response to tanDb in combination with CD28 costimulation. All samples from 16 untreated B-CLL patients were sensitive to tanDb-mediated cytotoxicity. The efficacy of killing induced by CD19×CD3 tanDb is determined by the ability of the patient's T cells to be activated as well as by responsiveness of the CLL cells. It is quite probable that in nonresponding patients a significant proportion of T cells are refractory to activation (anergic). However, some B-CLL cell subsets are able to secrete immunosuppressive cytokines.[33]

Considering the mechanism of leukemia cell elimination, tanDb comprises only CD19 and CD3 binding sites. We showed that CD3 binding alone does not lead to T-cell activation and B-cell killing. We also did not see any effect of CD19 crosslinking alone on the upregulation of costimulatory molecules and dying of CLL cells. Depletion of tumor cells was observed only when both specificities were present and was accompanied by T-cell proliferation. The only possible mechanism of killing is direct action of cytotoxic T lymphocytes on tumor cells *via* the formation of secretory synapses followed by release of the content of lytic granules, comprising proteases of the granzyme family (especially granzymes A and B), perforin and the recently discovered granulysin.[34] Both $CD8^+$ and $CD4^+$ T cells induced apoptosis of autologous B-CLL cells through a perforin-mediated pathway but not *via* Fas/FasL, TNF-α or TRAIL.[35]

Optimal activation of T cells requires TCR/CD3 engagement in addition to a costimulatory signal delivered by a distinct coreceptor. The best-characterized of these costimulatory molecules is CD28, which plays a multifaceted role in regulating T-cell function after interaction with its ligands, B7-1 (CD80) and B7-2 (CD86). Costimulation through CD28 in conjunction with triggering of the TCR/CD3 complex leads to high-level production of IL-2 and regulates T-cell cycle entry and progression through the G_1 phase. CD28 costimulation is thought to be required not only to activate T cells but also to protect them from apoptosis mediated by the CD95 (APO-1/Fas) death receptor.[14,36,37] Loss of CD80 and CD86 expression by immunogenic tumors may, therefore, lead to escape from host immunity.[38] Since the malignant cells of B-cell lineage express costimulatory molecules on their surface,[39,40] these expression levels might be high enough to provide a costimulatory signal, especially when high concentrations of the bispecific antibody (tanDb) are used. CD28-mediated signal causes upregulation of CD40 ligand on the surface of T cells, which in turn binds to CD40 on the B cells, thus enhancing B7-1/B7-2 expression and reinforcing the CD28/CD40-positive feedback loop.[41,42] However, the tetravalent CD19×CD3 tanDb by itself may impair the resistance of malignant B cells to T cell-mediated cytotoxicity. It has been previously shown that crosslinking of CD19 on the surface of tumor cells by homodimers of anti-CD19 MAb could induce G_0/G_1 cell cycle arrest and enhance sensitivity of xenografted tumor to doxorubicin *in vivo*.[43] It was therefore postulated that this inhibitory effect is mediated by intracellular signaling, which could modulate the regulatory signals of other receptors.[44] For example, crosslinking of CD19 was reported to increase the expression levels of B7 molecules, mainly B7-2, on the surface of resting splenic B cells.[45] In the present study, we have demonstrated upregulation of CD86 on PBMCs from B-CLL patients upon incubation with CD19×CD3 tanDb but only as a result of T-cell activation. CD19 crosslinking alone did not cause upregulation of the B7 molecules.

Once activated, T cells significantly increase membrane expression of CTLA-4 (CD152), which binds both B7-1 and B7-2 molecules with approximately 100-fold higher affinity than CD28 and, upon binding, transmits a signal to inhibit T-cell activation, leading to the Fas-independent death of T cells.[46] In our experiments, levels of CTLA-4 expression correlated with the degree of T-cell activation and antitumor response. It has been previously shown that CTLA-4 crosslinking leads to apoptotic death of a substantial fraction of activated $CD4^+$ T lymphocytes and to cell cycle arrest without apoptosis in resting $CD4^+$ T cells.[47] Accordingly, the attenuation of T-cell functions can be prevented by antibody blockade of CTLA-4/B7 interactions.[48,49] It is quite probable that the efficacy of T cell–mediated immunotherapy can be further enhanced by a combination of antitumor/anti-CD3 bispecific antibodies with antagonistic anti-CTLA-4 MAb. However, this hypothesis needs experimental examination.

When only a few tanDb molecules were present, the effect of CD28 costimulation on T-cell activation proved to be more pronounced. Depending on the patient specimen, we observed a 10- to 1,000-fold decrease of the half-maximal concentrations of tanDb for cell lysis. Upon CD28 costimulation, specific tumor cell lysis was found at tanDb concentrations as low as 0.5 pM. It is quite probable that the costimulatory signal provided by CD28 crosslinking lowers the TCR/CD3-triggering threshold necessary for T-cell activation.[50] Furthermore, it is quite plausible that crosslinking of CD28 with bivalent agonistic MAb 15E8 facilitates not only the amplification of TCR-coupled mitogenic signals but also the suppression of negative signals transduced through CTLA-4.

Efficient depletion of leukemic cells in PBMC cultures from B-CLL patients has also been demonstrated for an anti-CD19/anti-CD3 scFv–scFv fusion $[(scFv)_2]$.[51] Although the authors previously thought that the T-cell cytotoxicity mediated by $(scFv)_2$ is costimulation-independent,[16,52,53] they showed that a combination of their bispecific molecule with a costimulatory anti-CD28 MAb or IL-2 leads to increased lysis of B-CLL cells by T cells.[51] Although $(scFv)_2$ was produced using the more efficient folding machinery of mammalian cells, the data of Löffler *et al.*[51] indicate that their bivalent $(scFv)_2$ showed 10- to 20-fold lower activity on a molar basis in a similar autologous system compared to the bacterially expressed tetravalent tanDb described in the present study.

In conclusion, we have demonstrated that the tetravalent bispecific CD19×CD3 tanDb induces highly efficient T cell–mediated killing of autologous malignant B cells at very low E:T ratios, thus reflecting the clinical situation. Also, tanDb had superior properties compared to bivalent formats currently in use for the generation of bispecific molecules.

ACKNOWLEDGEMENTS

We thank Ms. B. Geweniger and Ms. S. Wolff for excellent technical assistance.

REFERENCES

1. Rozman C, Montserrat E. Chronic lymphocytic leukemia. N Engl J Med 1995;333:1052–7.
2. Kay NE, Hamblin TJ, Jelinek DF, Dewald GW, Byrd JC, Farag S, Lucas M, Lin T. Chronic lymphocytic leukemia. Hematology (Am Soc Hematol Educ Program) 2002:193–213.
3. Mavromatis B, Cheson BD. Monoclonal antibody therapy of chronic lymphocytic leukemia. J Clin Oncol 2003;21:1874–81.
4. Rai KR, Freter CE, Mercier RJ, Cooper MR, Mitchell BS, Stadtmauer EA, Santabarbara P, Wacker B, Brettman L. Alemtuzumab in previously treated chronic lymphocytic leukemia patients who also had received fludarabine. J Clin Oncol 2002;20:3891–7.
5. Rodon P, Breton P, Courouble G. Treatment of pure red cell aplasia and autoimmune haemolytic anaemia in chronic lymphocytic leukaemia with Campath-1H. Eur J Haematol 2003;70:319–21.
6. Manshouri T, Do KA, Wang X, Giles FJ, O'Brien SM, Saffer H, Thomas D, Jilani I, Kantarjian HM, Keating MJ, Albitar M. Circulating CD20 is detectable in the plasma of patients with chronic lymphocytic leukemia and is of prognostic significance. Blood 2003; 101:2507–13.
7. Huhn D, von Schilling C, Wilhelm M, Ho AD, Hallek M, Kuse R, Knauf W, Riedel U, Hinke A, Srock S, Serke S, Peschel C, et al. Rituximab therapy of patients with B-cell chronic lymphocytic leukemia. Blood 2001;98:1326–31.
8. van Spriel AB, van Ojik HH, van De Winkel JG. Immunotherapeutic perspective for bispecific antibodies. Immunol Today 2000;21:391–7.
9. Kipriyanov SM, Le Gall F. Recent advances in the generation of bispecific antibodies for tumor immunotherapy. Curr Opin Drug Discov Dev 2004;7:233–42.
10. Sieber T, Schoeler D, Ringel F, Pascu M, Schriever F. Selective internalization of monoclonal antibodies by B-cell chronic lymphocytic leukaemia cells. Br J Haematol 2003;121:458–61.
11. Anderson PM, Crist W, Hasz D, Carroll AJ, Myers DE, Uckun FM. G19.4(αCD3) × B43(αCD19) monoclonal antibody heteroconjugate triggers CD19 antigen-specific lysis of t(4;11) acute lymphoblastic leukemia cells by activated CD3 antigen-positive cytotoxic T cells. Blood 1992;80:2826–34.
12. Csóka M, Strauss G, Debatin K-M, Moldenhauer G. Activation of T cell cytotoxicity against autologous common acute lymphoblastic leukemia (cALL) blasts by CD3 × CD19 bispecific antibody. Leukemia 1996;10:1765–72.
13. Kipriyanov SM, Moldenhauer G, Strauss G, Little M. Bispecific CD3×CD19 diabody for T cell-mediated lysis of malignant human B cells. Int J Cancer 1998;77:763–72.
14. Daniel PT, Kroidl A, Kopp J, Sturm I, Moldenhauer G, Dörken B, Pezzutto A. Immunotherapy of B-cell lymphoma with CD3×19 bispecific antibodies: costimulation via CD28 prevents "veto" apoptosis of antibody-targeted cytotoxic T cells. Blood 1998;92:4750–7.
15. Kipriyanov SM, Moldenhauer G, Schuhmacher J, Cochlovius B, Von der Lieth CW, Matys ER, Little M. Bispecific tandem diabody for tumor therapy with improved antigen binding and pharmacokinetics. J Mol Biol 1999;293:41–56.
16. Löffler A, Kufer P, Lutterbuse R, Zettl F, Daniel PT, Schwenkenbecher JM, Riethmüller G, Dörken B, Bargou RC. A recombinant bispecific single-chain antibody, CD19×CD3, induces rapid and high lymphoma-directed cytotoxicity by unstimulated T lymphocytes. Blood 2000;95:2098–103.
17. Cochlovius B, Kipriyanov SM, Stassar MJJG, Schuhmacher J, Benner A, Moldenhauer G, Little M. Cure of Burkitt's lymphoma in severe combined immunodeficiency mice by T cells, tetravalent CD3×CD19 tandem diabody, and CD28 costimulation. Cancer Res 2000;60:4336–41.
18. Cochlovius B, Kipriyanov SM, Stassar MJJG, Christ O, Schuhmacher J, Strauss G, Moldenhauer G, Little M. Treatment of human B cell lymphoma xenografts with a CD3×CD19 diabody and T cells. J Immunol 2000;165:888-95.
19. Holliger P, Prospero T, Winter G. "Diabodies": small bivalent and bispecific antibody fragments. Proc Natl Acad Sci USA 1993;90: 6444–8.
20. Arndt MA, Krauss J, Kipriyanov SM, Pfreundschuh M, Little M. A bispecific diabody that mediates natural killer cell cytotoxicity against xenotransplanted human Hodgkin's tumors. Blood 1999;94:2562–8.
21. Kipriyanov SM, Moldenhauer G, Braunagel M, Reusch U, Cochlovius B, Le Gall F, Kouprianova OA, Von der Lieth CW, Little M. Effect of domain order on the activity of bacterially produced bispecific single-chain Fv antibodies. J Mol Biol 2003;330:99–111.
22. Kipriyanov SM, Cochlovius B, Schäfer HJ, Moldenhauer G, Bähre A, Le Gall F, Knackmuss S, Little M. Synergistic antitumor effect of bispecific CD19×CD3 and CD19×CD16 diabodies in a preclinical model of non-Hodgkin's lymphoma. J Immunol 2002;169:137–44.
23. Kipriyanov SM, Moldenhauer G, Martin ACR, Kupriyanova OA, Little M. Two amino acid mutations in an anti-human CD3 single chain Fv antibody fragment that affect the yield on bacterial secretion but not the affinity. Protein Eng 1997;10:445–53.
24. Binet JL, Auquier A, Dighiero G, Chastang C, Piguet H, Goasguen J, Vaugier G, Potron G, Colona P, Oberling F, Thomas M, Tchernia G, et al. A new prognostic classification of chronic lymphocytic leukemia derived from a multivariate survival analysis. Cancer 1981;48:198–206.
25. Kung PC, Goldstein G, Reinherz EL, Schlossman SF. Monoclonal antibodies defining distinctive human T cell surface antigens. Science 1979;206:347–9.
26. Pezzutto A, Dörken B, Rabinovitch PS, Ledbetter JA, Moldenhauer G, Clark EA. CD19 monoclonal antibody HD37 inhibits anti-immunoglobulin-induced B cell activation and proliferation. J Immunol 1987;138:2793–9.
27. Pohl C, Denfeld R, Renner C, Jung W, Bohlen H, Sahin U, Hombach A, van Lier R, Schwonzen M, Diehl V. CD30-antigen-specific targeting and activation of T cells via murine bispecific monoclonal antibodies against CD3 and CD28: potential use for the treatment of Hodgkin's lymphoma. Int J Cancer 1993;54:820–7.
28. Chambers CA, Allison JP. Costimulatory regulation of T cell function. Curr Opin Cell Biol 1999;11:203–10.
29. Jenkins MK, Taylor PS, Norton SD, Urdahl KB. CD28 delivers a costimulatory signal involved in antigen-specific IL-2 production by human T cells. J Immunol 1991;147:2461–6.
30. Schriever F, Huhn D. New directions in the diagnosis and treatment of chronic lymphocytic leukaemia. Drugs 2003;63:953–69.
31. Bohlen H, Hopff T, Manzke O, Engert A, Kube D, Wickramanayake PD, Diehl V, Tesch H. Lysis of malignant B cells from patients with B-chronic lymphocytic leukemia by autologous T cells activated with CD3×CD19 bispecific antibodies in combination with bivalent CD28 antibodies. Blood 1993;82:1803–12.
32. Grosse-Hovest L, Hartlapp I, Marwan W, Brem G, Rammensee HG, Jung G. A recombinant bispecific single-chain antibody induces targeted, supra-agonistic CD28-stimulation and tumor cell killing. Eur J Immunol 2003;33:1334–40.
33. Stevenson FK, Caligaris-Cappio F. Chronic lymphocytic leukemia: revelations from the B-cell receptor. Blood, 2004;103:4389–95.
34. Trambas CM, Griffiths GM. Delivering the kiss of death. Nat Immunol 2003;4:399–403.
35. Porakishvili N, Kardava L, Jewell AP, Yong K, Glennie MJ, Akbar A, Lydyard PM. Cytotoxic $CD4^+$ T cells in patients with B cell chronic lymphocytic leukemia kill via a perforin-mediated pathway. Haematologica 2004;89:435–43.
36. Daniel PT, Kroidl A, Cayeux S, Bargou R, Blankenstein T, Dörken B. Costimulatory signals through B7.1/CD28 prevent T cell apoptosis during target cell lysis. J Immunol 1997;159:3808–15.
37. Jones RG, Elford AR, Parsons MJ, Wu L, Krawczyk CM, Yeh WC, Hakem R, Rottapel R, Woodgett JR, Ohashi PS. CD28-dependent activation of protein kinase B/Akt blocks Fas-mediated apoptosis by preventing death-inducing signaling complex assembly. J Exp Med 2002;196:335–48.
38. Chen L, Ashe S, Brady WA, Hellstrom I, Hellstrom KE, Ledbetter JA, McGowan P, Linsley PS. Costimulation of antitumor immunity by the B7 counterreceptor for the T lymphocyte molecules CD28 and CTLA-4. Cell 1992;71:1093–102.
39. Trentin L, Zambello R, Sancetta R, Facco M, Cerutti A, Perin A, Siviero M, Basso U, Bortolin M, Adami F, Agostini C, Semenzato G. B lymphocytes from patients with chronic lymphoproliferative disorders are equipped with different costimulatory molecules. Cancer Res 1997;57:4940–7.
40. Damle RN, Ghiotto F, Valetto A, Albesiano E, Fais F, Yan XJ, Sison CP, Allen SL, Kolitz J, Schulman P, Vinciguerra VP, Budde P, et al. B-cell chronic lymphocytic leukemia cells express a surface membrane phenotype of activated, antigen-experienced B lymphocytes. Blood 2002;99:4087–93.
41. Frauwirth KA, Thompson CB. Activation and inhibition of lymphocytes by costimulation. J Clin Invest 2002;109:295–9.
42. Van den Hove LE, Van Gool SW, Vandenberghe P, Bakkus M, Thielemans K, Boogaerts MA, Ceuppens JL. CD40 triggering of chronic lymphocytic leukemia B cells results in efficient alloantigen presentation and cytotoxic T lymphocyte induction by up-regulation of CD80 and CD86 costimulatory molecules. Leukemia 1997;11:572–80.
43. Ghetie MA, Podar EM, Ilgen A, Gordon BE, Uhr JW, Vitetta ES. Homodimerization of tumor-reactive monoclonal antibodies markedly increases their ability to induce growth arrest or apoptosis of tumor cells. Proc Natl Acad Sci USA 1997;94:7509–14.
44. Ghetie MA, Ghetie V, Vitetta ES. Anti-CD19 antibodies inhibit the function of the P-gp pump in multidrug-resistant B lymphoma cells. Clin Cancer Res 1999;5:3920–47.
45. Kozono Y, Abe R, Kozono H, Kelly RG, Azuma T, Holers VM.

Cross-linking CD21/CD35 or CD19 increases both B7-1 and B7-2 expression on murine splenic B cells. J Immunol 1998;160:1565–72.
46. Sansom DM, Manzotti CN, Zheng Y. What's the difference between CD80 and CD86? Trends Immunol 2003;24:314–9.
47. Scheipers P, Reiser H. Fas-independent death of activated CD4$^+$ T lymphocytes induced by CTLA-4 crosslinking. Proc Natl Acad Sci USA 1998;95:10083–8.
48. Phan GQ, Yang JC, Sherry RM, Hwu P, Topalian SL, Schwartzentruber DJ, Restifo NP, Haworth LR, Seipp CA, Freezer LJ, Morton KE, Mavroukakis SA, et al. Cancer regression and autoimmunity induced by cytotoxic T lymphocyte–associated antigen 4 blockade in patients with metastatic melanoma. Proc Natl Acad Sci USA 2003; 100:8372–7.
49. Hodi FS, Mihm MC, Soiffer RJ, Haluska FG, Butler M, Seiden MV, Davis T, Henry-Spires R, MacRae S, Willman A, Padera R, Jaklitsch MT, et al. Biologic activity of cytotoxic T lymphocyte–associated antigen 4 antibody blockade in previously vaccinated metastatic melanoma and ovarian carcinoma patients. Proc Natl Acad Sci USA 2003;100:4712–7.
50. Valitutti S, Muller S, Cella M, Padovan E, Lanzavecchia A. Serial triggering of many T-cell receptors by a few peptide–MHC complexes. Nature 1995;375:148–51.
51. Löffler A, Gruen M, Wuchter C, Schriever F, Kufer P, Dreier T, Hanakam F, Baeuerle PA, Bommert K, Karawajew L, Dörken B, Bargou RC. Efficient elimination of chronic lymphocytic leukaemia B cells by autologous T cells with a bispecific anti-CD19/anti-CD3 single-chain antibody construct. Leukemia 2003;17:900–9.
52. Dreier T, Lorenczewski G, Brandl C, Hoffmann P, Syring U, Hanakam F, Kufer P, Riethmüller G, Bargou R, Baeuerle PA. Extremely potent, rapid and costimulation-independent cytotoxic T-cell response against lymphoma cells catalyzed by a single-chain bispecific antibody. Int J Cancer 2002;100:690–7.
53. Dreier T, Baeuerle PA, Fichtner I, Grün M, Schlereth B, Lorenczewski G, Kufer P, Lutterbüse R, Riethmüller G, Gjorstrup P, Bargou RC. T cell costimulus-independent and very efficacious inhibition of tumor growth in mice bearing subcutaneous or leukemic human B cell lymphoma xenografts by a CD19$^-$/CD3$^-$ bispecific single-chain antibody construct. J Immunol 2003;170:4397–402.

This Page is Inserted by IFW Indexing and Scanning Operations and is not part of the Official Record

BEST AVAILABLE IMAGES

Defective images within this document are accurate representations of the original documents submitted by the applicant.

Defects in the images include but are not limited to the items checked:

- ☐ BLACK BORDERS
- ☐ IMAGE CUT OFF AT TOP, BOTTOM OR SIDES
- ☐ FADED TEXT OR DRAWING
- ☐ BLURRED OR ILLEGIBLE TEXT OR DRAWING
- ☐ SKEWED/SLANTED IMAGES
- ☑ COLOR OR BLACK AND WHITE PHOTOGRAPHS
- ☐ GRAY SCALE DOCUMENTS
- ☑ LINES OR MARKS ON ORIGINAL DOCUMENT
- ☐ REFERENCE(S) OR EXHIBIT(S) SUBMITTED ARE POOR QUALITY
- ☐ OTHER: _____

IMAGES ARE BEST AVAILABLE COPY.
As rescanning these documents will not correct the image problems checked, please do not report these problems to the IFW Image Problem Mailbox.